

e-HIGHWAY 2050

Modular Development Plan of the Pan-European Transmission System 2050

Contract number	308908	Instrument	Collaborative Project
Start date	1st of September 2012	Duration	40 months
WP 8	Enhanced Pan-European Transmission Planning Methodology		
D8.2.a	Enhanced methodology for the computation of Demand/Generation scenarios		



Revision: 2.1

Due date of delivery: December 2014

		Date & Visa
Written by	Baptiste SEGUINOT, RTE	17/12/2014
Checked by	Patrick PANCIATICI, RTE, WP8 Leader Camille PACHE, RTE Jean MAEGHT, RTE Alessandro ZANI, RSE Alexander WEBER, TU Berlin Leif WARLAND, SINTEF	05/01/2015
Validated by	Brahim BETRAOUI, RTE Gérald SANCHIS, RTE, Coordinator	12/02/2015

Project co-funded by the European Commission within the Seventh Framework Program

Dissemination Level

PU	Public	X
PP	Restricted to other program participants (including the Commission Services)	
RE	Restricted to a group specified by the consortium (including the Commission Services)	
CO	Confidential, only for members of the consortium (including the Commission Services)	

Document information

General purpose

This document is the deliverable D8.2.a of the e-Highway2050 project. It contains the description of the work performed in the framework of Task 8.2, named “Computation of Demand and Generation Time Series”.

This deliverable:

- describes the method which has been developed and prototyped in the framework of this work package,
- discusses the modelling choices which have been made in the context of this long-term pan-European study and under the light of the state-of-the-art and sensitivity analyses,
- presents a literature review with alternatives to the retained method,
- and illustrates the methodology through test-cases and examples.

Change status

Revision	Date	Changes description	Authors
V0.0	05/12/2014	Initial version	B. SEGUINOT
V1.0	17/12/2014	Modifications after exchanges with WP 8 partners	B. SEGUINOT
V1.1	28/01/2015	Modifications after comments with coordinators	C. PACHE

EXECUTIVE SUMMARY

The present document is the final deliverable of Task 8.2 of e-Highway2050 project, named “Computation of Demand and Generation Time Series”.

It proposes a method to perform the first step of the enhanced Transmission Expansion Planning (TEP) methodology developed by Work Package 8 (WP 8). This first step consists in developing the macro-assumptions of each scenario and time horizon into balanced time series of demand and generation which will be later used as reference injections in the following steps of the TEP.

This task is performed with a stochastic adequacy model which simulates the behaviour of the power system using a “copperplate” approach (without grid constraints). The stochasticity of the problem is handled through a Monte Carlo method which consists in running numerous simulations with different samples of the uncertain phenomena affecting the system.

The method developed and prototyped contains four modules:

- A maintenance scheduling heuristic, which plans the maintenance of the thermal power plants.
- A time series generator, which samples new possible behaviours of the uncertain phenomena which affect the power system (intermittent RES, demand, hydrological inflows and thermal plant outages).
- A routine which allocates the hydro resources among the 52 weeks of the year, so as to decompose the problem into 52 sub-problems.
- An hourly adequacy model with a complete description of the hydro and thermal power plants, extra-European exchanges and demand response programs which computes the hydro and thermal dispatch of the system.

Significant work has notably been done on the modelling of dependencies between the uncertain phenomena affecting the system (both spatial and intermodal correlations), on the integration of an efficient unit commitment model (considering the limited flexibility of thermal units) and on the addition of demand response.

Recent literature has been reviewed on each of these points. Moreover, the role these modellings have in the adequacy simulator and the precision they bring to the results of the task have been analysed in a few test cases.

TABLE OF CONTENT

Document information	ii
EXECUTIVE SUMMARY	iii
TABLE OF CONTENT	iv
Introduction	ix
1. General presentation	11
1.1. PROBLEM STATEMENT	11
1.1.1. <i>Simulate the operation of the electrical system</i>	11
1.1.2. <i>Adequacy: a large-scale optimisation problem</i>	11
1.1.3. <i>Time-dependent issues: sequential approach</i>	12
1.1.4. <i>Copperplate system</i>	12
1.1.5. <i>Monte Carlo method</i>	13
1.1.6. <i>Operation of the power system facing uncertainties</i>	13
1.1.7. <i>Decomposition of the problem</i>	14
1.2. ARCHITECTURE OF THE DEVELOPED TOOL	15
1.2.1. <i>Inputs</i>	15
1.2.2. <i>Maintenance scheduling</i>	16
1.2.3. <i>Time series generation</i>	16
1.2.4. <i>Weekly allocation of the hydrological resources</i>	17
1.2.5. <i>Adequacy simulations</i>	17
1.2.6. <i>Outputs</i>	18
1.3. SENSITIVITY ANALYSES	18
1.3.1. <i>Spatial correlations</i>	19
1.3.2. <i>Modal correlations</i>	19
1.3.3. <i>Model of the flexibility of thermal units</i>	19
1.3.4. <i>Demand Response</i>	20
2. Maintenance Scheduling	21
2.1. THE DEVELOPED HEURISTIC	21
2.2. EXAMPLES: MAINTENANCE SCHEDULES OF THE IT INTEGRATION TEST.....	23
3. Modelling uncertainties	25
3.1. CHALLENGES RELATED TO THE GENERATION OF TIME SERIES	25
3.1.1. <i>The key characteristics to describe the uncertain phenomena impacting the power system</i>	26
3.1.2. <i>The use of historical data to learn the intrinsic characteristics of each time series</i>	27
3.1.1. <i>State-of-the-art on time series modelling</i>	28
3.2. DESIGN OF THE TIME SERIES GENERATOR	31
3.2.1. <i>The representation of one time series, univariate model</i>	31
3.2.2. <i>The generation of one time series</i>	35
3.2.3. <i>Modelling of spatial correlations</i>	36
3.2.4. <i>Architecture of the multivariate time series generator</i>	38
3.3. THE SPECIAL CASE OF THERMAL UNITS	39
3.4. PERFORMANCES OF THE TIME SERIES GENERATOR	40
3.4.1. <i>Reproduction of the intrinsic properties of hourly time series of demand</i>	40
3.4.2. <i>A univariate case with a monthly time step: hydro inflows</i>	43
3.4.3. <i>A multivariate case: reproduction of spatial correlations of WPG</i>	46
3.4.4. <i>An example of time series of thermal outages</i>	47
4. Allocation of hydrological resources	49
4.1. DECOMPOSITION OF THE PROBLEM	49
4.2. THE ROLLING PLANNING OF HYDRO RESOURCES	50
4.2.1. <i>Architecture</i>	50

4.2.2.	<i>Mathematical formulation</i>	52
5.	Adequacy simulations	54
5.1.	THE ADEQUACY MODEL	54
5.1.1.	<i>Thermal unit model</i>	54
5.1.2.	<i>Hydro unit model</i>	58
5.1.3.	<i>Demand response model</i>	60
5.1.4.	<i>Extra-European exchanges model</i>	63
5.1.5.	<i>National policy model</i>	64
5.1.6.	<i>Balancing between consumption and generation</i>	65
5.1.7.	<i>Minimization of the operational costs</i>	65
5.2.	IMPLEMENTATION	66
5.3.	EXAMPLE OF GENERATION SCHEDULES.....	66
6.	Sensitivity analyses	68
6.1.	THE INFLUENCE OF SPATIAL CORRELATIONS.....	68
6.1.1.	<i>Description of the test case</i>	68
6.1.2.	<i>Results</i>	70
6.1.3.	<i>Conclusions</i>	74
6.2.	THE INFLUENCE OF INTERMODAL CORRELATIONS.....	74
6.2.1.	<i>Modelling the intermodal correlations</i>	74
6.2.2.	<i>Description of the test case</i>	76
6.2.3.	<i>Results</i>	77
6.2.4.	<i>Conclusions</i>	79
6.3.	THE INFLUENCE OF THE MODEL OF THERMAL UNITS	80
6.3.1.	<i>Description of the test cases</i>	80
6.3.2.	<i>Results</i>	82
6.3.3.	<i>Conclusions</i>	86
6.4.	THE INFLUENCE OF DEMAND RESPONSE	87
6.4.1.	<i>Description of the test case</i>	87
6.4.2.	<i>Results</i>	87
6.4.3.	<i>Conclusions</i>	92
7.	Conclusions	93
8.	Annex A: Time series analyser	95
8.1.	LEARNING PROCESS OF UNIVARIATE TIME SERIES	95
8.2.	ESTIMATION OF THE CORRELATIONS BETWEEN THE INNOVATIONS	98
9.	Annex B: A few practical guidelines for the generation of time series	102
9.1.	WHERE TO FIND HISTORICAL DATA?	102
9.2.	HOW TO DEAL WITH THE LACK OF HISTORICAL DATA?.....	102
10.	Annex C: Weekly allocation problem	105
11.	Annex D: State-of-the-art of demand response models	108
11.1.	DIFFERENT DEMAND RESPONSE MECHANISMS	108
11.2.	DEMAND RESPONSE IN ADEQUACY MODELS.....	109
11.2.1.	<i>Modification of the demand time series</i>	109
11.2.2.	<i>Adjustment of the demand in the adequacy problem</i>	110
11.2.3.	<i>Maximisation of the social welfare</i>	111
11.2.4.	<i>Other approaches</i>	113
12.	References	115

List of figures

Figure 1. Enhanced Pan European Transmission Planning Methodology of WP 8	x
Figure 2. Decomposition of the 1-year problem into weekly sub-problems	14
Figure 3. Architecture of the adequacy simulator	15
Figure 4. Flowchart of the maintenance scheduling heuristic	22
Figure 5. Expected daily residual load and thermal capacity in maintenance in Spain (above) and France (bellow), based on the assumptions of the IT integration test	24
Figure 6. Interaction between TS analyser and TS generator	28
Figure 7. Seasonality of the load of France over 1 year (dimensionless).....	32
Figure 8. Characteristics of the stochastic component of load connected to the network of Amprion, learnt from 8 years of historical data	33
Figure 9. Characteristics of the stochastic component of wind power generation of France, learnt from 7 years of historical data	33
Figure 10. Decomposition of a time series of PV generation into a trend, a seasonality and a stochastic component. The trend has been exaggerated on purpose for the sake of understanding its role.....	35
Figure 11. Generation of one independent time series	36
Figure 12. Historical data of PV generation in two zones of France, with their associated trend and seasonality.....	37
Figure 13. Generation of correlated time series	38
Figure 14. Generation of the time series of thermal availability	40
Figure 15. One week of any generated MC year (blue) and expected seasonality (black) of French load.....	41
Figure 16. Probability Density Functions of the historical and newly generated time series of the French consumption.....	41
Figure 17. Monthly averages of the historical and newly generated time series of the French consumption	42
Figure 18. ACFs of the stochastic component of the historical and newly generated time series of consumption.....	43
Figure 19. Four consecutive historical years and four generated Monte-Carlo years of hydro inflows.....	44
Figure 20. pdf (left) and cdf (right) of historical and new time series of inflows.....	45
Figure 21. Monthly values of the historical and newly generated time series of inflows	45
Figure 22. Correlated time series of wind power generation in two zones of France (correlation of 78.7% between their stochastic components)	47
Figure 23. Thermal unavailability (maintenance + forced outages) of one MC year from the integration test of WP8, including France and Spain	48
Figure 24. Rolling planning of the hydro resources. The solid green line on the timeline represents a perfect knowledge of the uncertainties (inflows, intermittent RES, consumption) while the dotted grey line depicts the imperfect forecast of the inflows and the expected seasonality of the other uncertainties.....	51

Figure 25. Possible hourly dispatch vs. weekly average.....	52
Figure 26. Generation schedule over one week	67
Figure 27. Seven zones of the modelled French power system.....	69
Figure 28. Spatial correlations of load (a), wind power generation (b) and PV generation (c) between seven zones in France. The correlations have been calculated from historical data, after removing their trend and their seasonality (see Equation (4.1)). Correlations between zones which are not linked by an arrow are below 30%.	70
Figure 29. Probability density function (pdf) of the residual load of the scenario “Nouveau Mix”, with and without modelling the spatial correlations	72
Figure 30. Changes in the average injections when spatial correlations are neglected	72
Figure 31. Distribution of the injections of the West zone, with and without spatial correlations.....	73
Figure 32. Distribution of the injections of zone “Rhône Alpes Auvergne”, with and without spatial correlations.	73
Figure 33. Dependence between calculated time series of load, wind power generation and PV generation, modelled via the thermo-sensitivity of each time series.	75
Figure 34. Thermo-sensitivity of the load, wind power and PV generation (average of the thermo-sensitivities of the seven zones of the French power system).....	76
Figure 35. Unsupplied energy, with and without modelling the intermodal correlations.	78
Figure 36. Probability density function (pdf) of the residual load of the scenario “Nouveau Mix”, with and without modelling the intermodal correlations.....	78
Figure 37. Distribution of the injections of zone “Rhône Alpes Auvergne”, with and without intermodal correlations.	79
Figure 38. Energy mixes of scenarios low RES, intermediate and high RES.....	81
Figure 39. Distribution of the exchanges between France and Spain in the scenario "high RES" and for several thermal generators models	84
Figure 40. Generation schedule of the week with the most unsupplied energy of the scenario “High RES”, obtained with the complete model of thermal units.....	85
Figure 41. Generation schedule over one week of any MC year, with a fixed consumption (upper graph) and with 8% of the consumption which is controllable (lower graph).	89
Figure 42. Cost savings associated to demand response (the indirect savings due to the reduction of the spilled energy is indexed on the cost of nuclear generation).	90
Figure 43. Re-dispatching of thermal generators when 8% of the load is controllable via DR.....	91
Figure 44. Empirical computation of the correlation coefficient r_{ϵ}	99
Figure 45. Seasonality of wind power generation in the east and west of France (dimensionless).....	103
Figure 46. PDF and ACF of the stochastic component of the wind power generation in the east and west of France.....	103
Figure 47. Correlation between two areas as a function of their distance apart [14].....	104

Figure 48. Price taking and price responsive demands. The amount of power which will be generated corresponds to the intersection between the demand curve and the supply curve. It covers the demand which has a marginal value higher than the marginal supply price [54]111

List of tables

Table I. Average yearly sum of historical and generated time series41

Table II. Average durations of peak and off-peak for historical and generated time series.....42

Table III. Average and standard deviation of the yearly sum of historical and generated time series.....44

Table IV. Average duration of peak and off-peak for historical and generated time series45

Table V. Historical correlations between the stochastic components of WPG in France (%).....46

Table VI. Correlations between the stochastic components of the newly generated time series (%)46

Table VII. Installed capacities and load in the scenario Nouveau Mix at the horizon 203069

Table VIII. Reliability indicators for the scenario “Nouveau Mix”, with and without modelling the spatial correlations71

Table IX. Reliability indicators for the scenario “Nouveau Mix”, with and without modelling the intermodal correlations77

Table X. Installed capacities and yearly demand for the three scenarios.....80

Table XI. Standard characteristics of each type of thermal generation.....81

Table XII. Impact of the model of the thermal units on the results of adequacy simulations for the scenarios “low RES”, “intermediate” and “high RES”82

Table XIII. Generation of France of Spain during hour 67 and available capacity of each source of energy...86

Table XIV. Adequacy of both countries during hour 6786

Table XV. Impact of demand response on the results of adequacy simulations88

Table XVI. Impact of DR on the computational time.....91

Table XVII. Spatial Correlations of the stochastic components and innovations of historical and newly generated data98

Table XVIII. Estimated values of $r\epsilon$ 100

Introduction

Computation of demand and generation time series for the transmission expansion planning methodology

The Transmission Expansion Planning (TEP) methodology developed in the Work Package 8 (WP8) of e-Highway2050 project aims at building the optimal network expansion plan over the period 2020 to 2050. The TEP covers different hypothetical long-term visions, called “scenarios”, which depict possible evolutions of the generation mixes, demand and European energy policies.

Each of the considered time horizon and scenario is described by a set of “macro-assumptions” which is used as an input of the overall methodology. These macro-assumptions are broken down by country. They include the assumed installed capacity of different generation sources, the expected overall demand, the possible exchanges with external countries and the integration of demand response (see D1.2 “Structuring of uncertainties, options and boundary conditions for the implementation of EHS”).

The macro-assumptions inform about the general evolutions of the energy sector, but they do not contain the detailed mapped and operational information required by network studies. In order to have an idea of the grid capacities needed to ensure adequacy between consumption and generation, data must indeed be developed:

- under operational conditions, i.e. with actual output power of the generating units and real-time consumptions (and not total yearly consumptions),
- and for different possible situations, i.e. different moments of the year and under diverse random events.

For instance, the generation time series of each Combined Cycle Gas Turbine (CCGT) unit in Italy should be derived from the total installed capacity of CCGT in Italy, which corresponds to the macro-assumption of the given time horizon and scenario.

This part of the TEP methodology is ensured by Task 8.2, *Computation of Demand and Generation Time Series*, which simulates the operation of the electrical system in a copperplate model (without grid constraints) and develops the overall assumptions (installed capacity and yearly consumption) into balanced time series of consumption and generation. Similar simulations are also performed in WP2 through the use of ANTARES [32], a sequential Monte-Carlo system simulator developed by RTE (see D2.1 “Data sets of scenarios for 2050”). However, some modelling aspects are further studied in this deliverable.

The connexion of Task 8.2 with the other tasks of the *Enhanced Transmission Planning Methodology* of WP 8 is illustrated in Figure 1, where Task 8.2 is described as “STEP 1 – Adequacy without grid”. A copperplate approach has been retained for the first step of the methodology as its goal is to determine the optimal injections, i.e. the ones that the grid should ideally ensure. They are reference injections which are used in the following steps of the TEP and serve as a base to design the future grid expansions.

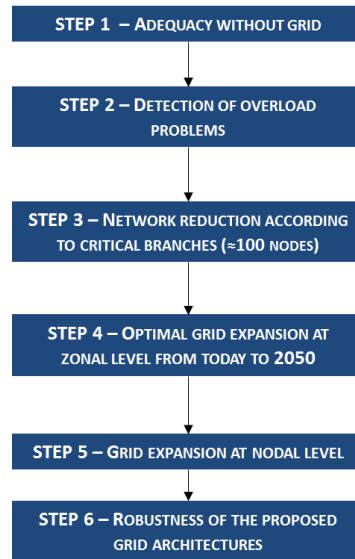


Figure 1. Enhanced Pan European Transmission Planning Methodology of WP 8

Objectives of this document

This document is the final deliverable of Task 8.2: *Computation of Demand and Generation Time Series*. It:

- describes the method which has been developed and prototyped in the framework of this work package,
- discusses the modelling choices which have been made in the context of this long-term pan-European study and under the light of the state-of-the-art and sensitivity analyses,
- presents a literature review with alternatives to the retained method,
- and illustrates the methodology through test-cases and examples.

A general presentation of the issues of the task and the developed methodology is presented in Section 1. Sections 2 to 5 explain in more details its four main components: scheduling of the maintenance of thermal units, generation of time series of the uncertain phenomena, weekly allocation of hydro resources and hourly simulations of the power system. The sensitivity of the methodology to some inputs is analysed in Section 6, through test cases. Finally, conclusions are presented in Section 7.

1. General presentation

1.1. Problem statement

This section presents some general issues of adequacy simulations and how they were addressed within the Work Package 8 of the e-Highway2050 project. Similar simulations were also performed in WP2 through the use of ANTARES (see D2.1 “Data sets of scenarios for 2050”). The model of this tool has been reviewed in the state of the art [32].

1.1.1. Simulate the operation of the electrical system

The role of Task 8.2 is to compute the power injections in each country of the system and for the different types of consumption and generation. Indeed, national policies and trends are considered to derive assumptions on generation (such as installed capacities) and consumption at the country level. Then, these power injections are distributed on each node of the reduced network using distribution keys (see D2.1 “Data sets of scenarios for 2050”).

For that purpose, the operation of the electrical system is simulated: given the available generation means and the consumption profiles of each country, the optimal (less-costly) dispatch of the generating units which meets the consumption is calculated. Storage, demand response, exchanges with neighbouring systems and other controllable elements of the system which participate in the balancing of consumption and generation can be simulated as well.

Such simulations are usually called “adequacy simulations”.

They answer – for instance – this type of questions: Which power plants will actually be operated and with which load factor? Is there any energy not served in the system? Does a part of the load or the renewable generation has to be curtailed to guarantee the adequacy of the system? For how long?

1.1.2. Adequacy: a large-scale optimisation problem

Adequacy simulations play an essential role in the long-term study of the electrical system.

Concretely, an adequacy simulator performs a balancing of the electrical market and computes the optimal generation dispatch which meets the consumption. Under the assumption of a perfect competition, it can be modelled as an optimization problem whose objective is to minimize the total expenditures of the system operators, while constraints describe the limitations in operating diverse elements of the power system, such as thermal power plants, hydro units, external exchanges, storage and demand response.

The most obvious constraint of such optimisation problem is the power adequacy, which ensures the equality between the overall generation and consumption of the system for each time step of the studied horizon. The other constraints of the problem are related to the technical limits of thermal units (e.g. minimum and maximum power, unit commitment, minimum up and down times), to the behaviour of hydro units (e.g. maximum power, description of the volume in hydro reservoirs, bounds of the reservoir) or to the description of the other controllable elements of the system (e.g. external exchanges, demand response, storage, curtailment).

With the recent restructuring of the power sector, some modelling trends also tend to integrate the competitive behaviour of market players, for example through the use of equilibrium models or game

theory. These approaches enable to describe the market mechanisms in an oligopoly [1] and therefore require a more in-depth knowledge of the market players and shares. They are typically used in market power analysis and market design studies. Within the 30 years' uncertain time frame of the e-Highway2050 project, we however do not aim at identifying the structure of the market and its actors. The competitive modelling seems unfitted in our case and we therefore assume the perfect competition at a European scale and keep a classic modelling approach where the expenditures of all the producers are gathered in one objective function.

1.1.3. Time-dependent issues: sequential approach

Adequacy modelling can be broadly divided into two categories of methods: sequential and non-sequential.

In the sequential approach, the simulation process evolves chronologically, considering that the system state at a given time depends on the states in the previous time steps. On the contrary, non-sequential approaches do not consider the chronology of the operations and assume that the system behaviour at a given time is independent from the system states in all the other time steps.

Non-sequential methods are naturally computationally faster. However, elements such as hydro, storage and demand response are defined with time-dependent constraints and cannot be properly modelled without a sequential approach. Moreover, the flexibility of the system – i.e. the ability of controllable units to adapt to the intermittencies of uncontrollable generation and load – is an important issue in a system with a high penetration of Renewable Energy Sources (RES), which is hardly assessed in a non-sequential approach. A sequential approach is therefore retained in this work package, with a classic hourly time step.

Although this method is computationally slower, it offers the advantages of:

- catching the high-variability and diurnal patterns of the RES¹ and the load,
- modelling the meteorological phenomena which can persist over time (e.g. cold spell of several days, dry year with low inflows) and
- taking into consideration time-dependent technological issues (e.g. limited flexibility of thermal units, management of the hydro reservoir and storage units, demand response with a maximum delay time).

A study period of 1 year is chosen in order to scope all the issues related to the seasonality of the load, hydrological inflows and RES.

1.1.4. Copperplate system

In this first step of the Transmission Expansion Planning (TEP) of WP8, the grid is not yet taken into account and the adequacy is solved in a “copperplate” model, i.e. with infinite transmission capacities [2].

Thus, the exchanges between areas are not bounded by the existing grid. The power injections calculated in this approach are the ones that the network should ideally guarantee. They will be used in the following tasks of the TEP in order to calibrate the network expansion.

¹ Considering the actual energy policies, we can assume that the RES will play an important role in most of the scenarios of 2050.

However, in order to avoid overoptimistic exchanges that would be unfeasible if the grid was taken into account, a constraint has been added in order to limit the total weekly imports of each country. This constraint can be used to describe the level of integration of the wholesale European electricity market, or the national policy of the European countries.

1.1.5. Monte Carlo method

Some inputs of the adequacy simulator are subject to a high degree of uncertainty, especially RES generation (wind and solar generation), load, hydro inflows and outages of the generating units – they will be referred to as “stochastic inputs”. These stochastic inputs are impacting the power system operation and its balancing: a system able to supply the demand under common conditions could indeed be insufficient when facing more unusual situations (drought, cold spell, loss of a thermal unit, critical combination of intermittent RES generation, etc.).

Two types of methods are usually considered to deal with probabilistic problems: analytical methods or Monte Carlo methods [3]. The first ones are computationally quick but require a simple description of the stochasticity and unavoidable approximations, while the second ones, although more time-consuming, are more flexible and can deal with complex stochastic inputs and a detailed modelling of the elements of the system.

In our case, two main aspects make the use of an analytical method difficult (if not impossible): firstly the high number of correlated stochastic inputs, each one with different statistical characteristics, and secondly the necessity of using a sequential approach with time-dependent constraints. A Monte Carlo method is more adapted to deal with that kind of complexities and a Monte Carlo algorithm will therefore be used to tackle the stochasticity of our problem.

The Monte Carlo procedure is an iterative method. For each of its iterations – called “MC-year”: i) a set of stochastic inputs is randomly sampled and ii) a deterministic adequacy simulation is performed on this set. On a final step, the results of all the simulations are aggregated and the probabilistic properties of these results are deduced.

The first part of the Monte Carlo iteration – the generation of new time series of the stochastic inputs – is a complex mathematical problem which is also addressed in this document. Its goal is twofold. Firstly, it converts a gross value (e.g. installed capacity of RES) into hourly and sequential figures which will be used to describe the real-time functioning of the electrical network. Secondly, it allows generating numerous random situations that the power system could face.

1.1.6. Operation of the power system facing uncertainties

Moreover, the management of the system is in practice affected by the uncertainties of some variables – for instance, most of the decisions are taken in advance, with forecasted values of the load, RES generation and inflows, and not with the real values of these inputs. It induces some sub-optimality in the operation of the system which will be later considered by differentiating the *real values* of the stochastic inputs, which are the values effectively sampled in one MC-year, from the *expected seasonality* of the stochastic inputs, which describes their general trend and seasonality. Typically, the expected value of a stochastic input is its seasonal average that has been observed in historical data.

1.1.7. Decomposition of the problem

The modelling of the elements of the system calls for different timescales:

- Some elements need to be managed on the *1-year basis*. This is the case of the scheduling of maintenance of thermal units, the management of the reservoir of hydro units, and equivalently the management of the energy stored in storage units. The whole scope of the problem's seasonality needs to be considered in order to handle efficiently those elements. For instance, the hydro reservoirs make the link between the seasonality of the inflows and the seasonality of the residual load, calculated as the demand minus the injection of non-dispatchable renewables.
- Moreover, most of the elements of the electrical network only require *shorter time considerations* (from one hour to a few hours). This is the case of the balancing of load, the operation of thermal units, the demand response mechanism, etc. The resulting constraints can be time-independent (e.g. bounding of the output power of a unit between its technical limits) or time-dependent with short time constants of only of few hours (e.g. minimum on-line and off-line durations of the power plants). We assume that the modelling of these elements on a period of 1 week can be made in exchange for minor approximations².

Due to these two levels of timescale, it has been decided to decompose the 1-year problem into weekly sub-problems, as illustrated in Figure 2.

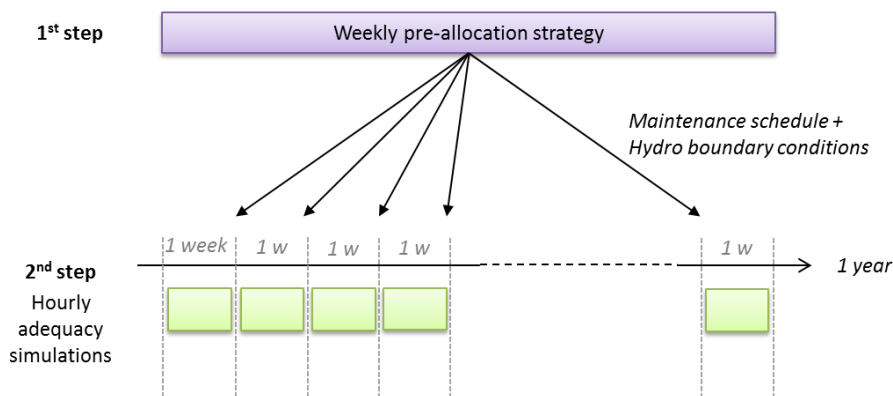


Figure 2. Decomposition of the 1-year problem into weekly sub-problems

In a first step, the yearly issues are dealt with, namely the scheduling of the maintenance of thermal units and the management of the reservoir of hydro units. The first step allocates the thermal maintenance for each hour of the year and sets volume targets to be reached at the end of each week for each reservoir.

In a second step, 52 hourly adequacy simulations are performed, one for each week of the year. The simulations are carried out with the reservoir boundary conditions defined in the first step and by forcing to zero the generation of the thermal units in maintenance. Instead of having one big problem of 8760 time steps, we therefore have to solve 52 smaller problems of 168 time steps.

This approach has two major advantages particularly appreciable in our context. Firstly, it implies a reduction of the computation time of the adequacy simulations – 52 problems of size n are quicker to solve than 1 problem of size $52n$ – and it decreases significantly the running time of the whole Monte Carlo

² The constraints which overlap two weeks indeed need to be handled with a sub-optimal method.

procedure. Secondly, it allows to approach the real operation of the system, which implies sub-optimal decision makings due to the imperfect forecast of the evolution of the uncertain phenomena.

The idea to divide the hydro-thermal scheduling in a multi-step mechanism with different timescales has already been exploited in [36]-[37]-[38]. For example, [36] decomposes the hydro allocation problem into a Long-Term Hydro Scheduling (LTHS) with a monthly time step and a Short-Term Hydro Scheduling (STHS) with an hourly time step.

1.2. Architecture of the developed tool

The global architecture of the developed tool is presented in Figure 3. The role of each block is briefly explained in this paragraph and is later detailed in the following sections of the document.

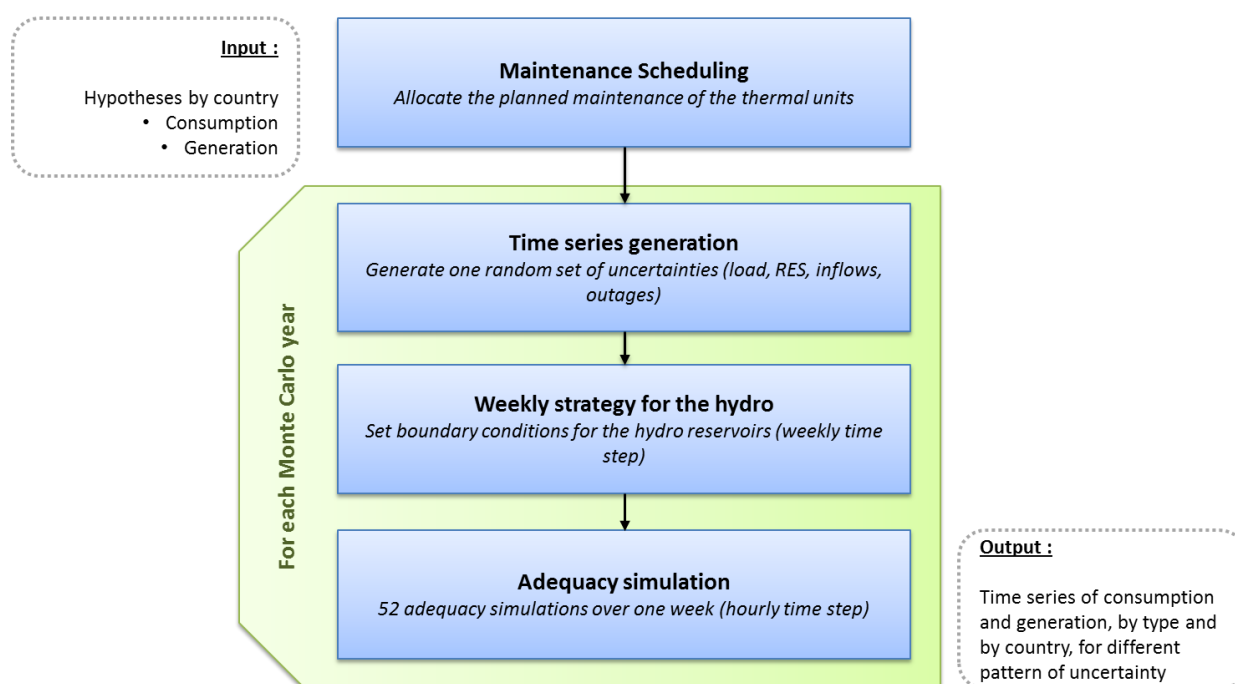


Figure 3. Architecture of the adequacy simulator

As explained in Section 1.1.5, a Monte Carlo approach has been retained to take into account the stochasticity of the problem and to study the response of the power system to diverse possible events. Consequently, the three last blocks of Figure 3 are repeated numerous times. The *high-level description of the methodology* of WP8 suggested running 2000 MC-years for each scenario and time horizon. This number may however be revised, depending on the data volumes and computation times implied by the algorithms.

1.2.1. Inputs

Each scenario and time-horizon is studied independently. For a given scenario and time-horizon (e.g. reference scenario in 2050), the required inputs are:

- The list of generating units with their nominal capacity, classified according to their generation source (e.g. nuclear, coal, lignite, gas, fuel, onshore wind, offshore wind, solar, biomass, hydro with reservoir, run of the river (RoR), pumped-storage hydro (PSP) etc.).
- A detailed description of the different thermal generation types, with their associated costs (linear, no-load cost³ and start-up cost), their technical limits (minimum up and down times⁴ and minimum stable operating power), their maintenance needs (yearly duration and minimal period) and their outage risks (outage rate and duration).
- A detailed description of the hydro resources of each country, with the expected yearly producible energy of the different hydro types (hydro with reservoir, PSP, RoR) and the overall size of the reservoirs for the hydro with reservoir and PSP.
- The list of the possible extra European exchanges, imports and exports, given as transfer capacities and associated costs.
- The yearly expected consumption of each country.
- The list of the deployed demand response initiatives, with their participation rate, associated delay time and costs.
- The list of the national energy policies, i.e. the objectives in term of self-generation for each European country.

1.2.2. Maintenance scheduling

Maintenance scheduling refers to the planned stops of thermal units, like the ones made to refuel the units or to perform preventive maintenance operations.

In this first step, the maintenance calendar is planned in adequacy with the needs of the power system. The method used to generate the maintenance schedule is a simple heuristic algorithm whose goal is to plan the stops of the units so as to affect security of supply as little as possible.

The maintenance program is designed in advance and is therefore based on the *expected seasonality* of the stochastic inputs, on an inaccurate forecast, and not on the final exact realization of those inputs. The maintenance schedule is therefore the same for all the MC-years and can be computed just once in the Monte Carlo procedure.

The proposed maintenance scheduling process is general, not specialized for a specific case. It can adapt to the whole scope of generation scenarios of the e-Highway2050 approach.

The maintenance scheduling algorithm is described in Section 2.

1.2.3. Time series generation

The second step of the whole approach consists in generating a Monte Carlo sample, i.e. a set of time series which describes the yearly evolution of the stochastic inputs affecting the power system.

³ The no-load cost is a constant cost representing the cost of fuel required to operate the generating unit at zero net output (i.e. to keep the unit running).

⁴ Once a unit is running, it may not be shut-down immediately but has to run a certain amount of time, which corresponds to the minimum up time. On the contrary, once a unit is shut down, it may not be started immediately (minimum down time).

The outages of the power plants are one of the stochastic inputs of the problem. Binary time series are generated. They describe the availability, hour per hour, of each thermal unit of the system. These time series are sampled in accordance with the outage rate and duration of the different thermal generation types.

The other stochastic inputs are: the load, the onshore wind power generation (WPG), the offshore WPG, the photovoltaic (PV) generation and the hydro inflows. They are generated by a module called Time Series (TS) generator which aims at replicating the intrinsic characteristics of the considered phenomena, notably their seasonality, autocorrelation and probability density function. The newly generated time series are moreover calibrated on a new trend, which represents the hypothetical vision of the considered long-term scenario (e.g. the installed capacity of PV in 2050).

The inter-dependencies between time series are also handled by the TS generator. Two types of dependencies have been investigated: intermodal correlations, which are the correlation between two phenomena (e.g. load and PV) in a same place, and spatial correlations, which are the correlations between two time series of a same phenomenon taken in two different places (e.g. WPG in Belgium and Denmark).

Significant amount of efforts were dedicated to the development of the TS generator. It is presented in more details in Section 3.

1.2.4. Weekly allocation of the hydrological resources

The goal of this next step is to allocate the yearly hydro resources among the 52 weeks of the year. It determines volume targets to be reached at the end of each week, for all the reservoirs of the system. These volume targets are the boundary conditions which will allow us to decompose the yearly adequacy problem into 52 weekly sub-problems.

This step consists in a rough adequacy problem with a weekly time step. One representative hour, with average values of generation and consumption, is used to represent each week. Hydro and thermal resources are scheduled so as to minimize the expected generation costs. The hydro resources are dispatched in accordance with the available inflows and the capacity of the reservoirs. A simplified model is used to describe the behaviour of the thermal units and extra-European exchanges. The decrease of the thermal capacity due to the planned maintenance is taken into account.

As it is unrealistic to consider a full knowledge of the stochastic inputs on a 1-year timeframe, the allocation of the hydro energy is made through an iterative method with a 1-week foresight rolling planning. The hydro schedule is recomputed each week with the *real value* of the stochastic inputs of the week to come and by assuming an imperfect forecast of the stochastic inputs of the following weeks.

The hydro allocation method is presented in Section 4.

1.2.5. Adequacy simulations

Finally, detailed adequacy simulations, with an hourly time step and a finer modelling of the elements of the system are performed.

52 simulations of 168 time steps are run iteratively. The commitment of the thermal units which are out-of-order or in maintenance is forced to zero. The volume targets obtained in the previous step are used as boundary conditions of the hydro reservoirs at the beginning and end of each week.

Simulations are run with a perfect foresight: the *expected seasonality* of the stochastic inputs is put aside and only the *real values* are considered. It seems indeed reasonable to assume an accurate forecast of the load and the RES generation on such a short time horizon (in practice, the deviation from the forecast are corrected by the intra-day market, the sub-optimality due to this adjustment process will be considered insignificant in our context). This perfect foresight allows us to focus only on the technical modelling of the system and to forget the probabilistic behaviour of its operations.

Different models of thermal generating units, with varying degrees of details, have been investigated in this project in the view of selecting a homogeneous final model with a good trade-off between accuracy and complexity.

The adequacy model includes a detailed representation of the thermal units, with unit commitment, minimum stable power and minimum on-line and off-line durations. The generation costs include three components, a linear cost (proportional to the output power of the unit), a constant cost (which takes effect only when the unit is online) and a start-up cost. A linear model is used for hydro and storage. Hydro resources are considered free, but they are limited by the bounds on the reservoirs determined in the previous step. Load can be controlled via Demand Response (DR) programs, which allow to shift a part of the load within a given delay time. Extra-European exchanges are possible and are bounded by the transmission capacities with the neighbouring countries of Europe. However, we have not considered maximal yearly imports or exports bounds, but weekly constraints on imports (see section 6.1.4). Import and export costs are assumed linear. Finally, the total imports of each European country can be bounded in accordance with its energy policy.

The adequacy problem is therefore a large Mixed-Integer Linear Program (MILP). For the case tested in the task, the problem has been solved with FicoXpress [62] on a server dedicated to WP 8.

The model is presented in more details in Section 5.

1.2.6. Outputs

For each scenario, each time-horizon and each MC year, the tool returns:

- Hourly time series of uncontrollable RES and load for each country. Uncontrollable RES are: wind power generation (onshore and offshore), solar generation and hydro run of the river generation.
- Hourly time series of generation and availability of each thermal unit.
- Hourly time series of generation and water value for each controllable hydro unit (hydro with reservoir and PSP)
- Hourly time series of exchanges, imports and exports, with the extra-European countries.
- Hourly time series of system cost.

1.3. Sensitivity analyses

Most of the complexity presented in this deliverable has also been tackled in WP2 through the use of ANTARES (see D2.1 “Data sets of scenarios for 2050”). However, further studies on some modelling aspects have been performed in task 8.2. The role of some innovative elements of the adequacy model has been analysed in a few test-cases, notably:

- The spatial correlations
- The intermodal correlations

- The modelling of the flexibility of thermal units (minimum up/down times, minimum stable power, start-up costs)
- The demand response

The impact they have on the results of adequacy simulations has been assessed.

This part presents the main conclusions which have been learnt from these sensitivity analyses. The complete results are presented in Section 6.

1.3.1. Spatial correlations

One hundred Monte Carlo years have been simulated on a French test case, with and without modelling spatial correlations. It has been shown that spatial correlations can have a significant impact on the results of adequacy simulations, and that neglecting them can:

- Induce an over-estimation of the reliability of the system,
- Significantly change the injections of several zones and gauge incorrectly the network needs.

The consideration of this type of correlations in the transmission expansion planning tools is recommended.

1.3.2. Modal correlations

One hundred Monte Carlo years have been simulated on a French test case, with and without modelling intermodal correlations. It has been shown that these types of interdependencies do not directly influence the network expansion needs. It has therefore been assessed that their modelling in a transmission expansion planning methodology is not essential.

However, it has also been noticed that these correlations can have an impact on some reliability indicators of the power system. They can therefore be worth thinking about in some other applications.

1.3.3. Model of the flexibility of thermal units

A complete unit commitment model which includes minimum up/down times constraints, minimum stable power constraints and start-up costs have been confronted to simpler models. The influence of the model of thermal units has been evaluated for different scenarios, integrating more or less uncontrollable renewable sources in their energy mixes.

In the scenarios with a large integration of RES, energy in excess is severely underestimated when the thermal unit model is simplified. However, the impact of the flexibility of the thermal unit on load curtailments, operational cost and cross-border exchanges has proved to be low in the analysed test cases. Consequent time savings (up to 75%) were made by simplifying the modelling of the flexibility of thermal units.

It has to be noticed that the assumptions made in the framework of Task 8.2 (notably the copperplate approach) do not necessarily enable to tackle all the issues related to the flexibility of the thermal park.

1.3.4. Demand Response

One hundred Monte Carlo years have been simulated on the French-Spanish system, with different participation rates of demand response. It has been shown that DR can have a significant impact on the results of adequacy simulations, even if its participation rate is low. Reduction of curtailed load, re-dispatching of thermal units and avoidance of spilled energy are the three main advantages of DR.

Moreover, DR does not increase the solving time of the adequacy simulator. On the contrary, it even slightly speeds the resolution of the MILP problem. We therefore recommend integrating the modelling of DR in the adequacy simulations, even if its deployment is at an early stage and its participation rate is low.

2. Maintenance Scheduling

Maintenance scheduling refers to the planned stops of thermal units, like the ones made for refuelling or to perform preventive maintenance operations. This type of stops can be scheduled in advance, and a maintenance calendar should therefore be planned in adequacy with the needs of the power system.

The state-of-the-art on maintenance scheduling is wide, with models based on a pure reliability criterion [4], with a multi-criteria optimization considering both economic and reliability issues [5], with a detailed modelling of the units of one company in a liberalized market [6]-[7], or even with multi-generation company problems and iterative processes with regulator interventions [8]. For our 2050 pan-European context, it is however unrealistic to consider a multi-agent model. The main goal here is to take into account the reduction of thermal availability due to maintenance operations. We will not try to mimic the real planning process or to put a cost on it.

A routine has been developed in the frame of the project in order to build coherent maintenance schedules. Its goal is to schedule the maintenance so as to affect security of supply as little as possible, by adapting it to the generation mix and the consumption of the considered country and scenario, and especially to the expected seasonality of uncontrollable generation and load. Maintenance scheduling was also tackled in WP2, but with a different heuristic (see D2.1 “Data sets of scenarios for 2050”).

The routine is described in Section 2.1. Examples of maintenance schedules are presented in Section 2.2.

2.1. The developed heuristic

The method used to generate the maintenance schedule is a simple heuristic whose goal is to program the stops of the units when it is the least troublesome. We assume it to be when the *expected* residual load – equal to the load minus the non-controllable generation – is low. The maintenance schedule is built with a daily time step.

For all thermal groups, the maintenance needs are described through two parameters:

- n_g^{maint} : number of required periods of maintenance, per year, for the thermal unit g .
- $d_{g,i}$: required duration of each period of maintenance, for all thermal units g and periods i .

Note that these parameters can be easily built on other pairs of inputs, such as the total number of days of maintenance required per year and the minimum duration of one period of maintenance.

The maintenance programs are built independently in each country, based on its own needs. In other words, no harmonization of the maintenance operations is performed at a European scale, the maintenance is scheduled on a national basis. As we do not have yet – in this step of the TEP – any knowledge of the future grid expansions, we indeed think it is more reasonable to keep a conservative approach and program the maintenance according to the local needs.

For each country, the developed heuristic considers iteratively the thermal units by decreasing order of nominal capacity. For each thermal unit, it plans the maintenance in the period where the expected residual load is the lowest and then virtually increases the residual load by the thermal unit capacity in order to represent the reduction of thermal availability. A condition is added in order to avoid the concentration of too much maintenance at a same moment, forbidding the addition of maintenance operation if a given percentage of the thermal capacity of a country is already unavailable.

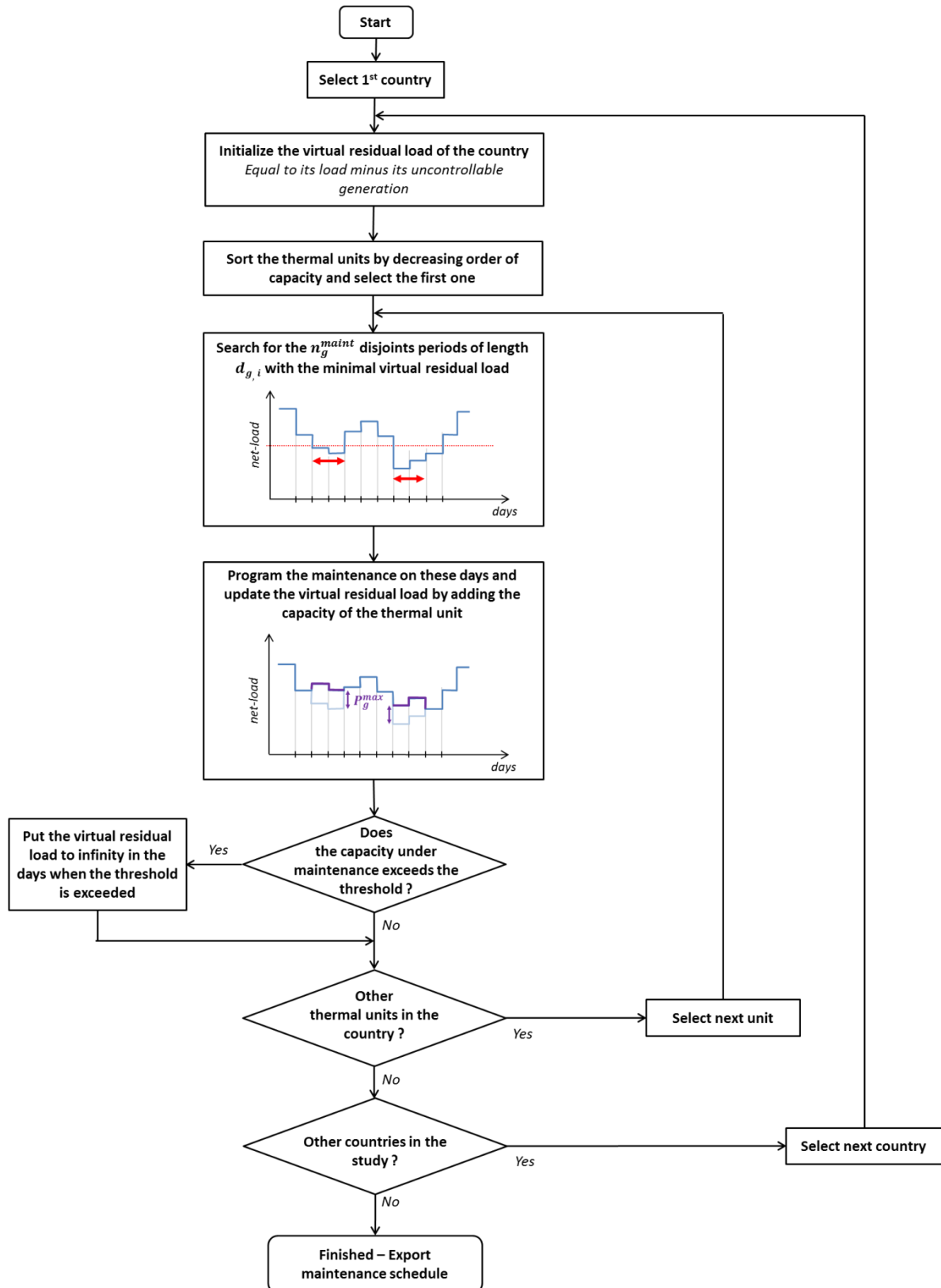


Figure 4. Flowchart of the maintenance scheduling heuristic

The flowchart of the algorithm is presented in Figure 4. The graphs are given for 2 periods of 2 days of maintenance. P_g^{max} is the unit capacity.

For each country, the thermal units are sorted by decreasing order of capacity. Thermal generators are then processed one by one. The units with the highest capacity – and whose maintenance can be more problematic – are therefore considered first.

The “virtual residual load” of each country is initialized. It is equal to the difference between the *expected* consumption of the country and its *expected* uncontrollable generation (PV generation, WPG and RoR). For each thermal unit g of the country, the algorithm programs the $n_{g,i}^{maint}$ periods of maintenance of duration $d_{g,i}$ when the virtual residual load is minimal, i.e. when the need for power is the lowest.

During the days when the unit is under maintenance, the total generation capacity is decreased of P_g^{max} , and so is the amount of load which can be supplied. We modelled this by summing the missing generation capacity P_g^{max} to the virtual net load.

The units are similarly processed one by one by decreasing order of capacity. After dealing with each unit, the algorithm checks, for each day of the year, if the total capacity under maintenance of the country exceeds a given threshold. The threshold is typically equal to a percentage of the total thermal capacity of the country. For the days when the threshold is exceeded, the virtual residual load of the country is set to infinity. During the following iterations of the algorithm those days will therefore not be selected as suitable for maintenance as they cannot minimize the virtual residual load anymore. This condition permits to avoid the concentration of too much maintenance operations at a same time.

Note that the maintenance scheduling method requires only the *expected seasonality* of the stochastic inputs (load, uncontrollable generation). In practice, the maintenance plan is indeed designed in advance and is therefore based on the expected evolution of the data, on an inaccurate forecast, and not on the final exact realization of those data. This means that the maintenance schedule is the same for all the MC-years and can be computed just once for each scenario and time horizon.

The scheduling of maintenance *a posteriori*, knowing the real values of the stochastic parameters, would have been unrealistic and could have led to excessively optimistic results.

The maintenance scheduling algorithm has been implemented in Matlab.

2.2. Examples: maintenance schedules of the IT integration test

One of the objectives of the developed routine is to build the maintenance schedule in adequacy with the consumption and generation mix of the country. To illustrate this fact, the maintenance schedules of the two countries of the IT integration test of WP 8, France and Spain, are analysed in this section.

This case has been built in order to test the integration of the tasks of WP 8 and to specify the interfaces and data formats. The starting year of the IT integration test has been used. It reproduces the 2012 installed capacities of France and Spain.

The *expected* daily residual load of both countries is plotted in blue in Figure 5. The installed capacity of uncontrollable RES of the two countries is similar to the one of 2012. The seasonality of the residual load is mainly explained by the seasonality of the consumption. The yearly cycles are quite different for the two countries: the one of France is more pronounced, with a load significantly higher during the winter than in the summer, while the one of Spain is flatter, with peaks both in winter and summer. Both residual loads are strongly affected by the weekly seasonality of the consumption habits.

Note than more information on the construction of the *expected seasonality* of the load and uncontrollable RES are given later in Section 3.

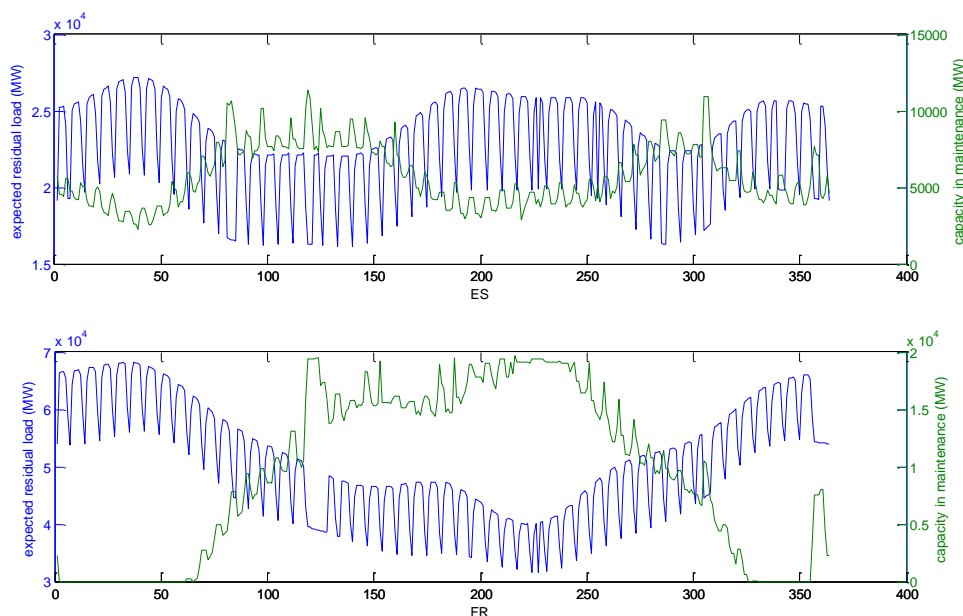


Figure 5. Expected daily residual load and thermal capacity in maintenance in Spain (above) and France (below), based on the assumptions of the IT integration test

In this example, Spain has 155 thermal units, for a total of 58.6 GW, while France possesses 132 thermal units for a total capacity of 94.9 GW. All thermal units require 36 days of maintenance per year. The number of periods of maintenance and their durations vary from one source of generation to another.

Maintenance schedules have been computed with the routine presented above. The total capacity in maintenance has been plotted in green, day by day, on the graphs of Figure 5. Residual load and capacity in maintenance have opposite variations: the capacity in maintenance is logically higher when the residual load is low. On the contrary, less maintenance operations are planned when the residual load is high, as the needs for available generation capacity are more important.

The comparison of the maintenance schedules of both countries confirms the ability of the routine to adapt the maintenance to the specificities of the local residual load. Equivalently, the routine is able to plan the maintenance in accordance with the hypothesis of each scenario and time horizon.

In the test case (Spain and France), the unavailable capacity due to maintenance reaches in some days more than 25 GW, that is to say 30% of the average consumption. This order of magnitude is such that neglecting the maintenance of the thermal units would lead to over-optimistic adequacy assessments. Considering the loss of generation capacity due to maintenance is therefore crucial.

3. Modelling uncertainties

The power system is subject to a large amount of uncertainties, such as the unplanned outages of thermal units, the uncontrollable generation of some renewable energy sources (RES), the electrical consumption and the hydrological inflows. These uncertainties are impacting the power system operation and its reliability: a network able to supply the demand under common conditions could indeed be insufficient when facing more unusual situations (drought, cold spell, loss of a thermal unit, critical combination of intermittent RES generation, etc.).

A robust transmission expansion plan should be able to supply the demand in most combinations of such random events. For this purpose, the stochasticity of the problem is taken into account in the methodology of WP8 through a Monte Carlo approach. Numerous situations are considered, each one based on one random realization of the uncertainties, and the response of the power system to all these situations is analysed.

The Monte Carlo approach implies the necessity of generating different samples of the stochastic inputs of the problem. A module has been developed to carry out this task, called Time Series (TS) generator.

The TS generator is applicable to different kinds of phenomena. More precisely, the ones considered in the scope of the WP8 are:

- Outages of thermal units;
- Electrical demand;
- Wind power generation (WPG), both onshore and offshore;
- Photovoltaic (PV) generation;
- Hydro inflows (which feed all types of hydro units);

Time series are generated with an hourly time step, over a period of one year and for each area of the modelled power system. In WP2, time series of load and uncontrollable generation were calculated from coherent historical data, keeping intermodal and spatial correlations (see D2.1 “Data sets of scenarios for 2050”).

Note that the interest of the TS generator is also the conversion of a gross value – typically, the installed capacity of an intermittent RES or the overall yearly consumption in a zone – into hourly and sequential figures which will be used to describe the real-time operation of the power system.

All the considered phenomena, except thermal outages, are defined on a continuous set – typically, the renewable generation is included between zero and the installed capacity of RES. The TS of the continuous phenomena are all generated with the same method, discussed in sections 3.1 and 3.2. On the other hand, the outages of thermal units are addressed independently, with a binary state either equal to zero (normal operation) or one (thermal unit out of order). The method to generate the TS of thermal outages is presented in Section 3.3.

Finally, examples of newly generated TS are presented and analysed in Section 3.4.

3.1. Challenges related to the generation of time series

This paragraph presents some issues related to the generation of continuous time series, namely uncontrollable renewable generation, hydro inflows and load. The time series of thermal outages is a special binary case which will be addressed independently.

3.1.1. The key characteristics to describe the uncertain phenomena impacting the power system

It can be expected that a majority of the scenarios integrate a lot of renewables in 2050. The detailed hourly description of these scenarios will therefore highly depend on the performances of the TS generator. For this reason a special attention has been given on its development, and especially on the characteristics presented below.

Time-dependence issues

The short-term intermittencies of the stochastic phenomena are an important issue which put to the test the flexibility of the power system [9]-[10]. The ability of hydro and thermal units to adapt to the intermittencies of RES generation can only be assessed if the sequential behaviour of the uncontrollable generation is properly described.

Moreover, a realistic management of the storage cannot be simulated without a temporal description of the consumption, uncontrollable RES and hydro inflows. Small storage units are usually used to compensate the daily variations of demand and RES, while large scale storage units can also adapt to the yearly seasonality of the electrical consumption and hydro inflows. Therefore, the impact of hydro storage can hardly be analysed without a proper representation of the temporal variations of the phenomena impacting the power system.

For these reasons, the evolution over time of the studied phenomena, i.e. their dynamic, is modelled. More precisely, two characteristics of the time series are considered in order to assess these time-dependent issues:

- **The seasonality.** Yearly, weekly or daily periodicities usually observed in the time series.
- **The temporal correlation, also called autocorrelation.** Correlation between the value of the time series at a time step t and the values at previous time steps.

Marginal distribution

In the view of extracting probabilistic indicators which assess the reliability of the power system, all types of situations, with their associated frequency, have to be represented. Extreme events, like the high loads resulting from the cold spell which struck Europe in winter 2012, are usually the most critical for the power system [11] and should be included in the model. On the other hand, most common situations are also essential to compute probabilistic indices (e.g.: loss of load probability) which describe the average response of the power system to all the space of possibilities, and not only for the worst-case or extreme situations.

For this purpose, the characteristics of a stochastic phenomenon should also include all the set of its possible realizations – including valleys, peaks but also intermediate values – with their associated probability of occurrence. **The marginal distribution** of a series, or univariate probability density function (pdf), is thus another property which is examined.

Interdependencies between time series

These three characteristics (seasonality, autocorrelation and marginal distribution) ensure a good modelling of a given time series, but a detailed description of the uncertainties affecting the power system should also include the interdependencies between time series. The positive dependency between two phenomena will highlight their intermittency – for example, the strong correlation between the loads of

two neighbouring zones will tend to gather the extreme situations (peaks or valleys) at the same time – while the independencies or negative correlations will smooth the variability of the time series considered altogether. Most of the interdependencies between time series are explained by **the spatial correlations**, which are the correlations between the time series of a same phenomenon taken in different zones.

Not taking the spatial correlations into consideration can lead to a severe underestimation of the intermittencies affecting the power system [12]. Moreover, spatial correlations directly impact the interest of pooling intermittent renewable energies in a spread area like Europe, and thus the interest of developing the grid in a system with a large amount of uncontrollable RES.

Sensitivity analyses have been performed to evaluate the influence of the spatial correlations (later presented in Section 6). It has been shown that they can have a significant impact on the results of the methodology and that neglecting them could lead to a severe over-estimation of the reliability of the system.

Correlations between different types of phenomena in a same area – called modal correlations, e.g. correlation between load and PV generation – have also been modelled and analysed for the purpose of this project. We show in Section 6 that the influence of the modal correlations on the exchanges in the power system is small. For this reason, it has been decided not to retain them in the final version of the TS generator.

3.1.2. The use of historical data to learn the intrinsic characteristics of each time series

Before being able to generate new time series, it is necessary to estimate the previously mentioned characteristics: seasonality, distribution, and correlations.

The most classic way to proceed is to suppose that these properties are constant over time and thus to use figures measured in the past to describe the future behaviour of the phenomena. This extrapolation of the past properties to the future horizon⁵ is an assumption which is not obvious and should be carefully considered. It is realistic in the case of a homothetic development of the system, i.e. a proportional and homogeneous growth of the current situation. Yet, their validity can be at stake if (e.g.):

- A technological breakthrough leads to new wind turbines or new solar generation technologies with significantly different behaviour.
- The spatial repartition inside an area of the wind or solar generating units follows a different tendency than the one observed in the past.
- Electrical uses appear or disappear, modifying significantly the consuming behaviours or the variability of the load.
- Global warming has an effect on consumption behaviours, hydro inflows, solar irradiation or wind speeds.

If those changes are assessed significant and can be quantified, the intrinsic characteristics of the time series should be accordingly modified in order to better represent the long-term behaviour of the power system.

⁵ The time horizons of e-Highway2050 are spread over the period 2020-2050. The properties learnt in the past will therefore be used to generate new time series up to 40 years ahead.

Moreover, this approach implies the availability of historical data in order to calibrate the intrinsic parameters of the time series. This methodology considers that such data are available for almost each area and each type of processes (WPG, solar generation, load, inflows)⁶. Yet, for the (rare) cases where no historical data can be found, *ad-hoc* routines are presented in Annex B.

A module called TS analyser, for time series analyser, is run *ex-ante* and extracts the intrinsic properties from historical data which are further used by the TS generator. The interaction between the TS analyser and TS generator is illustrated in Figure 6.

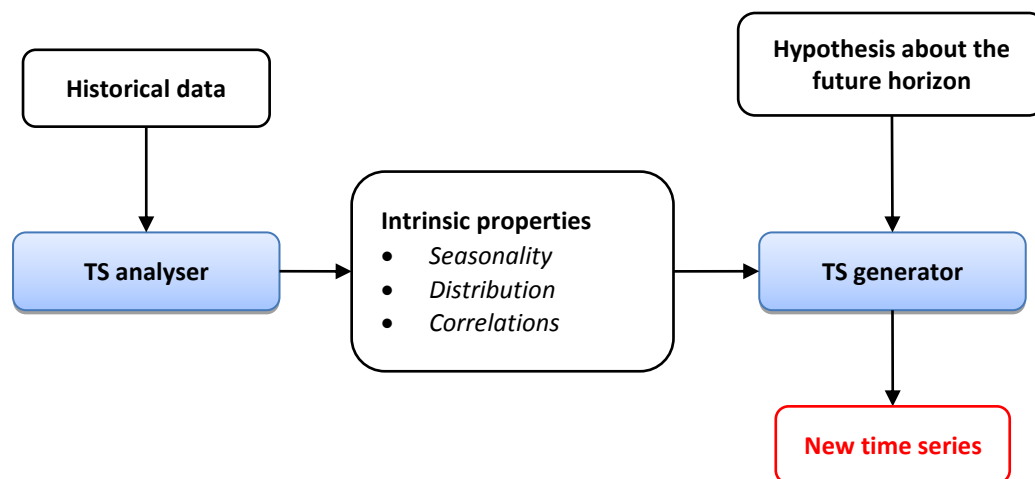


Figure 6. Interaction between TS analyser and TS generator

The TS generator also receives, as input, hypotheses about the future development of the power system, typically the installed capacity of RES or the overall yearly consumption which is forecasted for the studied time horizon. In this specific context, the construction of a time series is therefore based both on intrinsic characteristics of the phenomenon observed in its past realizations and on hypotheses about its future trend.

For the sake of brevity, this section focuses on the description of the TS generator. The TS analyser is presented in Annex A.

3.1.1. State-of-the-art on time series modelling

A state-of-the-art on time series generation is presented in this part. Its goal is to give the reader some landmarks on the different methods which were already developed by other authors, with their pros and cons. It also allows comparing the choices made in this work package with the other possibilities offered by the literature.

Time series decomposition, trend and seasonality

In the proposed methodology, time series are decomposed so as to extract their deterministic patterns, namely their trend and their seasonality.

⁶ At least one year of historical data is required in order to calibrate the seasonality. The calibration of the model on several years of historical data is moreover strongly advised in order to build a general model which does not contain the specificities of a given year (e.g. cold/hot or wet/dry year).

The interest of this decomposition is to isolate the random part of the time series from the one which can be logically explained, either by the evolution of the state of the power system (e.g. diffuse increase of consumption, expansion of the renewable generation fleet) or by the natural periodic patterns of the consuming behaviours and climatic conditions.

The seasonality of the phenomena we are dealing with is clear (see for example reference [13] on the illustration of the seasonality of wind power generation). When modelling the stochasticity affecting the power system, seasonality is therefore commonly isolated. For instance, Hill & al. [14] remove the seasonality of wind speed data using one standard diurnal profile for each of the four seasons of the year. Brunsh & al.[15] propose to identify the seasonality of the consumption via regression on Fourier series or spline functions, with dummy variables to distinguish the different hours of the day.

As raised by Zugno & al. in [16], the low-frequency dynamic of the trend also has to be filtered from large historical datasets in order to identify the variations which are due to random events from the ones which are due to structural changes of the power system. Typical time series decomposition models, including a trend and a seasonality, are presented in references [17] and [18]. The most popular ones are notably: moving averages, regression, X-12 and STL decompositions.

The framework of this project naturally pushes towards an identification of the trend and seasonality via regressions. It indeed presents the advantage of:

- identifying a *stationary* and *parametric* seasonality which can be re-used in the long-term horizon,
- offering the possibility of superposing several periodic cycles, typically yearly, weekly and diurnal cycles,
- distinguishing easily the days with an atypical demand (holidays, long week-ends), and
- having a common structure able to catch the specificities of all the considered phenomena (i.e. load, RES, inflows).

Stochastic time series models

Once the trend and the seasonality are extracted from the time series, the residual part – called stochastic component in this paper – is commonly represented by one of the family of models described below.

ARMA-type models are widely considered in power system applications. For instance, an autoregressive (AR) model is used in [19] to synthesise wind power generation time series. Its variant ARMA-GARCH is preferred in [20] in order to catch the homoscedasticity of wind speed. In [21], Sisworahardjo & al. preconize the seasonal ARIMA with a period of 24h to model the complex autocorrelation of the load. A seasonal ARMA is also applied in [14] to generate new time series of wind speed in the UK.

On a mathematical viewpoint, ARMA-type models present the advantage of fitting complex autocorrelation functions; however they can just handle Gaussian time series. References [19] and [20] propose to use the inverse cumulative distribution function of non-Gaussian processes in order to normalize them. With this routine they apply ARMA models on any time series.

Markov chains are also commonly employed in such application. For example, Papaefthymiou & al. [22] apply Markov chains up to the third order to sample time series of wind power generation. Birth and death Markov chains are used as well in [23] for wind speed time series. Markov chains are particularly efficient to fit all types of probability distribution functions (pdf). However, their application involves a discretization of the stochastic process into a finite number of states and so a possible loss of information. Furthermore, as highlighted in [24], Markov chains are not capable of fitting complex autocorrelation functions.

Finally, *diffusion-type models* have also been applied to the generation of wind power profiles [25]. As presented by Bibby & al. [26], this class of models derives from diffusion equations. It allows to represent

processes with diverse common probability distributions (e.g. Normal, Weibull, Beta, Gamma, etc.) and simple exponentially decaying autocorrelation. Contrary to ARMA and Markov chains, they also have the advantage of characterising the time series with only a few explicit coefficients: namely the parameters of the pdf (e.g. shape and scale parameters of a Weibull function) and the “slope” of the exponentially decaying autocorrelation function.

In our case, we want to sample new time series of several phenomena (load, intermittent RES, inflows). With the aim of covering the specificities of each of them, it has been decided not to settle on just one model. Two models have been retained so as to be able to capture numerous pdf and autocorrelation functions:

- Seasonal ARMA models for Gaussian time series with strong temporal correlations (typically applied to load time series)
- Diffusion-type models for non-Gaussian time series (typically applied to uncontrollable RES and inflows time series)

As explained in Section 3.2, depending on the intrinsic characteristics of the phenomenon we are dealing with, one approach or the other will be selected.

Dependencies between time series

The methods mentioned in the previous part allow the generation of univariate time series. The issues of correlations between several time series are discussed in this new section.

The literature on the sampling of correlated random variables expands in the past few years as the role of spatial correlations in probabilistic power system studies starts to become a topic of interest. The generation of correlated random variables is a complex mathematical problem; the tools mentioned in the state-of-the-art to tackle it are notably:

- *Copulas*: Copulas are a family of functions which allow the construction of multivariate distribution functions, based on the univariate marginal distributions and the correlation coefficients between each dimension. They have been employed in [27] and [28] in order to model the stochastic dependencies of the load, photovoltaic and wind power generation in uncertainty analyses of the power system. Copulas ensure an effective generation of correlated random variables with the expected pdf and cross-correlations. However, they cannot handle temporarily correlated time series.
- *Multivariate ARMA models*: Multivariate ARMA models have been used by Hill & al. [14] in order to model the spatial correlations of wind speed in Great Britain. Instead of building independently one model for each time series they consist in fitting one common model for all the time series, with cross-coefficients binding the evolution of the different processes. They are adapted to sample correlated Gaussian time series. However, the calibration of multivariate ARMA can be intractable when lots of time series are considered as they involve the estimation of a large number of parameters. Moreover, in order to be properly fitted, multivariate ARMA models require synchronised historical data for all the time series, i.e. historical data which overlap on a same period. It can be a limiting factor for a European study which collects data from numerous different sources.
- *Principal Component Analysis (PCA) and its variants such as Independent Component Analysis (ICA)*. These methods have been notably applied on multivariate hydrological series of Colombia in [29]. The principal components (or independent components) of a multivariate dataset explain most of its cross-correlations. PCA therefore allows to transform a set of correlated time series into a set of uncorrelated time series and to calibrate a classic univariate model on each of them. When time series are generated, the inverse transformation is applied so as to reconstruct the spatial dependencies. This

method is particularly flexible as it can be used with any of the univariate model presented in the previous section. However, as for multivariate ARMA, PCA requires synchronised datasets for all the areas of the system.

- *Transposition of the spatial correlations on the innovations:* Another approach consists in modelling the spatial correlations on the innovations – which are Gaussian white noises – instead of considering them on the stochastic components – which are complex stochastic processes. Methods for generating dependent Gaussian white noises are well-managed. This approach therefore simplifies drastically the mathematical complexity of the problem. It has been notably applied on the innovations of ARMA models by MacCormack & al [30] and Morales & al. [31] for time series of wind power generation and wind speed. To our knowledge, this approach was never applied on diffusion-type models, but considering their structure similar to the ARMA (see Equation 4.2), the extrapolation of this method to the innovations of diffusion-type models is feasible.

This last approach has been retained in the WP8 of e-Highway2050. It is applied in two steps. First, univariate models are calibrated independently on each time series of the system. And then correlations are modelled (if needed) between the innovations of the univariate models. The learning process in two steps is the asset of this approach. It provides the two following advantages:

- The accuracy of each univariate model is preserved. Each phenomenon is modelled as usual with the approach which better fits its characteristics. There is no need for a common approach or a pre-transformation which could degrade the representation of each time series considered independently.
- Dependencies are estimated two-by-two (i.e. independently for each pair of time series) based on the period of time which is common to the two historical datasets. Thus, the method can be applied even if the datasets of all the time series do not overlap.

The implemented solution is presented in the next subsection.

3.2. Design of the time series generator

This section tackles the problem of generating continuous time series, in particular:

- the representation of one independent time series is discussed in subsections 3.2.1 and 3.2.2;
- the correlations between several time series are addressed in 3.2.3;
- and finally, the architecture of the whole TS generator is presented in subsection 3.2.4.

The time series of load and uncontrollable RES generation are generated with an hourly time step. On the other hand, due to the lack of detailed historical data, hydro inflows are generated with a monthly time step and then rescaled on an hourly timescale with constant values over each month.

3.2.1. The representation of one time series, univariate model

We propose to model time series with a multiplicative model:

$$Y_t = T_t S_t X_t \quad (4.1)$$

Where Y is the final time series, T is the trend, S the seasonality, X the stochastic component of the phenomenon and t the time index. The four components of the model are described below.

The trend (T_t)

T_t is the trend, the average value of the time series. It can usually be assumed constant or linear on a given year. It represents the structural changes of the power system, more precisely:

- for load time series, the expected electrical consumption during the year,
- for time series of intermittent renewable generation, the installed capacity,
- and for time series of hydro inflows, the expected yearly producible energy.

T_t is evaluated with the given hypotheses of the long-term scenario and time horizon.

The seasonality (S_t)

S_t is the seasonality, i.e. the intra-year variations of the process. It represents the expected average behaviour of the studied phenomenon along the year and includes the periodic patterns observed in the historical data. It is mainly explained by the yearly, weekly and daily cycles of the climatic conditions and consuming behaviours. The seasonality also includes the irregularities which can appear during the time changes (seasonal adjustment of clocks) or on certain types of days, such as holidays and long weekends.

The seasonality is a deterministic and fixed sequence learnt from historical data with regression on Fourier series, using dummy variables to distinguish the different hours of the day or the different types of day (e.g. working day vs. non-working days). The learning process, performed by the TS analyser, is detailed in annex A. An example of the seasonality (S_t) _{$t=1..8736$} of the load of France is given in Figure 7.

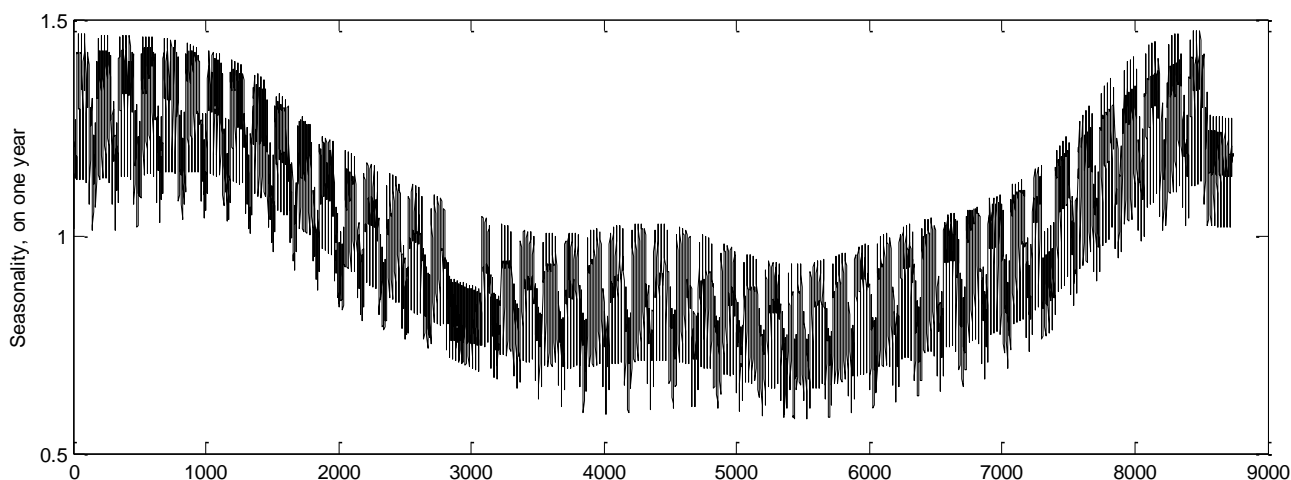


Figure 7. Seasonality of the load of France over 1 year⁷ (dimensionless)

Trend and seasonality are logically multiplied in the model (see Equation 4.1) as the yearly variations of the studied phenomena usually increase with its overall growth. For instance, if the installed wind power capacity is doubled, the gap between the average generation in December and June will also be doubled.

⁷ The TS Generator produces exactly 52 weeks of data, and so 8736 hourly time steps.

The stochastic component (X_t)

The stochastic component of a time series is its residual part, the one which cannot be explained by natural periodic cycles or by the low frequency dynamic of the trend.

Trend and seasonality are deterministic characteristics. They are the same for every Monte Carlo year. On the contrary the stochastic component includes random events and is different from one Monte Carlo year to another.

The stochastic component is characterised by its probability density function (pdf) and autocorrelation function (acf). They can be quite different from one time series to another. For instance, Figure 8 and Figure 9 show the pdf and acf of the stochastic component of the load connected to the network of Amprion (one of the four German TSOs), and the one of the French wind power generation. The pdf of the load’s residuals can be reasonably approximated by a Gaussian function while their acf has a complex periodic structure with peaks at multiples of 24 hours⁸. On the contrary, the pdf of the wind power generation is more complex, but its acf follows an exponential decay, typical of a memoryless process.

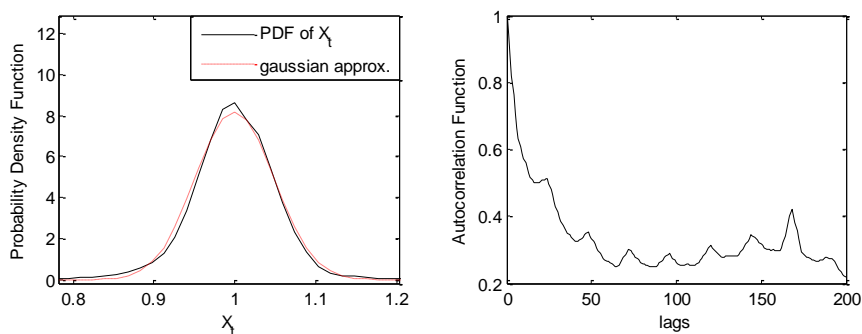


Figure 8. Characteristics of the stochastic component of load connected to the network of Amprion, learnt from 8 years of historical data

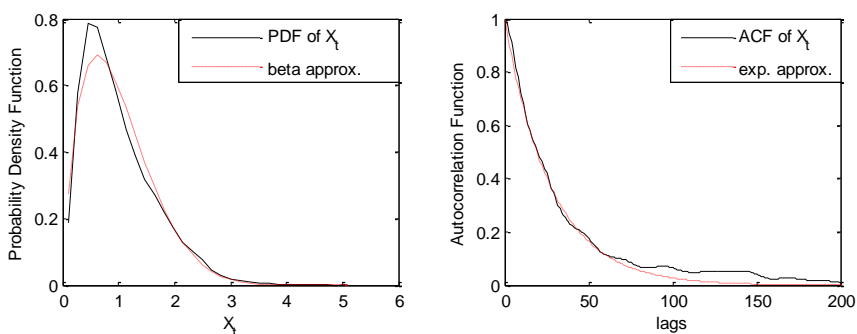


Figure 9. Characteristics of the stochastic component of wind power generation of France, learnt from 7 years of historical data

For each Monte Carlo year, the stochastic component is generated by a method which aims at replicating this pdf and acf. Depending on their nature, one method or another will be more efficient to generate a new stochastic component with the appropriate behaviour.

More precisely, two methods are advised to generate new time series of the stochastic component X_t :

⁸ Despite the removal of the seasonality, the residual part can still have slight daily and weekly correlations.

- **Diffusion-type models** [25]-[26], which can generate series with a given common pdf (Gaussian, Weibull, Beta, Gamma, Uniform...) and a simple exponential decaying autocorrelation.
- **Seasonal ARMA models** [14]-[18][19]-[20]-[30]-[31], which can only handle Gaussian processes but are especially adapted to complex autocorrelation structures. For instance, seasonal ARMA are particularly powerful to model series with periodic autocorrelations peaks as the ones of Figure 8.

On the datasets analysed by the author, diffusion-type models are more appropriate to describe the inflows, photovoltaic and wind power generation while the demand time series are better represented by the ARMA-type models.

Both methods have a similar structure and involves an iterative generation of X_t , where X_t is calculated as a function of its past realizations, $(X_\tau)_{\tau < t}$, and an innovative Gaussian white noise, ε :

$$X_t = \hat{f}((X_\tau)_{\tau < t}, \varepsilon) \quad (4.2)$$

The function \hat{f} is estimated by the TS analyser.

If the stochastic component is represented by an ARMA model, \hat{f} is linear. On the other hand, if it is represented by a diffusion-type model, \hat{f} is *a priori* non-linear and it just involves the previous time step of the stochastic component. In that second case: $X_t = \hat{f}(X_{t-1}, \varepsilon)$.

ε is the random source which contains the novelty of the time series. It is independent and identically distributed (i.i.d.) over a normal distribution and can therefore be easily obtained with a pseudorandom number generator. ε is usually called **innovation**.

The stochastic component is linked to the deterministic part of the time series through a multiplicative model – see Equation (4.1). A multiplicative model is adapted to the considered phenomena as it logically increases the range of the stochastic variation when the trend increases. Moreover, a multiplicative model allows to catch the seasonality of the intermittent RES and to isolate a stationary stochastic component: for example, in a multiplicative model, the seasonality of the photovoltaic generation contains the classic daily bell-shaped curve with zero values at night-time while the stochastic part represents the nebulosity, stationary along the day (see Figure 10).

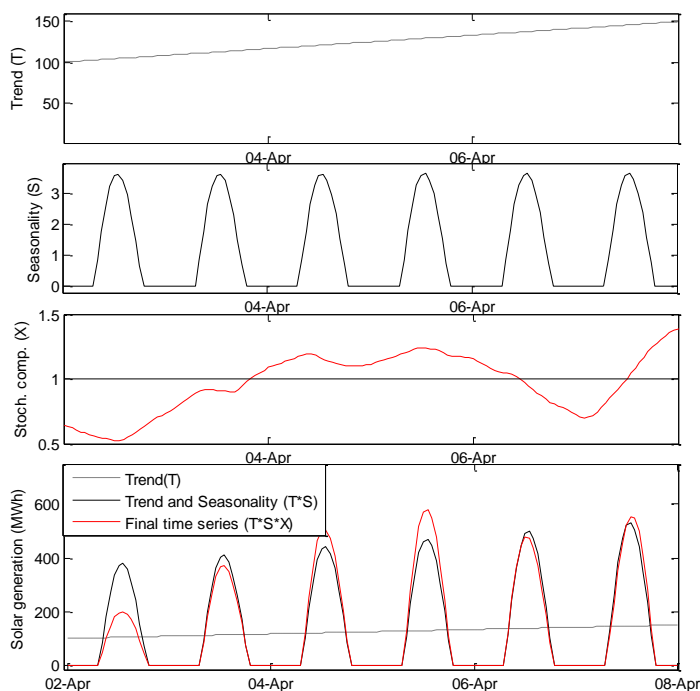


Figure 10. Decomposition of a time series of PV generation into a trend, a seasonality and a stochastic component. The trend has been exaggerated on purpose for the sake of understanding its role.

3.2.2. The generation of one time series

The generation of one independent time series is illustrated by Figure 11.

First, the innovation is sampled with a pseudo random number generator. The innovation includes the random source of the time series.

The pseudorandom generator is initialised by a seed: an integer value fixed by the user and different for each Monte Carlo year. The innovation, ε , is entirely determined by this integer. The interest of the seed is that it offers the possibility to re-generate identical time series. It can be useful in order to run the same simulation several times and analyse more deeply its results.

The stochastic part X , with its appropriate acf and pdf, is then iteratively generated, either with an ARMA or a diffusion-type model. The interest of this step is to convert a white noise into a temporally correlated and potentially non-Gaussian time series.

Finally, the stochastic component is combined with the trend and the seasonality in order to form the final time series Y .

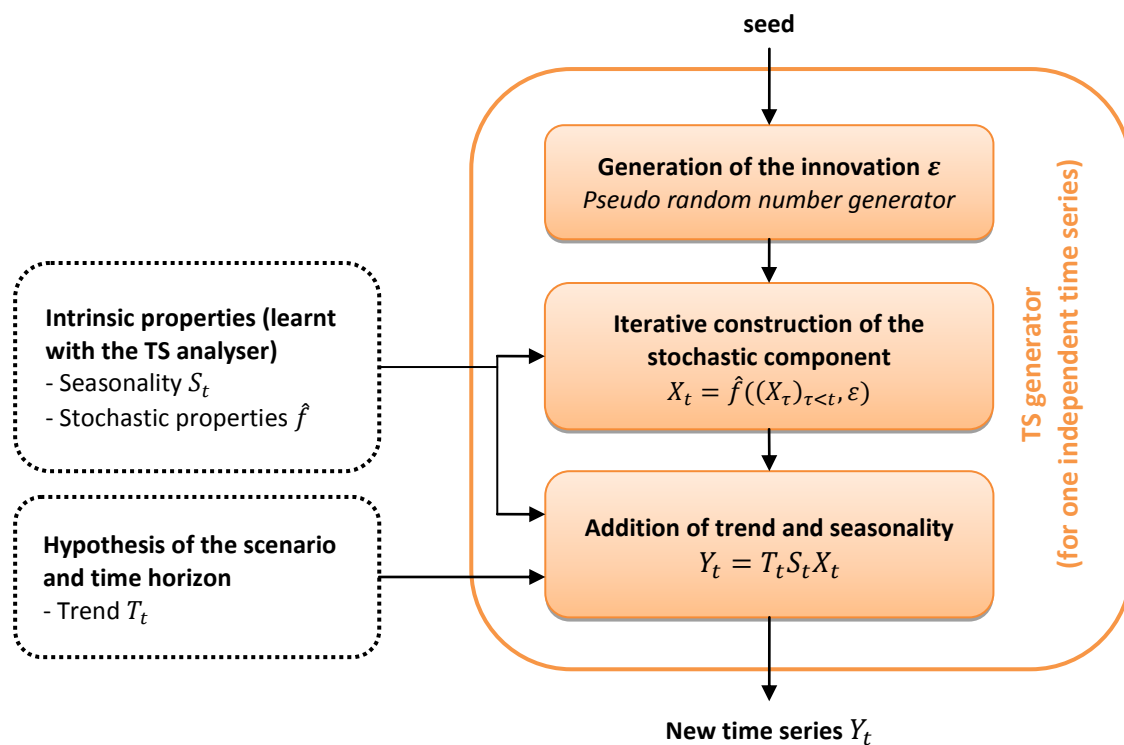


Figure 11. Generation of one independent time series

The TS generator requires, as inputs, both:

- information learnt on past realizations of the time series, their seasonality and stochastic properties, and
- hypotheses about the future tendency of each time series, namely their trend.

This approach allows generating univariate time series with the expected marginal distribution, autocorrelation and seasonality. Some examples presented in Section 3.4 attest the ability of the TS generator to reproduce the intrinsic characteristics of different phenomena into new synthetic samples.

The next sub-section addresses the problem of the dependencies between several time series.

3.2.3. Modelling of spatial correlations

What are spatial correlations?

The spatial correlations are the correlations between two time series of a same type in two different locations. They are typically due to the climatic conditions which tend to affect simultaneously neighbouring areas – for instance a similar cloud covering adjacent zones of the system which correlates their photovoltaic (PV) generation.

One part of these correlations is already included in the seasonality. For example, the photovoltaic generation of two areas is obviously highly correlated as they both have the same daily bell-shaped curve. However, the seasonality does not catch all the spatial correlation and the stochastic components of the two time series can still be correlated. In this same example, if the two areas are adjacent and subject to similar meteorological conditions, they will have similar variations around their seasonality, with cloudy (or sunny) days resulting in lower PV generation (or higher) than the seasonality occurring, most probably,

simultaneously. We focus on the correlations between the stochastic components, X_t , of several time series. An example of historical data of PV generation in two adjacent zones of France is given in Figure 12: both time series are clearly correlated.

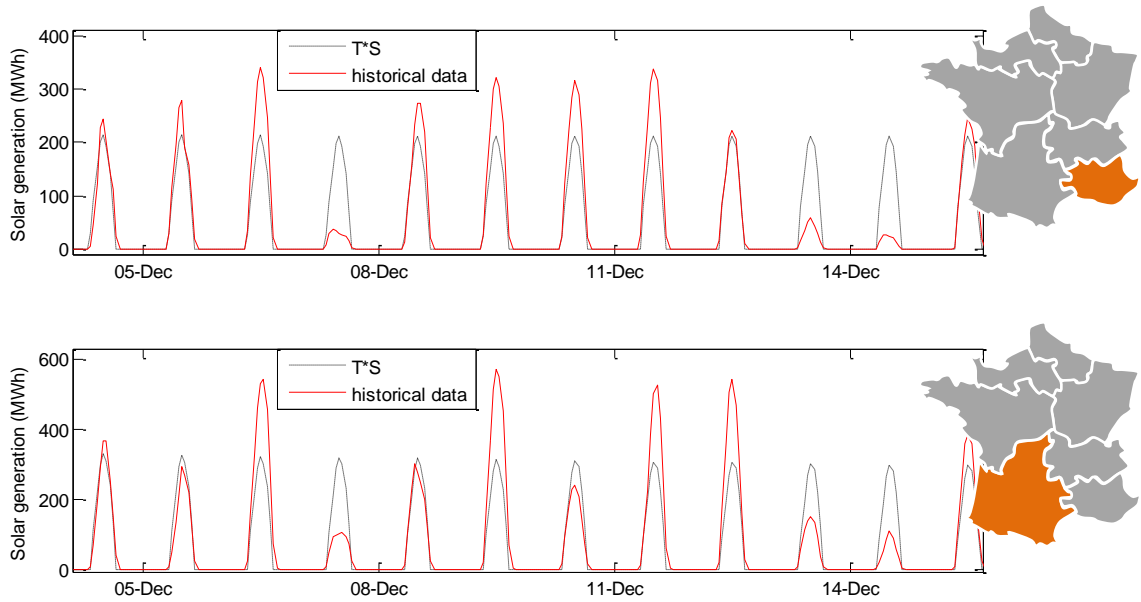


Figure 12. Historical data of PV generation in two zones of France, with their associated trend and seasonality

How are the correlations modelled in the e-Highway2050 project?

One of the classic methods to generate correlated samples of such time series is to focus on their innovations (ε). The innovations are Gaussian white noises and can therefore be easily handled using the approach presented in [30]-[31]. Let R_ε be the correlation matrix, positive semi-definite, between the n Gaussian white noises $\varepsilon_1, \dots, \varepsilon_n$ and $R_\varepsilon = L_\varepsilon L_\varepsilon^T$ the Cholesky decomposition of this correlation matrix. Then:

$$\begin{pmatrix} \varepsilon_1 \\ \dots \\ \varepsilon_n \end{pmatrix} = L_\varepsilon \begin{pmatrix} \xi_1 \\ \dots \\ \xi_n \end{pmatrix} \tag{4.3}$$

Where ξ_1, \dots, ξ_n are uncorrelated Gaussian white noises.

The generation of the correlated innovations $\varepsilon_1, \dots, \varepsilon_n$ can therefore be performed in two steps:

1. Spatially and temporally uncorrelated normal processes ξ_1, \dots, ξ_n are drawn independently using a classic pseudo random number generator.
2. Transformation (4.3) is applied to deduce the correlated sample $\varepsilon_1, \dots, \varepsilon_n$

The challenge of this method relies on the estimation of R_ε . The innovation is indeed an intermediate variable used for the purpose of generating new time series. The calculation of the correlation matrix R_ε is therefore not obvious as historical realization of ε depends on the model used and does not have any physical meaning. An empirical method has been developed to compute R_ε and is described in Annex A.

As shown in Section 3.4, this approach gives good results to model the interdependencies between time series with comparable intrinsic properties. It is therefore adapted to model spatial correlations, or possibly

correlations between onshore wind power and offshore wind power, which also have quasi-similar behaviours.

3.2.4. Architecture of the multivariate time series generator

The architecture of the complete time series generator of WP8 is finally sketched in Figure 13.

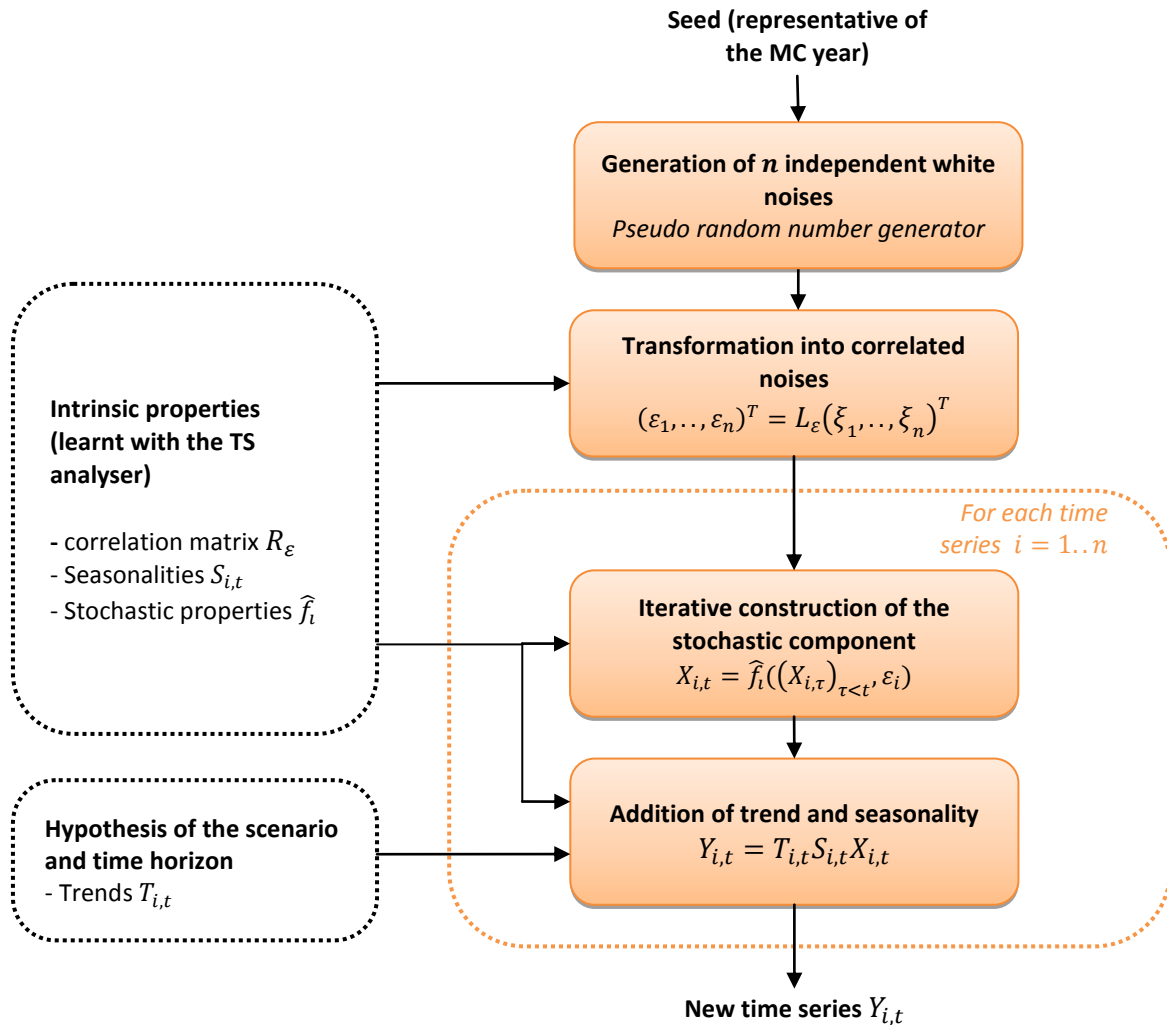


Figure 13. Generation of correlated time series

First, n independent Gaussian white noises, ξ_1, \dots, ξ_n , are sampled with a classic pseudo random generator.

They are then transformed into correlated innovations using Equation (4.3) where L_ε is obtained from the correlation matrix estimated between the innovations of the univariate time series model. Spatial dependencies as well as dependencies between offshore and onshore wind power generation can be integrated in the correlation matrix.

The generation method presented in Section 3.2.2 is then run for each time series. An ARMA or diffusion-type model is first used to transform the innovation into a stochastic component with the expected marginal distribution and temporal correlation.

The stochastic component is finally combined with the seasonality and the trend. The seasonality includes the natural periodic cycle of the series while the trend reflects the state of the power system.

The TS generator has been prototyped with Matlab.

3.3. The special case of thermal units

This section addresses the generation of time series of thermal units availability.

The method used to model the thermal availability is the one implemented in [32], described below. It offers a sequential two-state modelling of each thermal unit of the power system (each unit is either fully available or out of order) and therefore permits a realistically evaluation of the consequences of the loss of one or several units.

The outage of a thermal unit is a binary state: it is equal to 0 when the unit is available and equal to 1 when the unit is out of order. It is considered that the outages last at least one day and the time series are therefore generated with a daily time step. The daily time series are then rescaled on an hourly timescale with a constant state over each day.

Time series of outages are generated for each thermal units of the power system. More precisely, each thermal unit g is considered independently and characterised by two parameters:

- R_g : the outage rate. The average proportion of time during which a thermal unit is out of order.
- D_g : the outage duration, in days.

Thus, if a thermal unit fails in the beginning of day d , it will remain unavailable until the end of the outage period, that is to say until the end of day $(d + D_g - 1)$, and it will be operative again in day $d + D_g$.

From these two parameters, the failure rate, F_g , of the thermal unit is deduced (Equation 4.4). It corresponds to the probability of failure in the beginning of a day given that the thermal unit was available the day before.

$$F_g = \frac{R_g}{R_g + D_g(1 - R_g)} \quad (4.4)$$

The algorithm which draws the daily outage time series of a given thermal unit g is described in Figure 14.

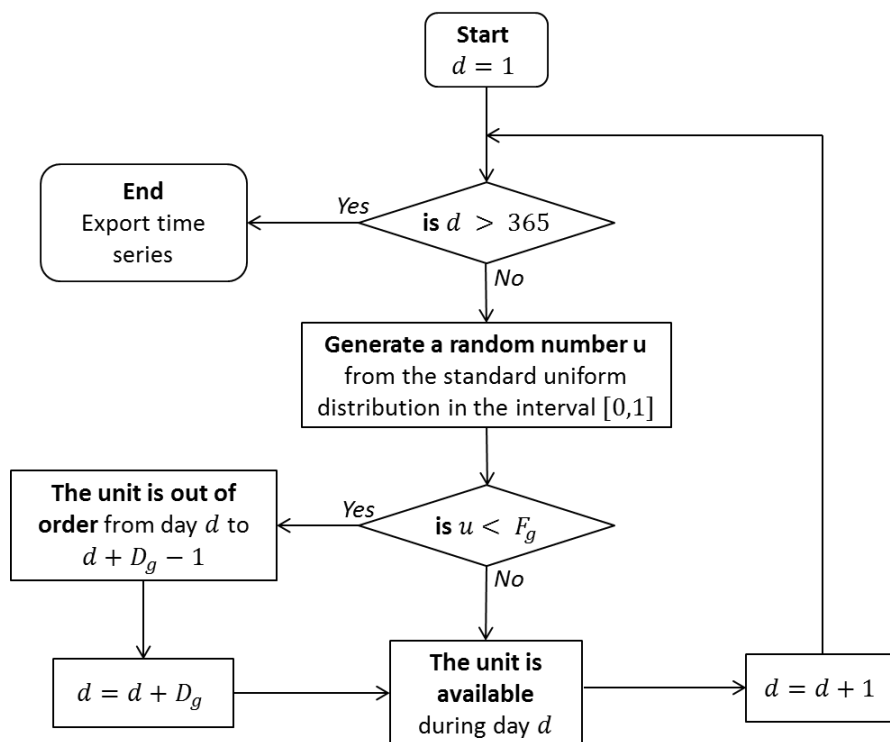


Figure 14. Generation of the time series of thermal availability

For every new day d , a random number is drawn from a standard uniform distribution. If this number is higher than the failure rate, the unit stays operative in day d and the procedure is iterated for day $d + 1$. Otherwise, if the random number is lower than the failure rate, the unit is unavailable from day d to day $d + D_g - 1$ (included), became operative again in day $d + D_g$ and the procedure is iterated for day $d + D_g + 1$, until the end of the year is reached.

This approach is repeated for all the thermal units of the power system. It has been implemented in Matlab.

3.4. Performances of the time series generator

This section presents some examples which were used to check the validity of the TS generator. First, two univariate cases are presented, one with hourly time series of demand, and one with monthly time series of hydro inflows. The replication of some historical properties of these time series is checked. Then, the performance of the generation of correlated time series of wind power generation is analysed. And finally, an example of time series of thermal outages is presented.

3.4.1. Reproduction of the intrinsic properties of hourly time series of demand

The stochastic phenomenon considered in this section is the French consumption. A time series model has been calibrated on 6 years of historical data. The seasonality is based on 120 Fourier series, one for each hour and for each type of day (Monday, Tuesday-Thursday, Friday, Saturday, non-working day). A seasonal ARMA is used to represent the stochastic component. 50 new MC years have been generated with this model.

One week of any newly generated Monte Carlo year is presented in Figure 15.

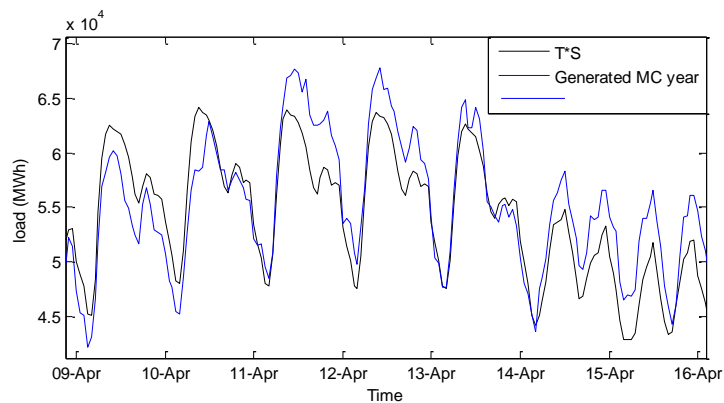


Figure 15. One week of any generated MC year (blue) and expected seasonality (black) of French load

The following of this sub-section compares some characteristics of the time series observed in historical data with the characteristics of the newly generated time series. Historical data have been re-scaled with the constant trend used to generate the new MC years.

The next table compares the average yearly sum of the time series, that is to say the average yearly consumption. The values observed in the historical data and the ones calculated in the generated data are very close: the TS generator therefore reproduces efficiently the average yearly sum of the time series.

Average yearly consumption	
Historical data	490 TWh
Newly generated MC years (50)	489 TWh

Table I. Average yearly sum of historical and generated time series

Instead of focusing on only one summed value, Figure 16 now presents the whole distribution of the time series, for both the historical data and the newly generated MC years (pdfs of the final time series are considered in these figures, including the trend, seasonality and stochastic components).

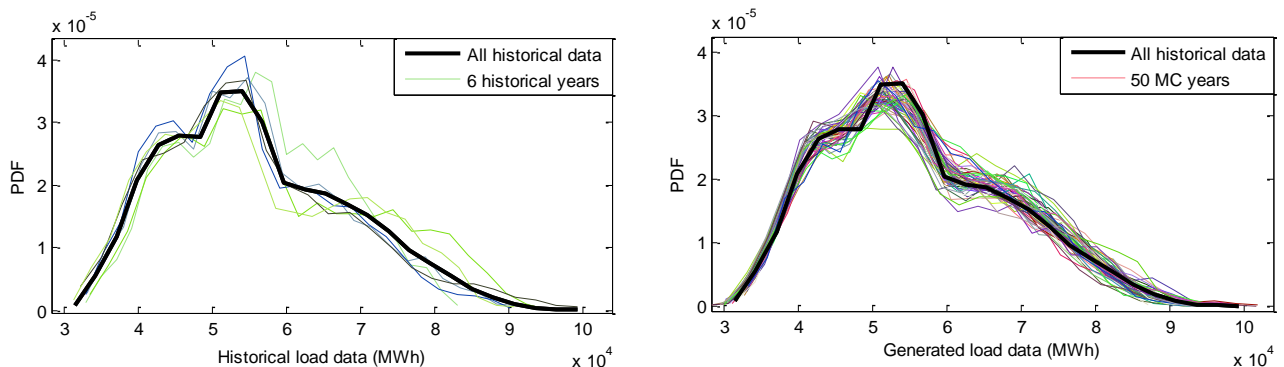


Figure 16. Probability Density Functions of the historical and newly generated time series of the French consumption

The pdfs of the newly generated time series are centred on the historical pdf and attest to the capacity of the TS generator to reproduce the historical distribution of the time series. The differences between the pdfs of the new MC years also show that the TS generator is able to create different possible situations, and not just to reproduce the average historical behaviour of the time series.

The next table focuses on the tails of the pdfs and indexes the average numbers of hours per year spent in the extreme peak and off-peak situations. The peak and off-peak bounds correspond to the first and 99th percentiles of the historical data.

	Peak hours (> 86 GWh)	Off-peak hours (< 34 GWh)
Historical data	88 h/year	88 h/year
Newly generated MC years (50)	67 h/year	96 h/year

Table II. Average durations of peak and off-peak for historical and generated time series

The reproduction of the tails is not fully accurate. The weight of the upper tail tends to be lower in the generated data. For instance, in the 6 years of historical data, there is in average 88 hours per year with a load higher than 86 GWh while in the newly generated data, there is only 67 hours per year with such a high consumption. The duration of peak events is therefore slightly underestimated in the new MC years. This inaccuracy is due to the fact that the PDF of the stochastic part of the time series is approximated by a common distribution, which fits the overall shape of the PDF but does not necessary ensure a good estimation of the tails.

The results are however satisfactory, with less than 15% difference between the weight of the extreme events for the historical and generated data.

The monthly averages of both historical and generated data are plotted in Figure 17. The monthly averages of the new time series are centred on the seasonality observed in the historical data. Moreover, the spread around this average value seems consistent with historical years: the TS generator is able to create different time series, scanning the space of possible situations already observed in the past.

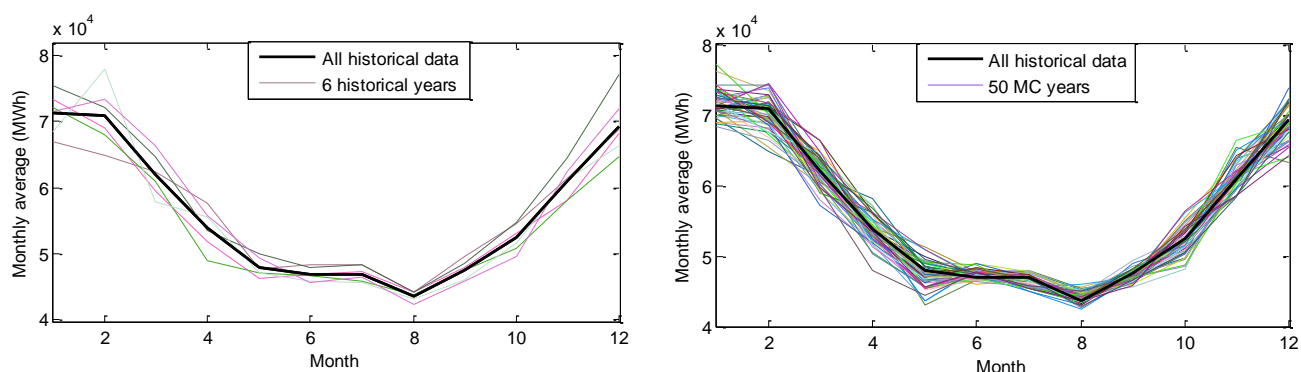


Figure 17. Monthly averages of the historical and newly generated time series of the French consumption

Finally, the autocorrelation of the time series is analysed. Due to the clear daily periodicity of the studied phenomenon, the autocorrelation of the whole time series (including seasonality) is similar for the historical and the newly generated data, with prevailing peaks at multiples of 24 hours. In order to refine the comparison, acfs of the stochastic components of the time series are studied. Figure 18 depicts the autocorrelation of the stochastic components of the historical data and the new MC years.

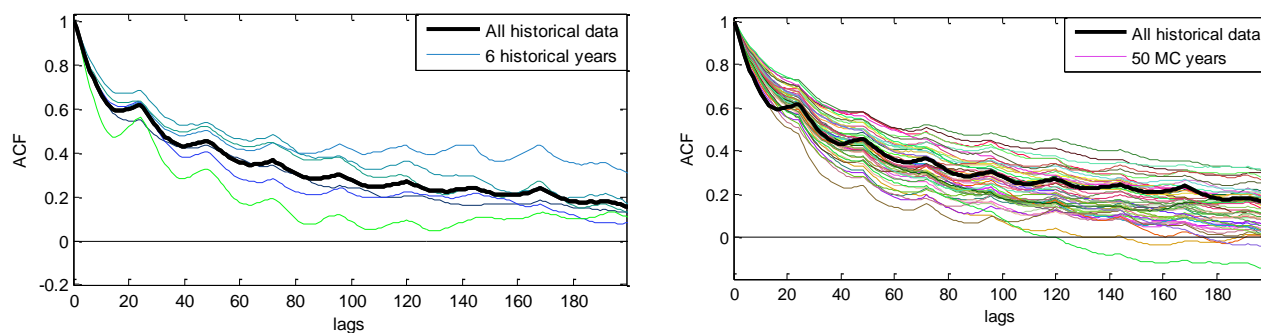


Figure 18. ACFs of the stochastic component of the historical and newly generated time series of consumption

The conclusion is the same than for the previous graphs: the TS generator reproduces, in average, the characteristics of the time series learnt in the past, with a dispersion around the average behaviour which seems consistent with the historical realization of the phenomena.

3.4.2. A univariate case with a monthly time step: hydro inflows

Contrary to load, solar and wind generation, historical data of hydro inflows are usually only available at monthly time step.

Models of hydro inflows are therefore built at this timescale and the procedure presented in Section 3.2.2 is also run with a monthly time step. In practice, the generated monthly time series are then converted into hourly time series by assuming a constant value over each month.

This sub-section presents some results obtained with the time series of hydro inflows in Spain⁹.

Firstly, the four consecutive years of available historical data are plotted along with four new Monte Carlo years, obtained with the TS generator (see Figure 19).

It can be noticed that the new time series follow similar seasonal variations than the historical ones, they contain both types of extreme events, wet and dry periods. They have a strong auto-correlation as well, i.e. the time series rarely intersect the seasonality, and phases when the inflows are higher and lower than the seasonal average tend to last at least six months, if not more.

⁹ As explained in annex B, historical data of run of the river generation has been used to calibrate the model of the inflows.

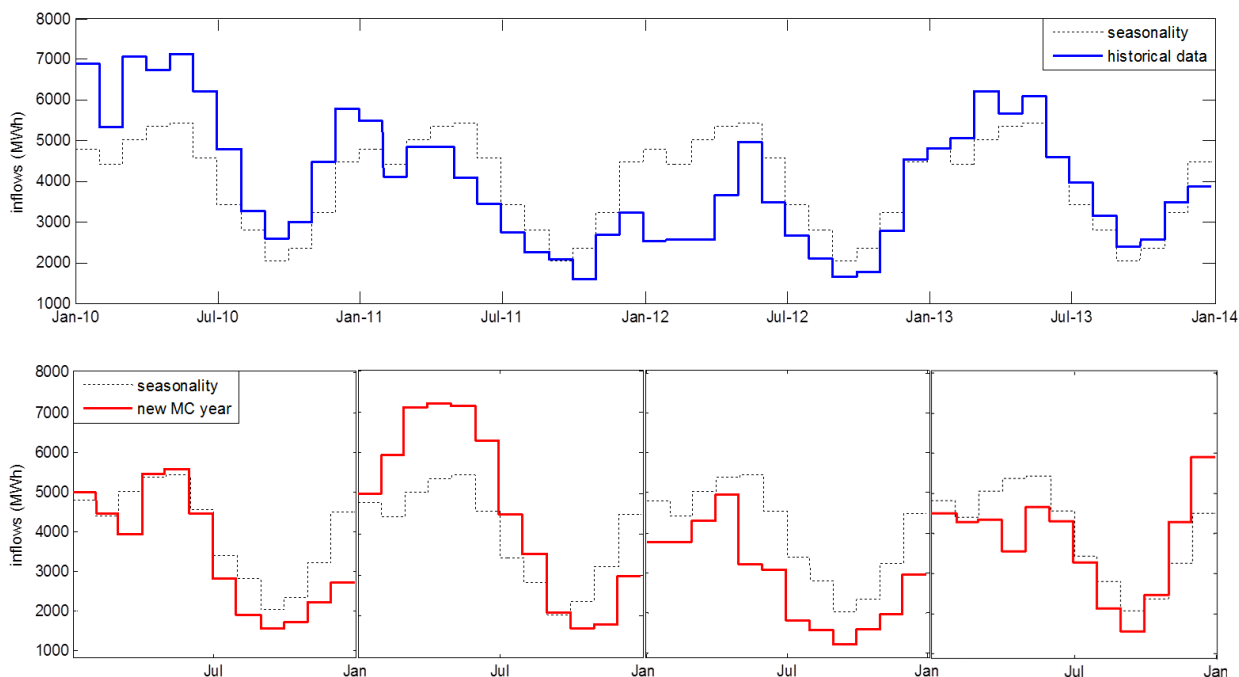


Figure 19. Four consecutive historical years and four generated Monte-Carlo years of hydro inflows

Like in the previous subsection, some characteristics of the original and new time series are compared. Table III. Average and standard deviation of the yearly sum of historical and generated time series

compares the average yearly producible energy, i.e. the total amount of inflows in the year, as well as the standard deviation of the producible energy between years. The average is similar for both historical and new time series. On the other hand, the TS generator slightly underestimates the standard deviation of the producible energy. This means that the dispersion of the new MC years around the average value of 35.0 TWh is slightly lower than the historical one.

	Average yearly producible energy	Standard deviation of yearly producible energy
Historical data	35.0 TWh	9.0 TWh
Newly generated MC years (50)	35.0 TWh	7.5 TWh

Table III. Average and standard deviation of the yearly sum of historical and generated time series

The Probability Density Function (pdf) and the Cumulative Distribution Function (cdf) of the historical data, and the 50 new MC years are plotted in Figure 20. Due to the limited amount of historical data in this example (48 monthly values of inflows), the historical pdf is logically irregular, with successive peaks and valleys, specific to the inflows during the short period between 2010 and 2013. On the contrary, the distribution of the newly generated data, with a total of 600 monthly values, is smoother and lies between the saw-tooth profiles of the historical pdf.

In this case, the TS generator does not follow the same behaviour than the one observed in the historical data, but tries to extrapolate something more general, less typical of the period 2010-2013. The smooth pdf seems indeed more realistic to describe a natural phenomenon. (On a modelling viewpoint, this is explained by the fact that the pdf of the historical stochastic component is approximated by a common

distribution, in this case a beta distribution, which is naturally smooth and cannot contain the irregularities of the historical pdf).

The two pdfs are therefore hard to compare. Yet, the two cdfs of Figure 20 are close and prove the consistency of the model.

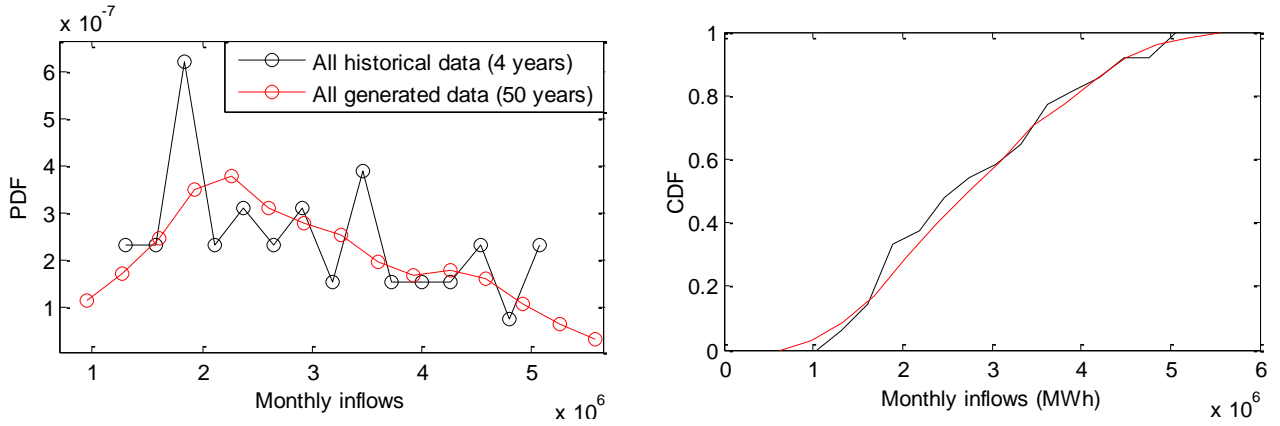


Figure 20. pdf (left) and cdf (right) of historical and new time series of inflows

The average duration of extreme events is presented in Table IV. Average duration of peak and off-peak for historical and generated time series

. The peak and off-peak bounds correspond this time to the first and 9th deciles of the historical data. The frequency of such events is similar in the historical and new generated time series.

	Peak months (> 4,54 TWh)	Off-peak months (< 1.53 TWh)
Historical data	1.25 m/year	1.25 m/year
Newly generated MC years (50)	1.15 m/year	1.30 m/year

Table IV. Average duration of peak and off-peak for historical and generated time series

Finally, the four historical years of inflows are plotted in Figure 21, next to the 50 new generated time series. The TS generator is able to create a large variety of new time series, centred on the seasonality, and with a dispersion around this average value similar to the one observed in the past.

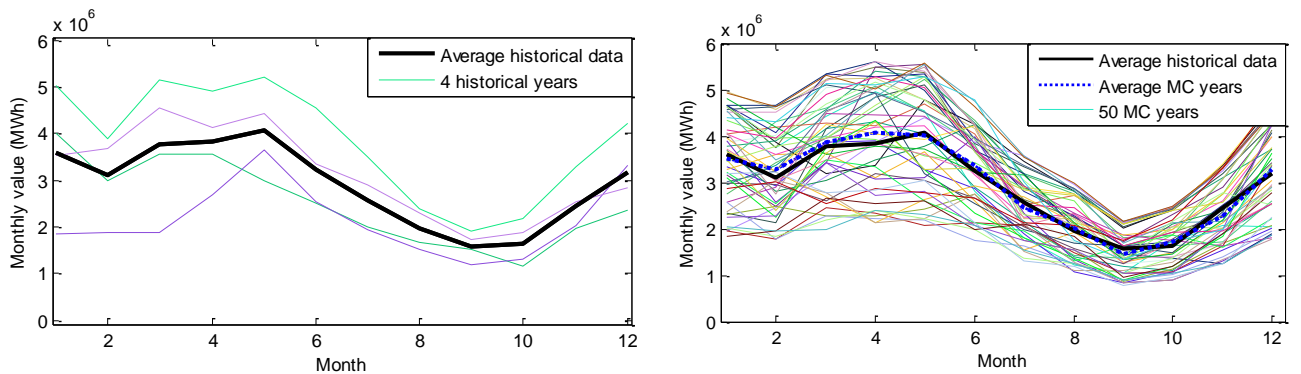


Figure 21. Monthly values of the historical and newly generated time series of inflows

For both hourly and monthly time series, and for the two presented phenomena (electrical demand and hydro inflows), the TS generator has proved efficient to reproduce the intrinsic characteristics observed in the past while proposing a vast variety of new time series. Results obtained with time series of wind power generation and solar generation, not presented in this document, are similar.

3.4.3. A multivariate case: reproduction of spatial correlations of WPG

This sub-section presents some results which show the ability of the TS generator to reproduce spatial correlations.

As explained in Section 3.2.3, spatial correlations are modelled between the stochastic parts of the time series, once the seasonality is removed. In this paragraph, correlations of historical stochastic components are thus compared with the correlations of new stochastic components drawn by the TS generator.

Time series of WPG from four areas of France (East, North-east, West and Rhône-Alpes-Auvergne) are considered. The spatial correlations between their stochastic components, learnt over 6 years of historical data, are indexed in the following table.

	East	North-East	West	RA-Auvergne
East	100	78.7	69.2	28.9
North-East	.	100	72.6	22.2
West	.	.	100	24.0
RA-Auvergne	.	.	.	100

Table V. Historical correlations between the stochastic components of WPG in France (%)

In a second step, a new set of 50 time series of wind power generation for the 4 zones previously mentioned has been drawn with the TS generator, taking into account the spatial correlations previously listed. The average correlation matrix of the time series obtained from these 50 new MC years has been computed and is given below. The resulting correlations are very close from the historical ones, within a range of more or less 1%.

	East	North-East	West	RA-Auvergne
East	100	78.5	69.4	29.5
North-East	.	100	72.2	23.1

West	.	.	100	24.4
RA-Auvergne	.	.	.	100

Table VI. Correlations between the stochastic components of the newly generated time series (%)

Newly generated time series of wind power generation for two zones (East and North-East) have been plotted in Figure 22. To facilitate the comparison, installed capacities have been assumed identical in both zones and equal to 1 GW. The high correlation between the two time series is obvious here.

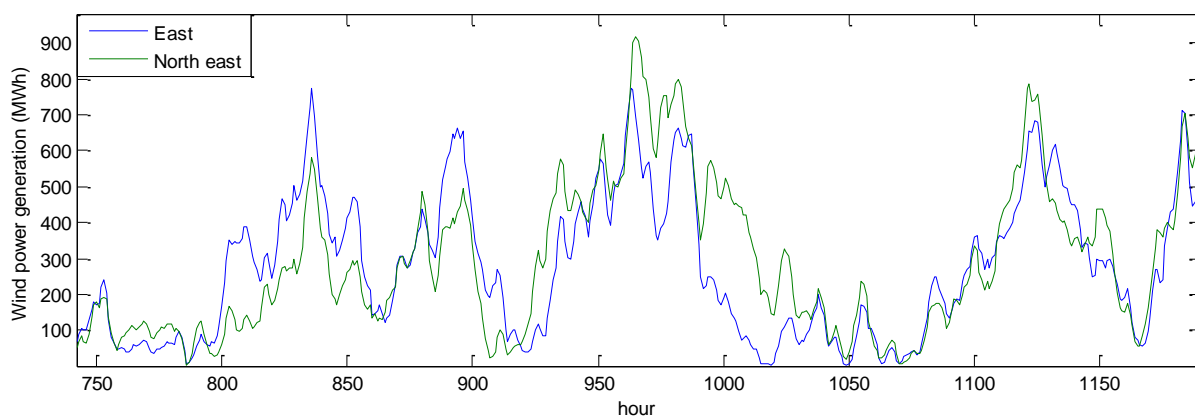


Figure 22. Correlated time series of wind power generation in two zones of France (correlation of 78.7% between their stochastic components)

Other tests have been performed with other types of time series and give similar results. The TS generator proves to be efficient to generate time series with the desired cross-correlations.

3.4.4. An example of time series of thermal outages

This sub-section presents a time series of the unavailability of thermal units sampled for the IT integration test of WP8. As presented in Section 2.2, this test contains 287 thermal units, for a total installed capacity of 154 GW. Most of the thermal units have a forced outage rate of 5% and are therefore out of order during, in average, 18 days a year. The failure of the thermal units is added to the scheduled maintenance (planned shutdown, refuelling,...), which is fixed deterministically, *ex-ante*, as presented in Section 2.

In short, for each thermal unit, 36 days of maintenance are already planned in the year. The forced outages are then randomly sampled, with the method presented in Section 3.3, and complete the time series of thermal unavailability. The 287 time series of outages are drawn independently for each thermal unit.

The sum of the total unavailable capacity has then been calculated, and the result obtained in any MC year is presented in Figure 23. The capacity in maintenance, identical for all MC years, is plotted in blue. The total unavailable capacity, also including the unplanned outages, generated by the TS generator, is plotted in green.

The planned maintenance is not constant over the year. Indeed, more maintenance is performed in summer when the load is expected to be lower. The forced outages are, in the contrary, more spread along the year. The expected thermal capacity subject to forced outages is indeed equal to 5% of the total capacity, that is to say 7.7 GW, and this for every day of the year.

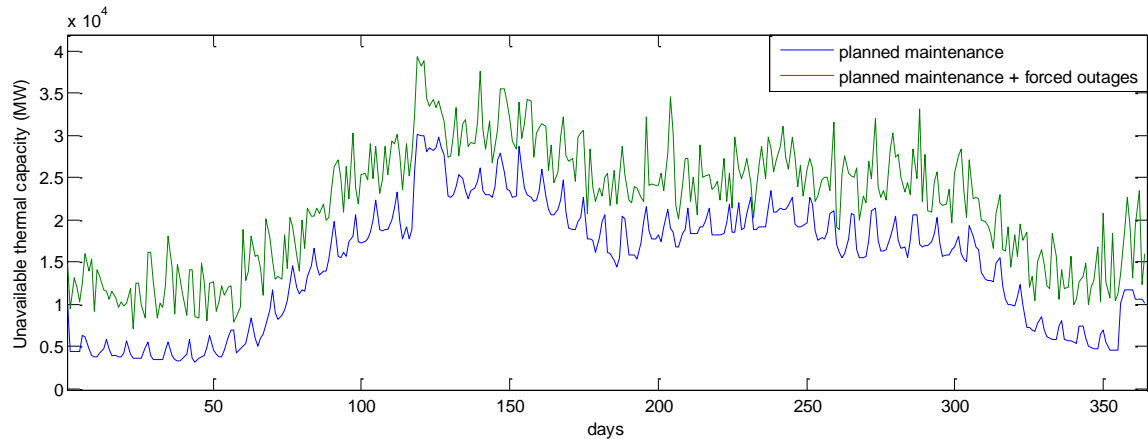


Figure 23. Thermal unavailability (maintenance + forced outages) of one MC year from the integration test of WP8, including France and Spain

Due to the high amount of thermal units in the system, the total unavailable thermal capacity is quite close from one MC year to another. However, the detailed time series of the state of each unit will be, most likely, different for every new generated year. Consequently, for a given day, the location of the non-functioning units should vary significantly from one MC year to another.

4. Allocation of hydrological resources

As presented in the introduction, it has been decided to divide the yearly adequacy problem into 52 weekly sub-problems. This decomposition requires dealing first with the issues of the system which needs to be handled on a one-year basis, and notably:

- the scheduling of the maintenance of thermal units, which has to be synchronised with the seasonality of the consumption and intermittent renewable generation. The maintenance schedule is determined with the heuristic presented in Section 2. And,
- the management of the hydro reservoirs, which has to be optimised so as to discharge the highly seasonal hydro inflows during the weeks when they are the most needed.

This second issue is presented in this section. It consists in optimising the dispatch of the water resources over the 52 weeks of the year.

More precisely, the hydro allocation strategy selects the amounts of hydro energy which will be used during each week of the year. Equivalently, it deduces the intermediary targets – volume to be reached at the end of each week – of the hydro reservoirs. This procedure is made in accordance with the capacity of the reservoirs and the inflows supplying each of them. A similar approach was used in WP2 using ANTARES (see D8.2 “Data sets of scenarios for 2050”).

Section 4.1 presents the concerns of the weekly division of the problem while Section 4.2 presents the general architecture of the hydro allocation problem

4.1. *Decomposition of the problem*

Decomposing the yearly adequacy problem allows to approach the real operation process

The division of the yearly adequacy problem is proper to the real operation of the electrical system.

The system is indeed subject to uncertain events (outages, inflows, intermittent RES, variations of the consumption) which cannot be precisely forecasted. The operation of the system has to deal with these uncertainties. For this reason, it can be seen as a dynamic process which is regularly adjusted as new information and new forecasts are available. For instance, a first generation schedule is cleared in the day-ahead market which meets the forecasted residual demand, and this schedule is then adjusted in the intraday market in order to fit the real (not forecasted) residual demand.

In any case it cannot be assumed realistic to plan the operation of the system with a 1-year perfect foresight. The uncertain events affecting the system cannot be predicted on such a long-term and the planned operation must be revised regularly so as to adapt to the evolution of the forecasts. The operation of the electrical system is therefore naturally sub-optimal. In other words, scheduling the generation on a 1-year period with exact values of the stochastic phenomena would be over-optimistic.

The weekly decomposition of the problem offers the advantage of mimicking this constantly evolving process.

Several methods have been developed in the literature to dispatch the hydro resources in a system subject to uncertainties [36]-[37]-[38]-[39]-[40]. The most popular ones are based on stochastic dynamic programming (SDP) [40]. They compute the optimal hydro dispatch of the current time step by considering all the possible evolutions of the stochastic phenomena (inflows, load, etc.). SDP requires a complete characterisation of the forecasts and forecasts errors of the stochastic phenomena; its implementation is

therefore quite heavy. It is typically used to operate the electrical system dominated by hydro generation, such as the Norwegian or Brazilian ones.

For the sake of simplicity, we decided to use a simpler version of SDP, called “Deterministic Dynamic Programming” and presented by Zambelli & al. in [36] and [39]. The approach is dynamic in the sense that it is based on an iterative algorithm – called rolling planning – which consists in iteratively calculating the dispatch of the current time step and updating the forecast of the stochastic variables. Contrary to SDP it is deterministic in the sense that it considers only the most probable evolution of the stochastic phenomena instead of considering all the range of their possible evolutions.

4.2. The rolling planning of hydro resources

4.2.1. Architecture

The method proposed for the WP 8 of e-Highway2050 project is based on this concept of deterministic dynamic programming. It is illustrated in Figure 24.

More precisely, the hydro allocation strategy comprises 52 iterative steps. For each step w ($w \in \llbracket 1; 52 \rrbracket$):

- The hydro dispatch of week w is determined by considering the possibilities offered by the hydro system during the two following years. The balancing of the hydro resources is therefore made with an overview of the yearly seasonality of the inflows, load and uncontrollable RES. The period between week w and week 104 (last week of the second year) is considered in this step.
- It is assumed that the uncontrollable RES generation (wind, solar, RoR), consumption and hydro inflows can be accurately forecasted for the week to come. Their *real values* (sampled by the TS generator) are then used for the week w . The hydro dispatch is therefore able to adapt to short disturbances (e.g. increase of the hydro generation when the load is especially high during one week).
- It is assumed that the stochastic phenomena cannot be accurately forecasted after 1 week.
- The *expected seasonality* of the wind power generation, solar generation and consumption are used from week $w + 1$ until the end of the period. These phenomena are highly intermittent and can hardly be forecasted after 1 week. It would be unrealistic (over-optimistic) to use the real values instead.
- An *imperfect forecast* of the hydro inflows is used from week $w + 1$ until the end of the period. As presented in Section 3.4.2 the hydro inflows are strongly temporally correlated and they can therefore be predicted on longer periods than the consumption and uncontrollable RES. The imperfect forecast of the inflows lies between their *real values* and *expected seasonality*.
- An optimisation problem – called weekly allocation problem – is solved under these conditions. It aims at finding the optimal (less expensive) generation schedule which balances the load. It is a sort of rough adequacy model, with just one representative hour for each week (with average values of power) and a simplified description of the behaviour of the system.
- The volume in each of the reservoir at the end of week w is saved. It defines the amount of water allocated to this week. The whole process is then iterated.

We make the approximation that the generating fleet is unchanged during the second year. *The expected seasonality* of the first year is therefore also used to describe the evolution of the stochastic inputs during the second year.

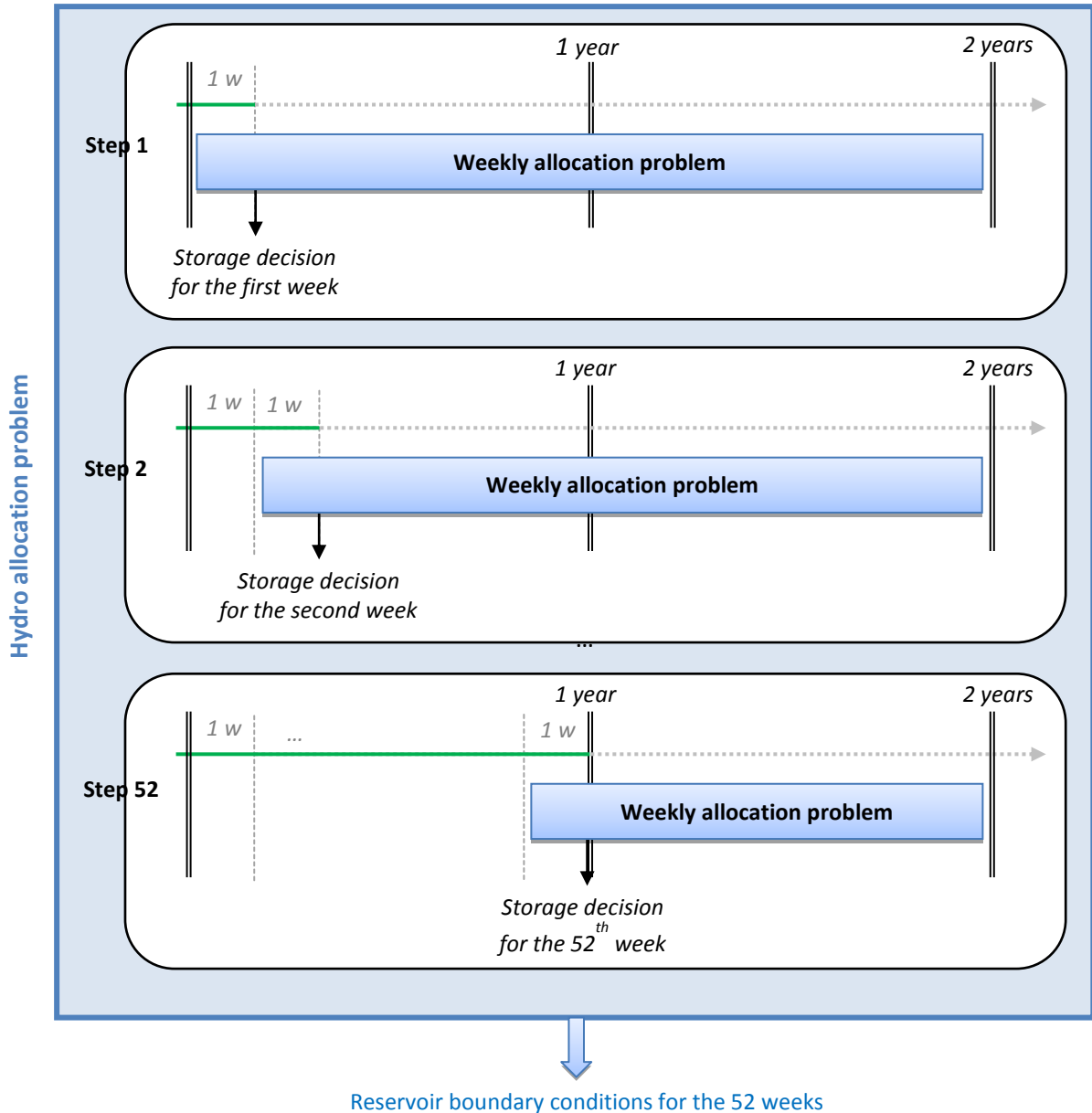


Figure 24. Rolling planning of the hydro resources. The solid green line on the timeline represents a perfect knowledge of the uncertainties (inflows, intermittent RES, consumption) while the dotted grey line depicts the imperfect forecast of the inflows and the expected seasonality of the other uncertainties.

Contrary to the approaches which solve the problem over one year with a pre-defined volume target at the end of the 52nd week [41], the approach employed here does not impose a fixed reservoir volume in the end of the first year. The hydro generation is adjusted to the inflows of the year and in practice, by using this method:

- extra stored water will be used if the realized inflows are lower than expected, and so the reservoir volume in the end of the year will be lower than the one in the beginning,
- the hydro units will store a higher volume than expected if the inflows are especially high, and so the reservoir volume in the end of the year will be higher than the one in the beginning.

The proposed method therefore provides a long-term management of the water resources which tends to compensate the meteorological conditions on a multi-year horizon.

The so-called “weekly allocation problem”, run in each step of the method, is presented in the next section.

4.2.2. Mathematical formulation

The weekly allocation problem

The weekly allocation problem is a linear optimisation program, used in each iteration of the hydro allocation problem. It is a rough adequacy model – with just one representative hour for each week (with average values of power) – whose goal is to dispatch the hydro and thermal resources at a minimal cost.

The weekly allocation problem is a simplified version of the hourly adequacy problem presented in section 5. Its objective is to minimise the thermal generation and exchanges costs. Thermal generation is simply bounded by the installed capacity (adjusted with the unavailability due to maintenance) and its flexibility is not modelled. A linear model is used to describe the management of the hydro resources and the evolution of the volume in the hydro reservoir.

For the sake of brevity, the objective and constraints of the weekly allocation problem have been put back in Annex C.

This weekly allocation problem is approximate as it is based on the weekly average values of the load, RES, hydro and thermal generation and it does not take into account the hourly variability of those parameters. However, its goal is just to obtain the intermediary targets of the hydro reservoirs. The real hourly dispatch is computed afterward at an hourly time step.

For instance, Figure 25 compares a theoretical average weekly value (in red) with a possible hourly dispatch (in blue). It has to be recalled that the hourly hydro-thermal dispatch is flexible – and can be therefore used to compensate the variability of the net load – even if it appears fixed in the weekly allocation problem. Moreover, as implied by Figure 25, it is also conceivable that the hourly dispatch which will be computed afterward includes both generation and pumping cycles even if one of these two average variables is equal to zero in the weekly allocation problem.

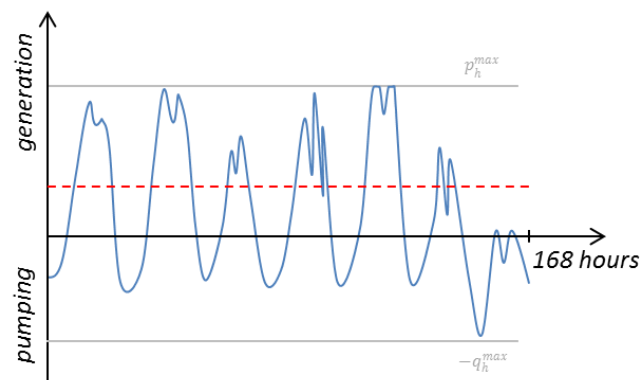


Figure 25. Possible hourly dispatch vs. weekly average

Post-processing

The hydro generation is provided free of charge in the weekly allocation problem. The optimisation problem is therefore not able to cleverly define a merit-order of the different hydro units. It has an infinite number of solutions, of which counterintuitive and unlikely ones.

For example, let's denote A and B two countries of a hypothetical power system. The weekly allocation problem will calculate the optimal yearly dispatch of the hydro resources taken altogether, but it will not be able to prioritize the ones of country A or B. One optimal solution could therefore be a hydroelectric production in country A during the first half of the period, followed by an inactivity of the hydro units of country A during the second half which are replaced by hydro generation in country B. This solution is obviously unlikely.

As explained in Annex C, a post-processing optimisation is therefore run in order to ensure that the hydro generation is logically divided among the hydro units.

Implementation

The weekly allocation problem and post-processing routine have been written in AMPL [61] and are solved with FicoXpress [62].

The iterative algorithm of the rolling planning is as well implemented in AMPL.

5. Adequacy simulations

This section presents the mechanisms of the hourly adequacy simulations – fourth and last step of Task 8.2.

For each hour of a given week, the operation of the electrical system is simulated. Given the available controllable generation means and the time series of non-controllable RES and demand, the optimal (less-costly) dispatch of the generating units which meets the consumption is calculated. Demand Response (DR), exchanges with neighbouring systems and other controllable elements of the system which participate in the balancing of the consumption and generation are simulated as well.

The goal of the TS generator was to determine time series of the non-controllable generation and demand. Adequacy simulations are performed in order to generate the time series of the controllable generation means as well.

We recall that the network is not modelled in Task 8.2. Adequacy simulations are performed in a copperplate model, i.e. with infinite transmission capacities between each zone of the system. Their goal is to determine the ideal generation dispatch, the one that the future grid should ideally transmit at the least system cost. Similar simulations are performed in WP2 using ANTARES (see D2.1 “Data sets of scenarios for 2050”).

The adequacy model implemented is described in Section 5.1 and 5.2. Typical results are presented and analysed in Section 5.3.

5.1. The adequacy model

The detailed mathematical formulation of the hourly adequacy model is presented in this part. It consists in one optimisation problem for each week of the year, where the optimal generation schedule which balances the load is calculated.

The 1-week simulations are computed with a perfect foresight, the *expected seasonality* of the stochastic inputs is put aside and only the *real values* (time series sampled in the MC year) are considered. It seems indeed conceivable to have an accurate forecast of the load and the uncontrollable RES generation on such a short horizon – in practice, the deviations from the forecast are corrected by the intra-day market, the sub-optimality due to this adjustment process will however be assumed insignificant in our context. This perfect foresight allows us to only focus on the technical modelling of the elements of the network and to forget the probabilistic behaviour of its operations.

Throughout the rest of this part, fixed parameters are represented by capital letters while lower cases are used for variables.

5.1.1. Thermal unit model

The thermal unit model is mainly based on the paper of G. Morales-España & al. [42][1]. It offers a unit commitment model, with a representation of the flexibility of the units via minimum up-down times constraints. Moreover, the formulation of the unit-commitment problem is tight and compact and particularly suited for commercial MILP solvers.

Characterisation of the thermal units

The set of all the thermal units of the system is denoted \mathcal{G} . Each thermal unit $g \in \mathcal{G}$ is characterised by the following parameters:

- P_g^{min} and P_g^{max} , minimum stable power and maximum output power of unit g . They define the stable power region within which a unit can be operated.
- D_g^{up}, D_g^{down} , minimum up and down times of unit g . The unit has to operate for a minimum time before it is shut down, in order to avoid component stresses (minimum up time). It also has to wait for a minimum time between two operational cycles (minimum down time).
- C_g^{lin} , linear variable cost of unit g , is the cost of operating the unit. It depends on the fuel cost and thermal efficiency, and is a linear function of the unit loading.
- C_g^{nl} , no-load cost (constant cost) of unit g . The no-load cost corresponds to the cost of fuel used to keep the unit warm in a stand-by phase.
- C_g^{start} , start-up cost of unit g
- $A_{g,t}$, availability of the unit g during the hour t , deduced from the maintenance schedule (see Section 2) and the time series of outages (see Section 3.3)

Except for the availability of the thermal units, which is deduced from the previous steps of Task 8.2, all the other parameters are general inputs of the methodology which must be determined for each scenario and time horizon.

We advise to use generic values for each type of generation source and/or technology. For example, one set of parameters for all the nuclear units, one other set for all the gas units, etc. Different technologies can also be distinguished if they have significantly different characteristics (e.g. units with carbon capture and storage). The description of technologies and types will depend on the study.

The calibration of these parameters is a sensitive task. Costs have to be calibrated in accordance with the planned evolution of fuel and CO₂ prices, while the technological limits must be based on average values of the installed units.

The operation of a thermal unit g is characterised by the following variables:

- $p_{g,t}$, power output at hour t of unit g , generation above the minimum stable power P_g^{min} (≥ 0)
- $u_{g,t}$, commitment status at hour t of unit g (binary)
- $u_{g,t}^{up}$, start-up status at hour t of unit g (≥ 0)
- $u_{g,t}^{down}$, shutdown status at hour t of unit g (≥ 0)

The commitment status of the thermal unit is a binary variable, equal to 1 if the unit is on, and 0 if it is off. Start-up and shutdown statuses follow the same logic, they are respectively equal to 1 if the unit is switched on or switched off during the considered hour and equal to 0 otherwise. Note that start-up and shutdown statuses are defined as positive continuous variables, but a constraint (Equation 6.5) forces them to take binary values.

In this model, $p_{g,t}$ is equal to the output power of the unit above the minimum stable power. It allows a tighter formulation of the adequacy problem and a shorter resolution time [42]. The total output power of unit g at hour t is therefore equal to:

$$u_{g,t} P_g^{min} + p_{g,t} \tag{6.1}$$

The cost of the thermal generation is composed of a linear cost, proportional to the total output power, a constant cost (also called no-load cost), which is proportional to the commitment status of the unit, and finally a start-up cost, which takes effect occasionally, when the unit is switched on. The total generation cost of unit g at hour t is given by Equation (6.2).

$$TC_{g,t}^{thermal} = \underbrace{(u_{g,t} P_g^{min} + p_{g,t}) C_g^{lin}}_{linear\ cost} + \underbrace{C_g^{nl} u_{g,t}}_{constant\ cost} + \underbrace{C_g^{start} u_{g,t}^{up}}_{start-up\ cost} \quad (6.2)$$

The operational constraints which bound and link the variables of the thermal units are described in the next paragraph.

Operational constraints

$p_{g,t}$ is limited by the capacity of the unit g via a constraint in Equation (6.3). This constraint also forces the output power to zero when the commitment status of the unit is off.

$$p_{g,t} \leq (P_g^{max} - P_g^{min}) u_{g,t} \quad \forall g, t \quad (6.3)$$

Moreover, the commitment status is fixed to zero when the unit is unavailable.

$$u_{g,t} \leq A_{g,t} \quad \forall g, t \quad (6.4)$$

The commitment status of the thermal units is logically linked to the start-up and shutdown statuses through the constraint in Equation (6.5). As both $u_{g,t}^{up}$ and $u_{g,t}^{down}$ are positive, they are forced to take the values of $|u_{g,t} - u_{g,t-1}|$ and they are inherently binary even if they are not defined so. Note that the minimum up-down time constraints (6.6) and (6.7) prevent the unit to start-up and shut-down at the same time t .

$$u_{g,t} - u_{g,t-1} = u_{g,t}^{up} - u_{g,t}^{down} \quad \forall g, \forall t > 1 \quad (6.5)$$

The minimum on and off time of the thermal units are imposed by the two following constraints. Equation (6.6) forces the commitment of the unit to 1 if it has been started up in the previous D_g^{up} hours, while Equation (6.7) forces the commitment of the unit to 0 if it has been shut down in the previous D_g^{down} hours. Thus, a thermal unit g has to be online during a period of at least D_g^{up} hours, and offline during a period of at least D_g^{down} hours.

$$\sum_{i=t-D_g^{up}+1}^t u_{g,i}^{up} \leq u_{g,t} \quad \forall g \in \mathcal{G}_1, \forall t \geq D_g^{up} \quad (6.6)$$

$$\sum_{i=t-D_g^{down}+1}^t u_{g,i}^{down} \leq 1 - u_{g,t} \quad \forall g \in \mathcal{G}_1, \forall t \geq D_g^{down} \quad (6.7)$$

\mathcal{G}_1 is the set of thermal units with minimum up and down times of less than 168h. For the special case of the nuclear units – which can have minimum up and down times of 168h, equal to the duration of the period on which the adequacy problem is solved – constraints in Equations (6.6) and (6.7) are replaced by Equation (6.8). This means that the nuclear units cannot be shut down or started up during the week. Changes in the commitment status of the nuclear units can only take place between two weeks.

$$u_{g,t} = u_{g,t-1} \quad \forall g \in \mathcal{G} \setminus \mathcal{G}_1, \forall t > 1 \quad (6.8)$$

Overlapping of the operational constraints between weeks

The adequacy problem is solved iteratively for each week of the year. Each week is considered knowing the previous weeks, but independently of the weeks to come. This poses the problem of the overlapping of the time dependent constraints between weeks. And notably:

1. How to ensure that the state of the system at the **beginning of the week** is coherent with the state of the system at the end of the previous week ?

Example: if a thermal unit g has been started up in the last hour of the week $w - 1$, we have to take into account that it has to remain online during the first D_g^{up} hours of the adequacy problem of week w .

Concerning this first point, constraints in Equations (6.6) and (6.7) are extended to the first time steps by considering the value of the variables obtained with the adequacy problem of the previous week. For example, Equation (6.7) is completed by Equation (6.9), where $U_{g,168}^{W-1}$ is the commitment status of unit g of the last hour of the previous week.

$$u_{g,1} - U_{g,168}^{W-1} = u_{g,t}^{up} - u_{g,t}^{down} \quad \forall g \quad (6.9)$$

2. How to constrain the units at the **end of the week** in order to propose a state at the beginning of the following week coherent with the expected needs of the power system ?

Example: should we shut down a unit with a long minimum down time at the end of week w while it could be useful to supply the load of the beginning of week $+1$?

The load in the end of the week (Sunday evening) is typically lower than the average weekly load, and the needs of thermal generation are therefore lesser. Thus, the adequacy problem solved on one week will tend to shut down thermal units the Sunday evening (whatever their minimum down times are). However, the load is usually increasing in the Monday morning and the units which have been shut down the Sunday evening might not be available to supply it. The second point listed above aims at preventing this situation.

Constraint in Equation (6.10) is added to the problem. It is a “rolled-up” version of constraint (6.7) where the shutdown statutes in the last D_g^{down} hours of the week are compared to the commitment status of the beginning of the week. More precisely, if the unit was used on Monday morning, shutdowns are forbidden in Sunday evening in order to make sure that the unit will be available in the beginning of the following week.

$$\sum_{i=168-D_g^{down}+t+1}^{168} u_{g,i}^{down} \leq 1 - u_{g,t} \quad \forall g \in \mathcal{G}_1, \forall t < D_g^{up} \quad (6.10)$$

Remarks on the complexity of the model of thermal units

The thermal unit model can seem quite complex for a study at a pan-European scale. The use of a unit-commitment model with binary variables and time dependent constraints on such a large area indeed implies a high computational complexity. This complexity has already been tackled in the literature and it is also taken into account with ANTARES in WP2 (see D2.1 “Data sets of scenarios for 2050”).

Sensitivity analyses were performed in section 6 in order to evaluate the impact of this modelling on the accuracy of the results of adequacy simulations.

5.1.2. Hydro unit model

Required data and aggregated model

Hydro units are represented by an aggregated linear model.

In order to model properly the behaviour of such units, large amounts of data are required: the capacity of the unit, but also the size of the reservoir associated to this unit, the inflows which supply its reservoir (time series), the pumping capacity of the pumped-storage hydro power plants (PSP) and their pumping rate.

The literature offers numerous models of hydro units, from simple linear models [37] to complete models which take into account head losses and the dependence of the efficiency of the unit to the water level of its reservoir [39]. Some authors also propose to model the interlinking of the inflows in the hydro valleys [41]. The obstacle to the use of such complete models is that they require large amounts of data on each of the hydro unit of the system. They are interesting for energy producers who have a perfect knowledge of their installed power plants, or for TSOs who can get access to detailed data on the hydro power plants connected to their network. However, they seem inappropriate to European projects: the gathering of detailed and homogeneous data on a large-scale system (which implies numerous stakeholders) is often a thorny task.

An aggregated model has therefore been retained in the WP8 of e-Highway2050. Hydro units are aggregated by country and by type. Three types are distinguished: run of the river (RoR) units, hydro with storage and pumped-storage power plants (PSP). Each country therefore possesses three aggregated units.

RoR are non-controllable. They therefore participate as a fixed parameter in the optimisation problem. On the contrary, hydro with storage and PSP are controllable and their management is modelled in the adequacy.

Characterisation of the hydro resources of a country

For each country $c \in \mathcal{C}$, the hydro resources are characterized by:

- $I_{c,t}$, hourly time series of inflows of the country
- R_c^{RoR} , ratio of the inflows of the country which supply RoR power plants,
- R_c^{stor} , ratio of the inflows of the country which supply hydro with storage power plants,
- R_c^{PSP} , ratio of the inflows of the country which supply PSP,

$I_{c,t}$ is the time series of inflows of the country, sampled by the TS generator. R_c^{RoR} , R_c^{stor} and R_c^{PSP} are respectively the ratio of the inflows which supply the RoR, storage power plants and PSP. The sum of the three ratios is obviously equal to 1. There are specific to each country and can be estimated on the base of historical data.

The generation of RoR is equal to $I_{c,t}R_c^{RoR}$ and is a fixed parameter of the problem. The models for hydro power plants with reservoir and PSP is presented in the next paragraph.

Characterisation of the aggregated hydro units

We denote $\mathcal{H}(c)$ the set of aggregated hydro units of country c . $\mathcal{H}(c)$ usually contains two elements, one for the hydro with storage, and one for PSP. Each aggregated hydro unit $h \in \mathcal{H}(c)$ is characterised by the following parameters:

- P_h^{min} , minimum output power
- P_h^{max} , maximum output power

- V_h^{max} , reservoir limit
- V_h^0 and V_h^{168} , amount of water in the reservoir in the beginning of the week, and objective for the end of the week.
- Q_h^{max} , pumping capacity
- $\lambda_h^{pumping}$, pumping rate

P_h^{min} , P_h^{max} , V_h^{max} and Q_h^{max} are the aggregated technical limits, obtained by summing the limits of all the hydro units represented by h . They are specific to each scenario and time horizon. This generic model embraces both hydro plants with storage and PSP, but the aggregated hydro plant with storage obviously has a pumping capacity equal to 0. The volumes in the beginning and the end of the week, V_h^0 and V_h^{168} , are calculated during the weekly allocation of the hydro resources (see Section 4).

Hydro generation is supposed to be costless. However, the volume in the reservoir of unit h at the end of the week has to meet the objective defined in the previous step of the methodology. Equivalently, the weekly generation of the unit is limited to a fixed amount. The goal of the model is to allocate optimally this amount among the 168 hours of the week.

The operation of an aggregated hydro unit h is modelled by the following variables:

- $p_{h,t}$, energy generated during hour t (≥ 0)
- $q_{h,t}$, energy pumped during hour t (≥ 0)
- $v_{h,t}$, amount of water in the reservoir at the end of hour t (≥ 0)

The operational constraints which bound and link the variables of aggregated hydro units are described in the next paragraph.

Operational constraints

The hydro generation and pumping are naturally bounded by their technical limits:

$$P_h^{min} \leq p_{h,t} \leq P_h^{max} \quad \forall h, \forall t \quad (6.11)$$

$$0 \leq q_{h,t} \leq Q_h^{max} \quad \forall h, \forall t \quad (6.12)$$

The volume in the basin of the unit is as well bounded by the reservoir limit V_h^{max} , as imposed by the following constraint:

$$0 \leq v_{h,t} \leq V_h^{max} \quad \forall h, \forall t \quad (6.13)$$

The evolution of the volume in the reservoir is explained by Equations (6.14) and (6.15). The evolution of the reservoir volume during two consecutive time steps is balanced with the difference between water supply (inflows plus pumping) and water losses (generation). Moreover, the constraint in Equation (6.15) fixes the initial volume of the reservoir of the aggregated unit h , equal to V_h^0 .

$$v_{h,t} = v_{h,t-1} + I_{c,t}R_c^h + \lambda_h^{pumping} q_{h,t} - p_{h,t} \quad (6.14)$$

$$v_{h,1} = V_h^0 + I_{c,1}R_c^h + \lambda_h^{pumping} q_{h,1} - p_{h,1} \quad (6.15)$$

Finally, the volume in the reservoir of unit h at the end of the week has to reach the target V_h^{168} , as imposed by the constraint below.

$$v_{h,168} = V_h^{168} \quad (6.16)$$

Disaggregation

The adequacy problem is solved with the aggregated hydro units.

In a post-processing step, the aggregated generation and pumping – $p_{h,t}$ and $q_{h,t}$ – are divided among all the singular units represented in h . The interest of this disaggregation is to map the global values of generation and pumping among the different units – and so the different nodes – of the power system. Nodal values are indeed needed in order to perform the TEP afterwards.

$p_{h,t}$ and $q_{h,t}$ are divided proportionally to the capacities of each unit which forms the aggregate h .

Let's note i a singular unit of the aggregate h , $\rho_{h,i}^{min}$ and $\rho_{h,i}^{max}$ its minimum and maximum output powers and $q_{h,i}^{max}$ its pumping capacity, then the final generation and pumping of unit i are calculated with the two following equations:

$$generation(i, h, t) = \rho_{h,i}^{min} + (p_{h,t} - P_h^{min}) \frac{\rho_{h,i}^{max} - \rho_{h,i}^{min}}{P_h^{max} - P_h^{min}} \quad (6.17)$$

$$pumping(i, h, t) = q_{h,t} \frac{q_{h,i}^{max}}{Q_h^{max}} \quad (6.18)$$

5.1.3. Demand response model

Demand response (DR) has been identified as one of the controllable elements of the system which could be deployed to a great extent in the next decades. As it could have a substantial role in some of the 2050's scenarios, it has been integrated in the adequacy model. One of our goals is also to analyse its impact on the balancing of the electrical system. A study has been realised in this purpose and is presented in Section 6.

Introduction on demand response

Demand Response refers to the changes in the electric usages of the consumers in response to signals transmitted by the system operator. Reference [55] identifies different actions by which a consumer response may be achieved. The most common one is the load-shifting, which consists in rescheduling – anticipating or postponing – one part of the demand. Some end-use consumptions of electricity are naturally flexible and can therefore be rescheduled in exchange for a low loss of comfort. These end-use consumptions possess a good potential for DR, this is for instance the case of the charging of Electric Vehicles (EVs), heating and cooling, white goods (e.g.: washing machines, dryers, dishwashers) and some industrial processes.

DR offers a new flexibility to the load which can be used to balance the power system. The impacts of this new controllability of the load have been largely studied in the literature. DR has been proven efficient to reduce the operational cost of the system, to reduce the congestions in the network, to avoid the curtailment of intermittent Renewable Energy Sources (RES), to decrease the emissions of CO₂, to diminish the need of new peaking units, to strengthen the reserve and to increase the reliability of the system. A

state-of-the-art on DR models has been written for the purpose of this project and is transcribed in Annex D.

Characterization of demand response

We denote $\mathcal{D}(c)$ the set of types of demand response of country c . If the considered long-term scenario is detailed enough, a distinction can indeed be made between different types of demand response (typically, DR of different sectors or different end-use consumptions). Yet, if such details are not available, countries can contain only one type of demand response, covering all sectors and end-use consumptions.

For each country c , each type of demand response $j \in \mathcal{D}(c)$ is characterised by the three following parameters:

- $R_{c,j}^{DR}$, the participation rate, i.e. the percentage of the total load which participate in DR
- $L_{c,j}^{DR}$, the delay time
- $C_{c,j}^{DR}$, the associated cost

No distinction is made between price-based and incentive-based mechanisms (see annex D for more details on the different mechanisms of demand response). It is indeed quite optimistic to assume that level of detail for a scenario at the horizon 2050. It seems therefore more reasonable to represent all mechanisms of DR within a common model. The model implemented in the WP 8 of e-Highway2050 is described below.

For each country c and each type of demand response $j \in \mathcal{D}(c)$, the demand response actions are managed through the following variables:

- $d_{c,j,t}^+$ upward demand modification
- $d_{c,j,t}^-$ downward demand modification
- $dh_{c,j,t}$ demand on hold

The adjusted time series of load of country c , after the modifications due to DR, is as well a variable of the optimization problem:

- $d_{c,t}$, adjusted time series of demand

Operational constraints

DR is directly modelled in the adequacy problem, through a set of new variables and constraints which allow changes in the load time series. The model retained is mainly based on the one of Göransson & al [44].

In the adequacy problem, time series of demand can be modified according to constraint in Equation (6.19), where $L_{c,t}^0$ is used to denote the initial time series of consumption of country c (sampled by the TS generator). $d_{c,t}$ is the adjusted time series of demand, after the upward and downward modifications – respectively $d_{c,j,t}^+$ and $d_{c,j,t}^-$ – brought by DR. Different types of demand response $j \in \mathcal{D}(c)$ can be operative in a same area.

$$d_{c,t} = L_{c,t}^0 + \sum_{j \in \mathcal{D}(c)} (d_{c,j,t}^+ - d_{c,j,t}^-) \quad \forall c, t \quad (6.19)$$

The modifications of the demand are caused by load shifting actions and are constrained by Equations (6.20-6.23). $dh_{c,j,t}$ is the demand put on hold at time t . It is defined through Equation (6.20). It is equal to

the demand which has been reduced and not postponed yet (positive) or to the demand which has been anticipated and not reduced yet (negative).

$$dh_{c,j,t} = dh_{c,j,t-1} + d_{c,j,t}^- - d_{c,j,t}^+ \quad \forall c, j, t > 1 \quad (6.20)$$

The demand on hold at the beginning of the week is initialised to zero. Moreover, to guarantee that all the shifting actions have been completed, the demand on hold of the last time step of the week is also forced to zero.

$$dh_{c,j,1} = 0 \quad \forall c, j \quad (6.21)$$

$$dh_{c,j,168} = 0 \quad \forall c, j \quad (6.22)$$

Furthermore, the demand which is shifted has to be rescheduled before the delay time $L_{c,j}^{DR}$. Equation (6.23) ensures that the demand put on hold is recovered in the next $L_{c,j}^{DR}$ hours, while Equation (6.24) ensures that the demand which has been anticipated is reduced in the next $L_{c,j}^{DR}$ hours.

$$dh_{c,j,t} \leq \sum_{l=1}^{L_{c,j}^{DR}} d_{c,j,t+l}^+ \quad \forall c, j, t < 168 - L_{c,j}^{DR} \quad (6.23)$$

$$-dh_{c,j,t} \leq \sum_{l=1}^{L_{c,j}^{DR}} d_{c,j,t+l}^- \quad \forall c, j, t < 168 - L_{c,j}^{DR} \quad (6.24)$$

Finally, the modifications of the demand time series, $d_{c,j,t}^+$ and $d_{c,j,t}^-$, are bounded by the amount of demand which participates in DR: a percentage of the total demand defined by the participation rate $R_{c,j}^{DR}$.

$$0 \leq d_{c,j,t}^+ \leq R_{c,j}^{DR} L_{c,t}^0 \quad \forall c, t, j \quad (6.25)$$

$$0 \leq d_{c,j,t}^- \leq R_{c,j}^{DR} L_{c,t}^0 \quad \forall c, t, j \quad (6.26)$$

Note that the demand is modified through load shifting actions only – load shaving actions are not considered. We indeed think that the model would be more reliable if the total yearly consumption of each country is preserved. This model is similar to the one used in WP2 (see D2.1 “Data set of scenarios for 2050”).

Cost of demand response

A linear cost is associated to demand response:

$$TC_{c,j,t}^{DR} = C_{c,j}^{DR} d_{c,j,t}^- \quad \forall c, \forall j, \forall t \quad (6.27)$$

Assuming the cost of DR on a long-term horizon is not an easy task. We propose here some guidelines in order to build this cost depending on the place of DR in the merit order. Three possible cases are distinguished below.

1st case: $C_{c,j}^{DR} = 0$, demand response is free. In this configuration DR is highly competitive. It will encourage re-dispatching toward less expensive generation means and will be used to reduce both the unwanted curtailment of load and the energy in excess in the system. Furthermore, it will be economically preferred

to more classic storage means, such as pumped-storage hydro plants. We advise to use free demand response to represent price-based mechanisms, which imply high investments costs (meters and smart-grids) but low operational costs.

2nd case: $C_{c,j}^{DR} = C^{base} (1 - \lambda^{pumping}) / \lambda^{pumping} + 1$, demand response has a low cost and is competitive. In the previous equation C^{base} represents the typical costs of cheap thermal generation means (e.g. nuclear) and $\lambda^{pumping}$ a typical value of hydro pumping efficiency (e.g. 75%). Demand Response is economically competitive in the electricity markets, it will favour re-dispatching toward less expensive generation means and will contribute to reduce the amount of unsupplied and in-excess energy. Traditional hydro storage will therefore be preferred to demand response initiatives. This case is suited to represent well integrated incentive-based programs.

3rd case: $C_{c,j}^{DR} = C^{peak} + 1$, demand response has a high cost and is not competitive. In the previous equation C^{peak} is the typical cost of peak thermal units. It will only be used in order to avoid the unwanted curtailment of load. Its cost is too high to compete on the power markets and the start-up of peaking power units will be preferred to the use of DR. Moreover, under such conditions, the reduction of in-excess energy will not be favoured and the demand will not adapt to the intermittencies of the RES. We advise to use this case to model market-based programs in their infancy.

5.1.4. Extra-European exchanges model

Extra-European exchanges refer to the exchanges across the present EU borders, mainly with North Africa and Russia.

Characterisation of the extra-European exchanges

We denote \mathcal{E} the set of possible extra-EU exchanges. Each of its members e is characterised by the following parameters:

- P_e^{min} , minimum capacity of extra-European exchange e
- P_e^{max} , maximum capacity of extra-European exchange e
- $C_e^{exchange}$, cost of exchange extra-European e

The same structure is used for imports and exports. Imports typically have a P_e^{min} equal to zero and a P_e^{max} equal to the transfer capacity with the neighbouring country. On the contrary, exports have a negative P_e^{min} and a P_e^{max} equal to zero. This distinction between exports and imports is necessary if they have different costs or if the transfer capacities are different for both directions.

For the sake of simplicity, the three previous parameters have been noted without time index. However, for some scenarios and interconnections, we can imagine capacity and costs signals which vary over time. For example, in a scenario with a massive solar generation in North Africa, the import cost could vary over the 24h of the day, with low prices during daylight and higher prices during dark hours.

For each $e \in \mathcal{E}$ and each time-step, the extra-European exchange is modelled with a single variable:

- $p_{e,t}$, the exchanged energy at hour t

$p_{e,t}$ is positive when energy is imported, and negative when energy is exported.

The exchange cost is linear, simply equal to:

$$TC_{e,t}^{exchange} = C_e^{exchange} p_{e,t} \quad \forall e, \forall t \quad (6.28)$$

Operational constraints

Exchanges are naturally bounded by the maximum transfer capacity with the neighbouring country, as imposed by the following constraint:

$$P_e^{min} \leq p_{e,t} \leq P_e^{max} \quad \forall e, \forall t \quad (6.29)$$

5.1.5. National policy model

National policies reflect the level of integration of the European electricity markets. They represent the amount of energy that each country agrees to import. For instance, a wholesale integrated European electricity market would be characterized by flexible energy policies, and unconstrained cross-border exchanges.

This constraint can also be used in practice to avoid overoptimistic exchanges that would be senseless when the grid will be considered.

Characterisation of the extra-European exchanges

For each country $c \in \mathcal{C}$, the energy policy is characterised by a unique parameter:

- R_c^{policy} , the import ratio.

R_c^{policy} is the percentage of the weekly consumption of country c which must be supplied by self-production. It is an input of the overall WP8's methodology, specific to each scenario and time horizon. The choice of a weekly constraint was arbitrary. We could also have imposed that the annual imports should be lower than a certain ratio of the yearly consumption (same modelling than for hydro).

The following slack variable is used in the model of the national policies. For each country $c \in \mathcal{C}$:

- i_c^{excess} , the excess of import (≥ 0).

i_c^{excess} acts as a slack variable which allows – in compensation of a high cost – the infringement of the energy policy. It is notably used to arbitrate between unsupplied energy and excess of imports: excess of imports will be allowed if they can avoid curtailing the consumption of the country.

Operational constraints

For each country $c \in \mathcal{C}$, the total generation of the week should be equal or above the imposed ratio of the consumption, as imposed by constraint in Equation (6.30). $\mathcal{G}(c)$ and $\mathcal{H}(c)$ are respectively the sets of thermal and hydro units of the country c . $P_{c,t}^{res}$ is the time series of uncontrollable RES generation of country c and $L_{c,t}^0$ the time series of demand of the country (both generated by the TS generator).

$$\sum_t \left[\sum_{g \in \mathcal{G}(c)} (u_{g,t} P_g^{min} + p_{g,t}) + \sum_{h \in \mathcal{H}(c)} p_{h,t} + P_{c,t}^{res} \right] \geq R_c^{policy} \sum_t L_{c,t}^0 - i_c^{excess} \quad \forall c \quad (6.30)$$

$P_{c,t}^{res}$, the uncontrollable renewable generation, comprises the generation of run of the river ($I_{c,t} R_c^{RoR}$), onshore wind, offshore wind and PV. It is obtained with the TS generator.

5.1.6. Balancing between consumption and generation

Finally, the adequacy constraint ensures the equilibrium between the generation and the consumption during each hour of the studied week:

$$\underbrace{\sum_{g \in \mathcal{G}} (u_{g,t} P_g^{min} + p_{g,t})}_{\text{thermal generation}} + \underbrace{\sum_{h \in \mathcal{H}} (p_{h,t} - q_{h,t})}_{\text{hydro generation}} + \underbrace{\sum_{c \in \mathcal{C}} P_{c,t}^{res}}_{\text{uncontrollable RES}} + \underbrace{\sum_{e \in \mathcal{E}} p_{e,t}}_{\text{exchanges}} = \underbrace{\sum_{c \in \mathcal{C}} d_{c,t}}_{\text{demand}} + \underbrace{p_t^{exc} - p_t^{uns}}_{\text{slack variables}} \quad \forall t \quad (6.31)$$

In order to guarantee the feasibility of the problem, the two following slack variables are needed:

- p_t^{exc} , energy in excess in the system at hour t (≥ 0).
- p_t^{uns} , shortage of energy at hour t (≥ 0).

Energy in excess is in practice handled by curtailing RES generation.

Shortage of energy causes curtailment of consumption. For this reason, it is also often called “unsupplied energy”.

5.1.7. Minimization of the operational costs

The objective of the problem is the minimization of the operational costs (6.32) which contain the cost of thermal generation, the cost of extra-European exchanges, the cost of demand response and the penalization costs of unsupplied energy and excess of imports.

$$\min \sum_t \left[\sum_{g \in \mathcal{G}} TC_{g,t}^{thermal} + \sum_{e \in \mathcal{E}} TC_{e,t}^{exchange} + \sum_{c \in \mathcal{C}} \sum_{j \in \mathcal{D}(c)} TC_{c,j,t}^{DR} + c^{uns} p_t^{uns} \right] + \frac{c^{uns}}{2} \sum_{c \in \mathcal{C}} i_c^{excess} \quad (6.32)$$

Under the assumption of a perfect competition, the solution found by minimizing the operational cost is identical to the equilibrium which would result from the clearing of the electricity market. By searching for the less-costly generation dispatch, the adequacy model therefore aims at simulating the behaviour of the different actors of the power system. The goal of this simulation is indeed to determine how the available resources would be used in practice, hour by hour.

In Equation (6.32), c^{uns} is the cost of unsupplied energy, also called value of loss load (VOLL). Its estimation, based on the damages caused by load curtailments, is a thorny problem. Yet, from a modelling viewpoint, what matters is to fix it to a high value in order to avoid, as often as possible, the curtailment of load. For instance, a VOLL of 10.000 €/MWh has been used in the test cases of this document.

The cost associated to the infringement of the national policies over a week has been arbitrarily fixed to half of the VOLL. Excess of imports will therefore be preferred to situations which imply curtailments of consumption.

Note that no direct cost has been associated to energy in-excess. However, energy in excess implies an over-generation, and therefore the indirect generation cost of the energy which is not consumed.

5.2. Implementation

The adequacy model is defined by the objective (6.32) and constraints (6.2-6.31)

It has been written in AMPL [61].

Several solvers have been tried, notably FicoXpress [62], Cplex and Gurobi. Comparable solving times have been obtained with the three of them.

A loop has been coded in AMPL in order to solve consecutively the 52 adequacy problems of the 52 weeks of the MC year.

The implemented algorithm returns time series of generation for each of the thermal and hydro units, time series of consumption with and without demand response as well as time series of extra-European exchanges. In addition, several output files with aggregated values or reliability indicators are written in order to analyse more easily the results. Some of these results are presented in the next paragraph.

5.3. Example of generation schedules

This section presents a typical result of adequacy simulations.

The adequacy model calculates the optimal generation schedules which meet the load. Time series of generation, for each hour and each generating unit of the system, are returned by the adequacy simulator. Figure 26 depicts a typical generation schedule, where each source of energy is distinguished.

The system modelled in Figure 26 is based on the IT integration test which includes France and Spain. The generation fleet is derived from on the one of 2012, of which nuclear and coal powers have been decreased by respectively 29 GW and 8 GW and replaced by solar and wind energy. The energy mix of the system includes 32% of uncontrollable RES generation (hydro RoR, wind and solar). This test case has been built for the purpose of testing the adequacy simulator and does not aim at being realistic.

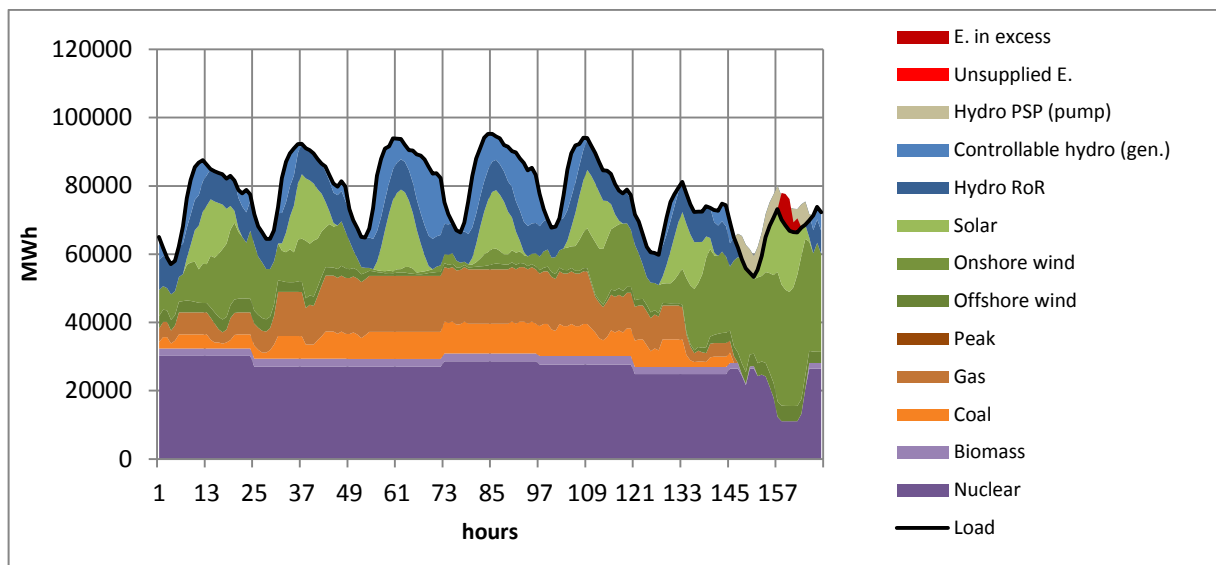


Figure 26. Generation schedule over one week

In this case, nuclear power is the cheapest thermal generation source and therefore plays the role of base load. Except during the two last days, it always attains its full generation capacity. The variations of nuclear power during the week are due to units which are turning on or off because of forced outages or maintenance operations.

The generation of the uncontrollable RES, namely wind generation, solar generation and hydro RoR, is the one sampled by the TS generator, which is fixed in the adequacy model.

The other hydro and thermal generation sources – namely hydro with storage, PSP, biomass, coal and gas units – compensate the variations of the uncontrollable RES generation and consumption so as to balance the system.

PSP units are pumping on Sunday, when the cost of electricity is low (equal to the cost of nuclear energy) and are redelivering this energy during the week, when the price of electricity is higher.

On Sunday, the system presents some energy in excess. It is favoured by a low demand and a high solar and wind power generation. The nuclear power plants are constrained by their minimum stable power and they cannot follow the intermitencies of the RES generation.

The example of Figure 26 does not contain demand response. The consumption profile is therefore fixed, equal to the one sampled by the TS generator. Moreover, the system is isolated and exchanges with neighbouring countries are not allowed.

Detailed test-cases are presented in the next section, notably to assess the influence of the model of the thermal power plants and the role of DR.

6. Sensitivity analyses

This section aims at analysing the interest of some modelling aspects of the proposed methodology. Its goal is notably to distinguish the improvements of the model which are justified on account of the precision they bring to the results from the elements whose contribution on the accuracy of the method is low.

We decided to focus on the elements which are quite innovative in adequacy simulations over large systems, notably:

- spatial correlations
- intermodal correlations
- modelling of the flexibility of the thermal units (minimum up/down times, minimum stable power, start-up costs)
- demand response

The precision they bring to the results of the adequacy simulations is analysed in a few test cases, as well as their impact on the complexity of the problem.

6.1. The influence of spatial correlations

In this first case, the influence of spatial correlations on the results of the adequacy simulator has been analysed. We recall that spatial correlations refer to dependencies of time series of the same type taken in different areas of the system. They are modelled on the innovations of the time series, as explained in Section 3.2.3.

6.1.1. Description of the test case

The French power system has been modelled using the hypotheses of the scenario “Nouveau Mix” proposed in the 2012’s adequacy report of RTE [63]. This scenario assumes a favourable RES integration at the horizon 2030, with 40% of the load supplied by renewable sources, of which respectively 14% and 6% supplied with wind and solar energy.

The system has been divided into 7 zones, depicted in Figure 27. The installed capacities of the scenario “Nouveau Mix” have been mapped over these zones and are reported in Table VII. Installed capacities and load in the scenario Nouveau Mix at the horizon 2030

. A proportional and homogenous development of the demand and RES capacities has been assumed, i.e. they have been distributed among the seven zones with the same proportions as the current ones.

The location of the hydro and thermal units is based on the current one. In order to match the evolution between the present situation and the scenario “Nouveau mix”, the oldest nuclear and coal power plants have been closed and new gas, peaking units and hydro capacities have been randomly distributed over the seven zones.

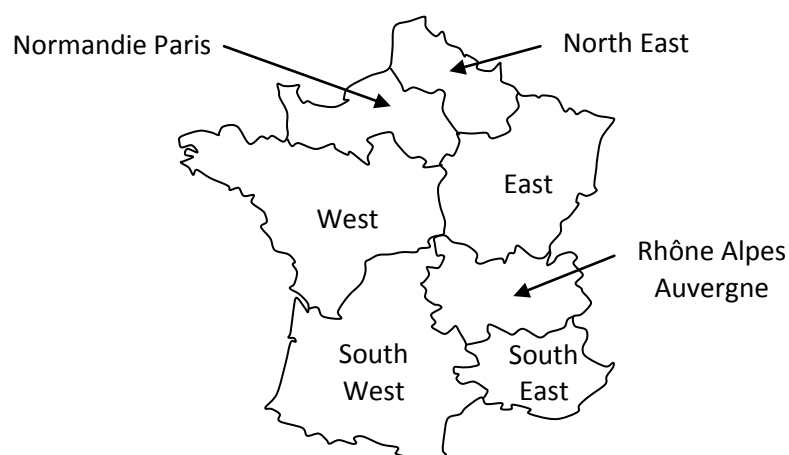


Figure 27. Seven zones of the modelled French power system

	Wind (GW)	PV (GW)	Hydro (GW)	Nuclear (GW)	Other thermal (GW)	Demand (TWh/year)
North East	9,7	0.9	0	2.9	4.6	54
Normandie Paris	6.1	1.2	0	12.0	5.8	115
East	5.3	3.6	3.1	7.8	7.9	68
West	12.6	5.7	2.5	9.2	5.6	84
Rhône Alpes Auvergne	0.8	2.4	14.1	2.6	2.6	67
South West	4.8	9.9	4.2	2.6	2.7	66
South East	0.6	6.3	4.2	2.7	7.4	62
Total	40	30	28.1	40	36.5	516

Table VII. Installed capacities and load in the scenario Nouveau Mix at the horizon 2030

The stochastic phenomena considered in this test case are the load, the wind power generation, the PV generation, the inflows and the outages of the thermal units.

Time series models of wind power generation, PV generation and demand have been calibrated for each zone, based on historical data provided by RTE. 6 years of historical have been used for the load and wind power generation, and two years of historical data for PV generation. For the three phenomena, the spatial correlations have been estimated as explained in annex A. They are illustrated in Figure 28.

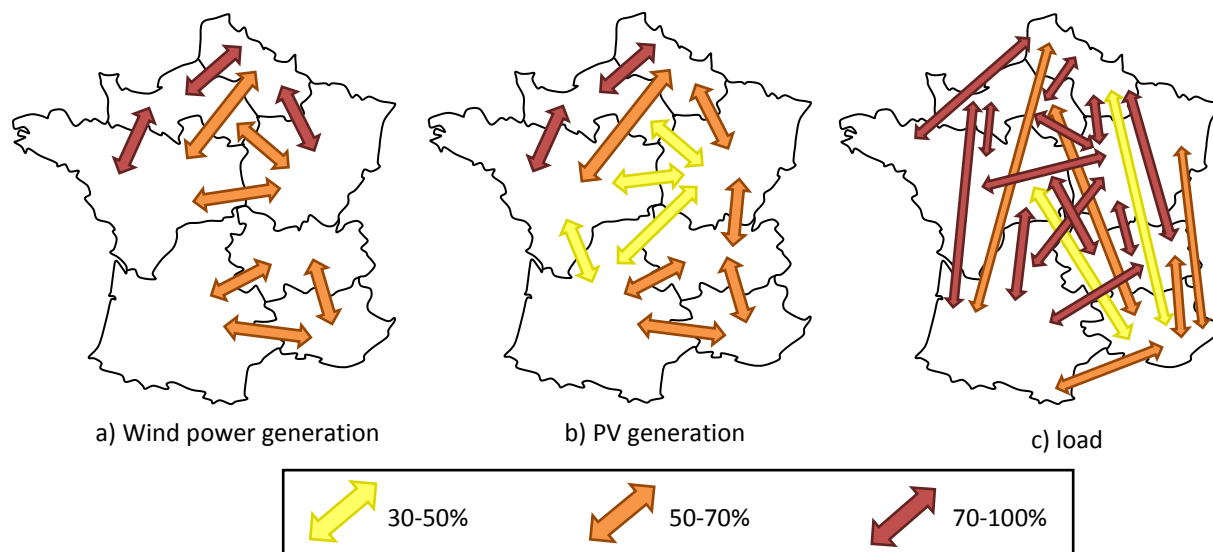


Figure 28. Spatial correlations of load (a), wind power generation (b) and PV generation (c) between seven zones in France. The correlations have been calculated from historical data, after removing their trend and their seasonality (see Equation (4.1)). Correlations between zones which are not linked by an arrow are below 30%.

The interdependencies are significant here. For instance, two zones with highly correlated wind power generation can be distinguished: the first one, which includes the four regions in the North of France, has correlation coefficients which range between 67% and 91% and the second one, with the three regions in the South of France has correlation coefficients which range between 57% and 70%. Spatial dependencies in PV generation follow a different logic where the time series of one zone is significantly correlated with the time series of the adjacent zones. Finally, the demand between the seven zones of France is highly correlated, even on long distances.

Due to the lack of available historical data, the inflows of France are modelled with only one time series common to the seven zones. This test case therefore focuses on the spatial correlation of PV, wind power and consumption.

The whole adequacy simulator – including the scheduling of the maintenance of the thermal units, the generation of the time series, the allocation of the hydro resources and the computation of the generation schedules with an hourly time step – has been run. Simulations have been performed with and without modelling the correlations depicted in Figure 28.

We recall that this task uses a “copperplate” approach. In other words congestions are not taken into account and transfer capacities between the zones are supposed infinite. Moreover, in order to highlight the influence of the spatial correlations, cross-border exchanges with neighbouring countries are not modelled and France is supposed to be an isolated system.

6.1.2. Results

100 Monte Carlo years have been simulated for both cases:

- Taking into account the spatial correlations, and
- Assuming that time series are independent.

Reliability of the power system

For each Monte Carlo year, a few reliability indicators have been retrieved: the total operational cost, the unsupplied energy, the loss of load duration (LOLD – number of hours per year during which one part of the load has to be curtailed), the energy in excess (EIE – amount of curtailed RES) and the 5% Value at risk (VaR) of the French residual load (value of the residual load which is exceeded with a probability of 5%).

The total cost includes the cost of unsupplied energy, considered equal to 10 000 €/MWh.

The expectation of the reliability indicators (i.e. their average on the 100 Monte Carlo years) is reported in Table VIII. Reliability indicators for the scenario “Nouveau Mix”, with and without modelling the spatial correlations

	Total cost (G€/year)	Energy in excess (GWh)	Unsupplied energy (GWh)	LOLD (h)	VaR of the residual load (MW)
With spatial correlations	5.4	312	20	10	6600
Neglecting spatial correlations	5.0	49	0	3	6244

Table VIII. Reliability indicators for the scenario “Nouveau Mix”, with and without modelling the spatial correlations

The unsupplied energy is clearly underestimated when the spatial correlations are neglected, it drops below 0.1 GWh while it is 20 GWh when the correlations were modelled. Equivalently, the loss of load duration is reduced when spatial correlations are not taken into account.

The total cost is underestimated by about 7 % when the spatial correlations are neglected. Around half of this difference is due to the unsupplied energy (10 GWh of unsupplied energy cost 0.1 G€) while the other half is due to the use of more expensive thermal units.

The energy in excess is also clearly undervalued when the correlations are neglected.

Finally, the 5% value at risk of the residual load is higher when spatial correlations are modelled. In other words, periods with a high residual load happen more frequently when spatial correlations are taken into account.

In this case, not taking into consideration the spatial correlations clearly biases the results of the adequacy simulations. It can mainly be explained by the fact that positive spatial correlations tend to gather extreme events (peaks and valleys) at the same moment. For instance, the simultaneity of peaks in the load will call for the use of expensive peaking power plants, or even load curtailments. On the contrary, when spatial correlations are not considered, peaks will less probably occur simultaneously and the different zones of the system will therefore be able to cooperate to compensate local extreme events. The same kind of reasoning can be made with the valleys of the load in order to explain the differences in the energy in excess.

This phenomenon is illustrated by Figure 29, which depicts the pdf of the total residual load (load minus uncontrollable generation, summed for the seven zones of the test case). The tails of the pdf are shorter when spatial correlations are neglected as extreme events (high/low load or high/low intermittent RES generation) are less likely to occur simultaneously. The variability of the residual load is undervalued when spatial correlations are neglected.

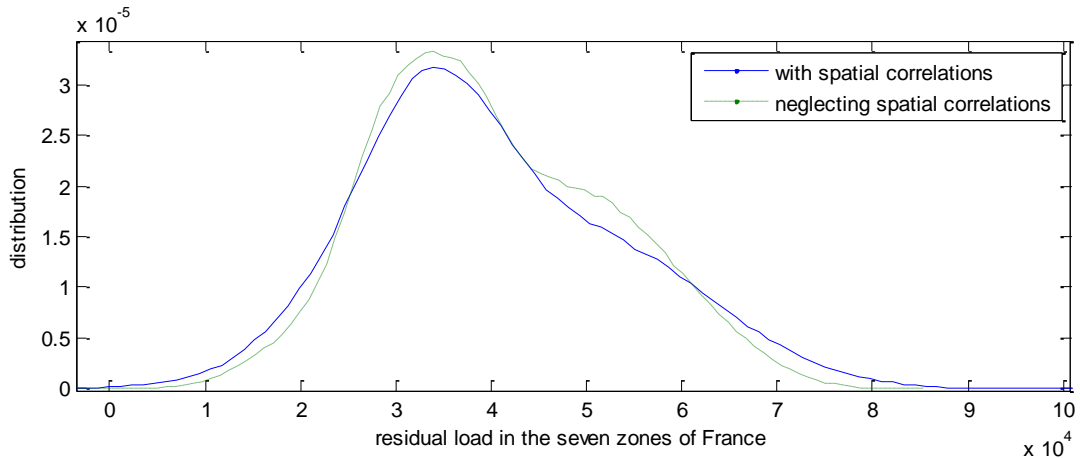


Figure 29. Probability density function (pdf) of the residual load of the scenario “Nouveau Mix”, with and without modelling the spatial correlations

Injections in each zone of the power system

The impact of the correlations on the exchanges in the system has been assessed. To do so, the time series of injections (generation minus consumption) of each zone have been analysed.

The average injection of each zone is slightly affected by the modelling of the spatial correlations. As explained in the previous part, the spatial correlations tend to stress the intermittencies of the load and RES, and so can call for the use of less base-load units and more peaking units. That is to say, spatial correlations can change the energy mix and – depending on the location of each type of generation – they can also impact the average exchanges in the system.

The differences in the injections of the studied scenario are illustrated in Figure 30. The zone with the biggest change is “Normandie Paris”; this is the zone with the highest installed nuclear capacity (see Table VII. Installed capacities and load in the scenario Nouveau Mix at the horizon 2030

). When spatial correlations are neglected, the generation of this zone increases by 7% (64 MWh/h in average). On the contrary, the generation of the zones with few nuclear power plants and a larger fleet of more expensive thermal units (e.g. South East and North East) tends to decrease. This illustrates the changes in the energy mix due to spatial correlations.

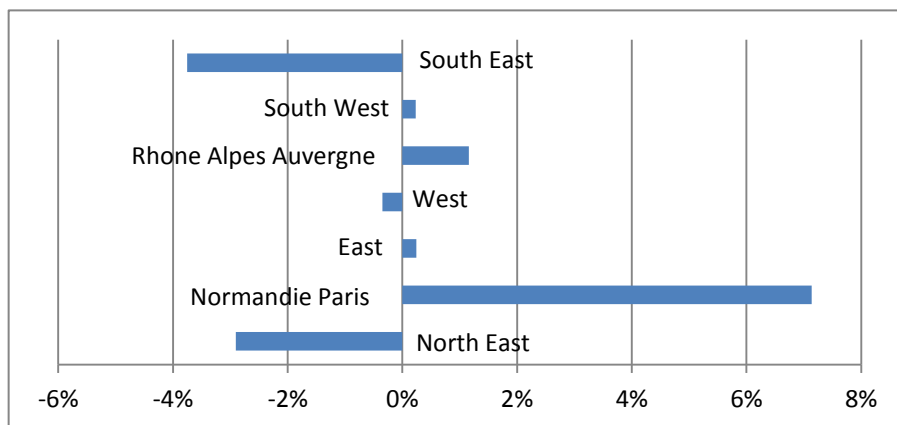


Figure 30. Changes in the average injections when spatial correlations are neglected

Moreover, the variability of the injections is also impacted by the spatial correlations. For example, Figure 31 depicts the distribution of the injection of the zone “West” over the 100 Monte Carlo years.

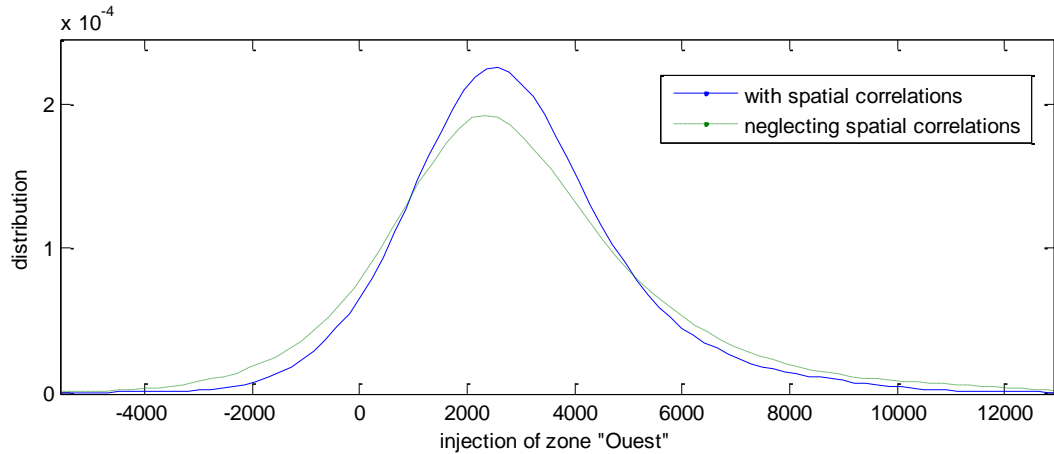


Figure 31. Distribution of the injections of the West zone, with and without spatial correlations.

For this zone, the distribution is less spread out when the spatial correlations are modelled. Four other zones of the system follow the same logic (South East, West, Normandie Paris and North East). We could explain this behaviour with the fact that, when spatial correlations are taken into account, the same variations of the residual load occur more likely simultaneously in different zones of the system. Exchanges between zones are therefore less often solicited to compensate the variability of the residual load.

On the other hand, the injections of the zone Rhône Alpes Auvergne have the opposite behaviour: injections are more spread out when spatial correlations are taken into account (see Figure 32). The same behaviour has also been observed in the South West zone. These are the two zones with the highest shares of hydroelectric power plants. The flexibility offered by this type of energy is visibly more often exploited when spatial correlations are modelled.

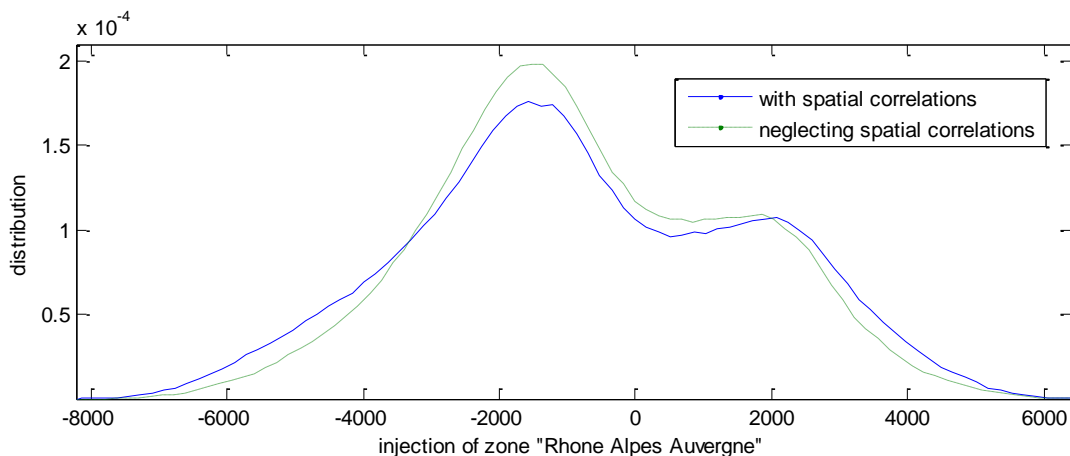


Figure 32. Distribution of the injections of zone “Rhône Alpes Auvergne”, with and without spatial correlations.

The modelling of spatial correlations therefore impacts the injections computed in Task 8.2. Both the average values and the distributions of the injections are affected by the spatial correlations. There is no clear pattern. Depending on the energy sources of each zone, average injections can be increased or reduced, and the distribution around this average can be spread out or tightened.

Note that the time series of injections are used as a reference to calibrate the grid expansions in the following steps of the TEP methodology. Significant changes in the injections imply different needs of exchanges and can therefore lead to different network expansion plans.

6.1.3. Conclusions

One hundred Monte Carlo years have been simulated in this test case, with and without modelling the spatial correlations. In this test case, it has been shown that spatial correlations have a significant impact on the results of adequacy simulations, and that neglecting them can:

- Induce an over-estimation of the reliability of the system,
- Significantly change the injections of several zones and gauge incorrectly the network needs.

For these reasons, we therefore strongly advise to include this type of correlations in transmission expansion planning tools.

6.2. *The influence of intermodal correlations*

A similar study has been performed on the influence of intermodal correlations.

Intermodal correlations refer to dependencies between different kinds of phenomena. Typically, dependencies between several sources of RES (e.g. wind vs. PV), or dependencies between demand and intermittent RES (e.g. load vs. PV).

6.2.1. Modelling the intermodal correlations

We decided to model the intermodal correlations through an intermediate variable: the temperature.

The dependence of each time series toward the temperature – called “thermo-sensitivity” – has been added in the model. To take into account the intermodal correlations, the time series decomposition henceforth includes a trend, a seasonality, a stochastic component, and also a thermo-sensitive component, denoted H_t :

$$Y_t = T_t S_t (1 + H_t) X_t \quad (7.1)$$

The thermo-sensitive component is a function of the temperature. For each zone of the system, a time series of temperature is first sampled¹⁰. The thermo-sensitive components of all the other time series of the zone are then calibrated on this time series of local temperature.

More precisely, the thermo-sensitive component is a linear function of the deviation of the temperature from its seasonal average, ΔT_t .

$$H_t = \alpha_t \Delta T_t \tag{7.2}$$

Where α_t is the thermo-sensitive coefficient, learnt from historical data. A classic approach consists in considering 12 thermo-sensitive coefficients, constants over each month of the year. For instance, a thermo-sensitive coefficient of -1% in January means that the time series tends to decrease of 1% when the temperature is 1°C above its seasonal average.

Within the same zone, all the time series are generated with the same chronicle of temperature, ΔT_t . If two time series are dependent toward the temperature, these interactions will be caught by the model and the resulting time series will naturally be correlated.

The role of the thermo-sensitivity is illustrated in Figure 33, with 6 days of any Monte Carlo year generated for one zone of France. During these 6 days (April), the thermo-sensitivity of the load is negative equal to -2%. The load is therefore higher than its seasonality during the first three days when the temperature is below its seasonal average. On the contrary, during the last three days, the temperature is slightly above its seasonality and tends to decrease the consumption.

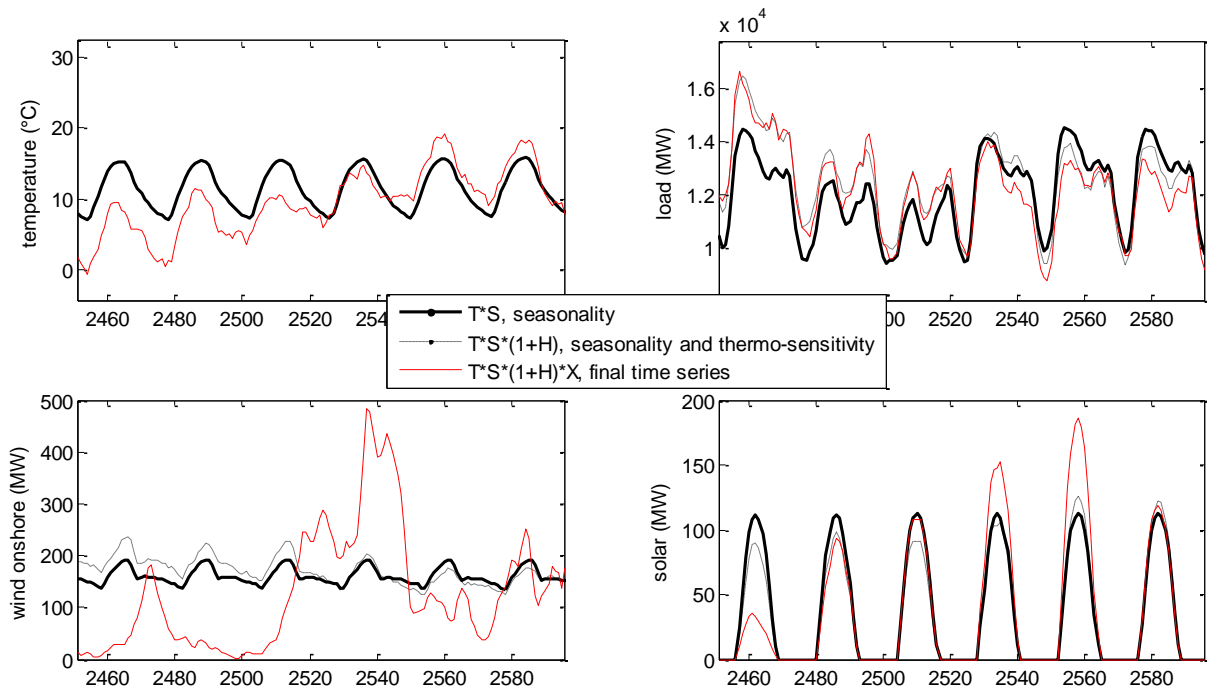


Figure 33. Dependence between calculated time series of load, wind power generation and PV generation, modelled via the thermo-sensitivity of each time series.

¹⁰ When intermodal correlations are taken into account, the temperature is itself an uncertainty of the problem, modelled with a similar approach as the one described in section 3.2 and sampled for each Monte Carlo year.

The thermo-sensitivity of the wind power is also negative, equal to -3.2%. The variability of the stochastic component of the time series of wind power generation is however high compared to its thermo-sensitivity. For this month, the deviations from the seasonality due to the temperature only have a small impact on the final time series of wind power.

Finally, the thermo-sensitivity of the solar generation is positive, equal to 3.5%. The PV generation therefore tends to be lower than its seasonality during the first three days, with low temperatures, and higher than its seasonality during the last three days, with high temperatures.

Discussion on the modelling of intermodal correlations

Intermodal correlations are due to complex meteorological events. In our approach, we modelled them in a first approximation through a simple linear dependence with only one meteorological variable: the temperature. We however do not pretend to explain the evolution of the time series with this variable only. We added the information brought by the temperature in the statistical model, but this is clearly not enough to explain the whole behaviour of the time series. The stochastic component still has a large spread which includes all the variations that cannot be explained by the periodic cycles of the seasonality or the thermo-sensitivity (see for example the time series of wind power and PV generation of Figure 33).

This approach could obviously be refined using several meteorological variables (e.g.: wind speed, nebulosity). Yet, such data were not available in the framework of this project.

6.2.2. Description of the test case

The scenario “Nouveau Mix” presented in section 6.1 for the study on spatial correlations has also been used in this test-case.

The thermo-sensitivity of the load, wind power generation and PV generation has been modelled. One thermo-sensitive coefficient has been learnt in the historical data related to each month of the year. The obtained thermo-sensitivities of the three considered stochastic phenomena are illustrated in Figure 34. Historical data of temperature have been found for central locations of the seven zones of France in the National Climatic Data Center (NCDC) database [64].

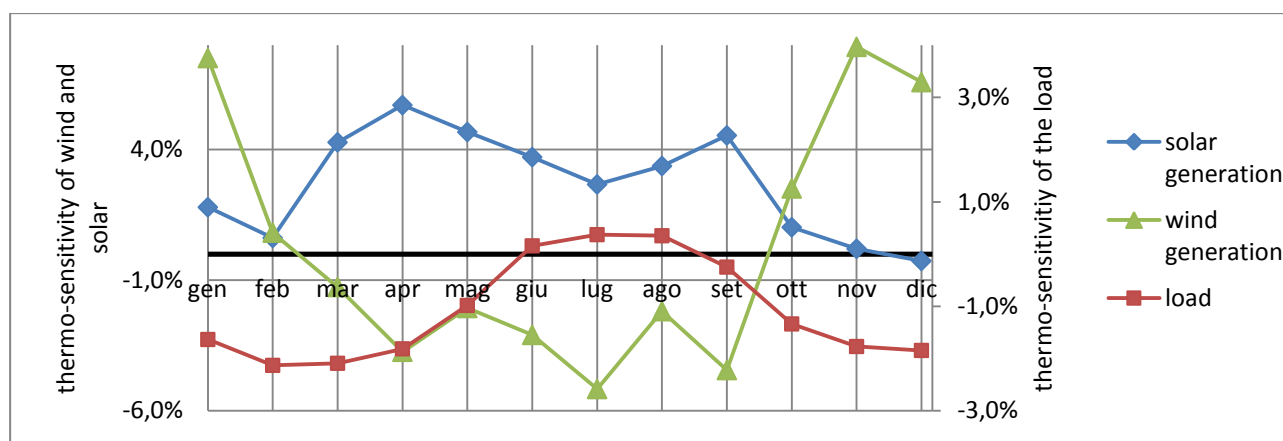


Figure 34. Thermo-sensitivity of the load, wind power and PV generation (average of the thermo-sensitivities of the seven zones of the French power system).

Due to the large integration of electrical heaters in France, the consumption naturally has a negative dependence to the temperature in winter: when the temperature drops, the consumption tends to

increase and vice versa. On the contrary, the thermo-sensitivity is slightly positive in summer, probably due to the use of cooling devices.

The solar generation has a positive dependence on the temperature. In other words, high temperatures are usually associated with a clear sky. This dependence varies over time and is particularly high during Spring and in the beginning of Autumn. As the nebulosity is more stable in summer, the variability of the PV generation is lower and so is its thermo-sensitivity. This dependence is less pronounced in winter.

Finally, the wind power generation has a strong positive dependence on the temperature in winter, when cold days visibly seem to cause high winds. The dependence however reverses from March to September. The oscillating variations of the thermo-sensitivity in summer (July-September) is quite odd but may probably be refined by calibrating the model on a longer period of historical data.

Note that the results presented in Figure 34 have been learnt from historical data of France. It has been noticed that they are specific to this area and they cannot be extrapolated to other zones of Europe.

The thermo-sensitivity of the inflows has not been modelled. This test case therefore focuses on the intermodal correlations of PV, wind power and consumption.

The whole adequacy simulator – including the scheduling of the maintenance of the thermal units, the generation of the time series, the allocation of the hydro resources and the computation of the generation schedules with an hourly time step – has been run. Simulations have been performed with and without modelling the thermo-sensitivity of the time series. Spatial correlations of the load, wind power, PV generation and temperature are taken into account.

We recall that this task uses a “copperplate” approach. In other words congestions are not taken into account and transfer capacities between the zones are supposed infinite. As in the previous test case, cross-border exchanges with neighbouring countries are not modelled and France is supposed to be an isolated system.

6.2.3. Results

100 Monte Carlo years have been simulated for both cases:

- Taking into the account the inter-dependences between PV, wind generation and demand via the thermo-sensitivity, and
- Considering that these three phenomena are independent.

Reliability of the power system

For each Monte Carlo year, the same reliability indicators as in the previous example have been retrieved, namely the total operational cost, the unsupplied energy, the loss of load duration (LOLD), the energy in excess (EIE) and the 5% Value at risk (VaR) of the residual load.

The total cost includes the cost of unsupplied energy, considered equal to 10 000 €/MWh.

The expectation of the reliability indicators (i.e. their average on the 100 Monte Carlo years) is reported in Table IX. Reliability indicators for the scenario “Nouveau Mix”, with and without modelling the intermodal correlations

	Total cost (G€/year)	Energy in excess (GWh)	Unsupplied energy (GWh)	LOLD (h)	VaR of the residual load (MW)
With intermodal correlations	5.4	312	20	10	6600
Neglecting intermodal correlations	5.3	323	11	7	6533

Table IX. Reliability indicators for the scenario “Nouveau Mix”, with and without modelling the intermodal correlations

In this case, intermodal correlations impact the reliability of the power system.

The unsupplied energy is divided by two when intermodal correlations are not modelled. As a consequence, the LOLD and the operational cost are also reduced. The difference in the operational cost is mainly due to the unsupplied energy (10GWh of unsupplied energy cost 0.1 G€).

The repartition of the unsupplied energy in the 12 months of the year is plotted in Figure 35. More than 98% of the load curtailments occur during the months of December, January and February. These are the three months with the highest consumption (see Figure 7). The main differences in the unsupplied energy are gathered in January and December, two months during which demand and wind power generation are negatively correlated. When intermodal correlations are taken into account, the peaks in the load which are due to cold weather are more likely to be accompanied with a low wind power generation. This explains such a difference between the unsupplied energy of the two cases.

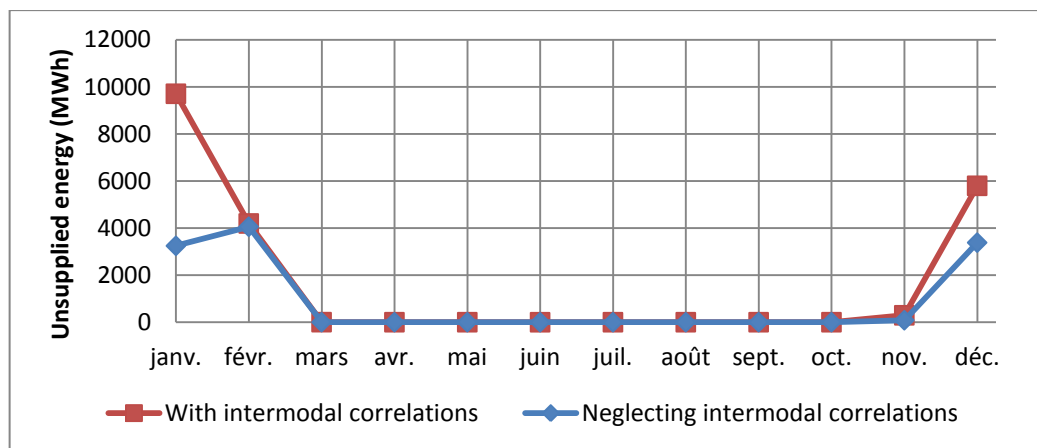


Figure 35. Unsupplied energy, with and without modelling the intermodal correlations.

However, the impact of the intermodal correlations on the distribution of the residual load is weak (see Figure 36). The intermodal correlations slightly change the upper tail of the distribution – which contains the most critical events for the power system – but they do not provoke major changes in the residual load. As a consequence, the energy in excess is not affected by the modelling of the intermodal correlations.

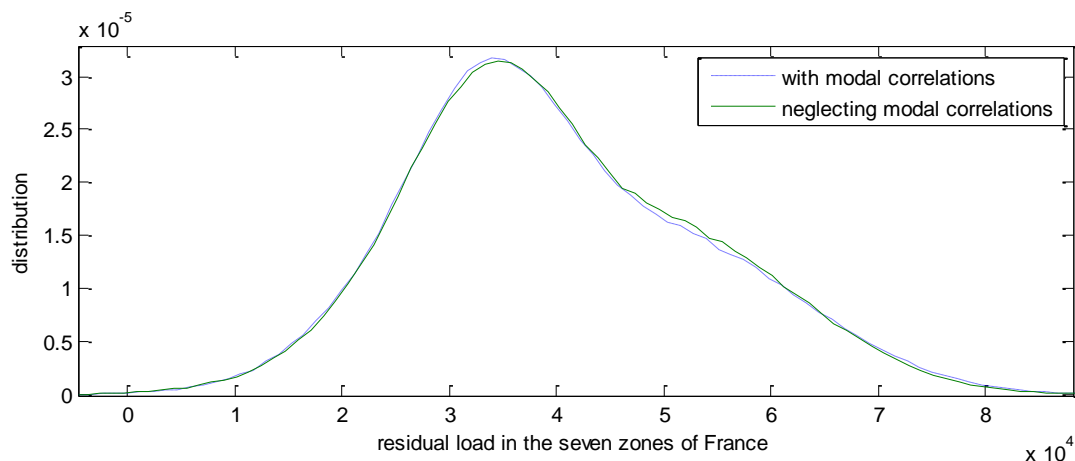


Figure 36. Probability density function (pdf) of the residual load of the scenario “Nouveau Mix”, with and without modelling the intermodal correlations

Note that the influence of the intermodal correlations is case-dependent. In a system with a slightly higher thermal capacity or with possible exchanges with neighbouring countries, the impact of the intermodal correlations on the unsupplied energy would have been lower. Moreover, in a country with a high load in summer and a high installed capacity of PV, the effect of intermodal correlations on the reliability would probably be opposite.

Injections in each zone of the power system

The impact of the correlations on the exchanges has been assessed. To do so, the time series of injections (generation minus consumption) of each zone have been analysed.

In this case, the average injection of each zone is not significantly sensitive to the intermodal correlations. Their differences with and without modelling the intermodal correlations only range between -1.7 % and 1.6 % (-11 MW to 16 MW in the average flows). As the intermodal correlations do not significantly change the distribution of the residual load, they do not modify the generation mix and they therefore do not visibly affect the average exchanges in the system.

The distribution of the injections of each zone has also been analysed. Once again, no major changes have been observed. For instance, the distribution of the injections of one zone of France with and without modelling the intermodal correlations is plotted in Figure 37.

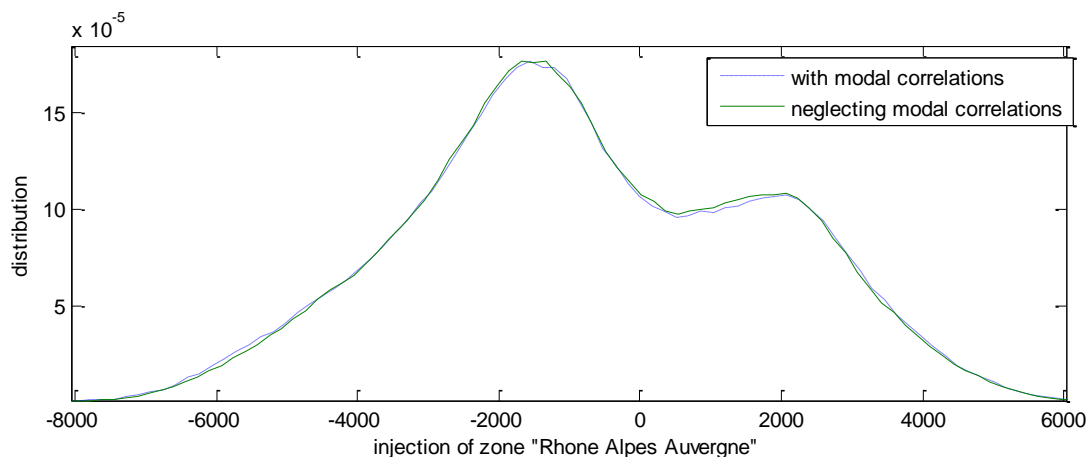


Figure 37. Distribution of the injections of zone “Rhône Alpes Auvergne”, with and without intermodal correlations.

As the intermodal correlations do not significantly impact the time series of injections, we can expect that they will not affect the planning of the grid expansions.

6.2.4. Conclusions

Although we could believe that wind generation, solar generation and load are not totally uncorrelated, this study in which temperature is used as a common factor does not reflect this correlation. One hundred Monte Carlo years have been simulated in this test case, with and without modelling the intermodal correlations through temperature, and it did not directly influence the network expansion needs.

It would have been obviously preferable if coherent time series of wind speed, solar irradiation and temperature were available. These factors could be directly implemented in the method and developed modules.

6.3. *The influence of the model of thermal units*

The model of thermal units proposed in this task (presented in section 5.1.1) includes:

- Unit commitment consideration with minimum stable power,
- Start-up costs, and
- Minimum up and down times.

The goal of this sub-section is to assess the influence of these elements on a few test cases.

6.3.1. Description of the test cases

We can expect that the flexibility of thermal power plants will be more sought in contexts with larger shares of uncontrollable intermittent RES generation. The influence of the model of thermal unit has therefore been evaluated in three scenarios with different energy mixes.

The three scenarios are based on the French/Spanish system of the IT integration test of WP 8. Two zones are considered in this system, one for each country. The generation fleet is derived from the one of 2012, of which some nuclear and coal power plants have been shut down and replaced by solar and wind energy. The replacement of conventional power plants by renewable sources is more or less pronounced in the three test cases. The installed capacities are reported in Table X. Installed capacities and yearly demand for the three scenarios

, as well as the demand of the three scenarios. Note that the test cases have been built for the purpose of evaluating the influence of the thermal unit model and that they do not represent the expected future development of the French/Spanish system.

	Wind (GW)	PV (GW)	Hydro (GW)	Nuclear (GW)	Other thermal (GW)	Demand (TWh/year)
Low RES	30.0	9.8	44.9	65.2	72.1	732
Intermediate	69.4	29.5	44.9	42.0	63.7	732
High RES	131.4	55.5	44.9	20.3	56.8	737

Table X. Installed capacities and yearly demand for the three scenarios

The three studied scenarios are called “low RES”, “intermediate” and “high RES” in reference to the quantity of renewables they integrate. The energy mixes of the three scenarios are given in Figure 38.

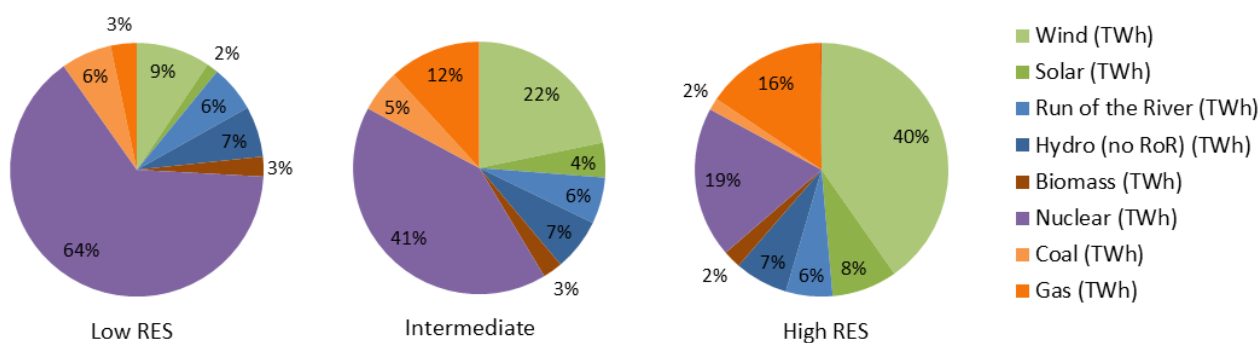


Figure 38. Energy mixes of scenarios low RES, intermediate and high RES.

In the scenario low RES, 26 % of the demand is supplied by RES generation, of which 17 % by uncontrollable RES. On the other hand, the energy mix of the scenario high RES contains 65 % of renewable energy, of which 55 % coming from uncontrollable sources. From one scenario to another, the increase of the installed RES capacity is compensated by a reduction of the traditional thermal capacities.

The three scenarios include respectively 268, 242 and 218 thermal power plants. The typical characteristics of each technology are given in Table XI. Standard characteristics of each type of thermal generation

Fuel	Minimum stable power (%Pmax)	Minimum down time (h)	Minimum up time (h)	Generation cost (€/MWh)	Start-up cost (€)
Biomass	50	3	3	16	3 000
Nuclear	50	168	168	14	25 000

Coal	50	24	24	50	15 000
Gas	50	24	24	50	15 000
Oil	50	3	3	80	3 000

Table XI. Standard characteristics of each type of thermal generation

In this test case, we did not seek to build exact values of each of these parameters. We just took order of magnitude close enough to the reality so as to be able to consistently model the behaviour of the thermal generators. Our goal is here to measure the influence of the technical constraints in which those parameters are taking part (e.g. minimum stable power, minimum up/down times).

The three scenarios do not include DR. Moreover, no external exchanges have been modelled.

For the three scenarios, the adequacy simulator has been run with different modelling of the thermal units:

1. **With the complete model**, as presented in Section 5.1.1, which includes a binary commitment status for each thermal unit, minimum stable power constraints, start-up costs in the objective function and minimum up/down times constraints.
2. **Without minimum up/down times**, i.e. with the complete model of Section 5.1.1 of which the minimum up/down times constraints have been removed. In this case, thermal units are free to turn on and off any time.
3. **Without considering the start-up costs** in the objective function. Start-up costs are removed from the objective function (the MILP is simplified), but they are still computed afterward. In this case, the resolution of the adequacy problem is then sub-optimal.
4. **Without minimum up/down times constraints and start-up costs** (combination of the two previous cases).
5. **With fully flexible thermal units**. In this case, the minimum up/down times constraints are not considered, start-up costs are removed from the objective function and UC variables are relaxed. The optimisation problem is continuous. Start-up costs are re-computed afterward and are not part of the optimisation problem anymore. Moreover, thermal power plants are able to have an output power below their minimum stable power.

6.3.2. Results

10 Monte Carlo years have been simulated:

- For the three scenarios low RES, intermediate and high RES
- With the 5 modelling approaches of the thermal units mentioned in the previous part.

The adequacy problem is solved with FicoXpress[62], using an optimality gap of 0.1%.

The same list of 10 seeds has been used for each modelling approach. Time series of the uncertain inputs are thus identical in each case. Differences between the results are then due to the modelling of the thermal units and not to different Monte Carlo samples.

For each Monte Carlo year, a few indicators have been retrieved: the solving times of the 52 weekly optimisation problems, the operational cost, the energy in excess (EIE), the unsupplied energy and the loss of load duration (LOLD).

The operational cost includes the cost of unsupplied energy, considered equal to 10 000 €/MWh.

The expectation of the reliability indicators (i.e. their average on the 10 Monte Carlo years) are reported in Table XII. Impact of the model of the thermal units on the results of adequacy simulations for the scenarios “low RES”, “intermediate” and “high RES”

for the three scenarios.

		Solving time (min)	Total cost (G€/year)	Energy in excess (GWh)	Unsupplied energy (GWh)	LOLD (h)
Low RES	Complete model	19' 58''	11.27	0	0	0
	No minimum up/down times	21' 56''	11.26	0	0	0
	No start-up costs	20' 55''	11.29	0	0	0
	No min. up/down & start-up costs	6' 57''	11.35	0	0	0
	Fully flexible thermal units	4' 07''	11.35	0	0	0
Intermediate	Complete model	18' 46''	11.63	19	1.1	3
	No minimum up/down times	17' 13''	11.63	1	0.5	1
	No start-up costs	20' 07''	11.66	19	0.5	2
	No min. up/down & start-up costs	5' 38''	11.77	1	0.5	1
	Fully flexible thermal units	3' 47''	11.77	0	0.5	1
High RES	Complete model	17' 10''	9.32	4 746	81	20
	No minimum up/down times	13' 49''	9.22	2 976	75	16
	No start-up costs	18' 49''	9.31	4 765	79	19
	No min. up/down & start-up costs	5' 42''	9.38	2836	75	15
	Fully flexible thermal units	4' 04''	9.38	2835	75	15

Table XII. Impact of the model of the thermal units on the results of adequacy simulations for the scenarios “low RES”, “intermediate” and “high RES”

Impact on the operational cost

When minimum up/down times constraints are removed from the problem, the space of possible solutions widens and the minimum cost logically decreases. Thermal units are made more flexible and new less-costly solutions are therefore offered to balance the system. In these test cases, the reduction of the operational cost is however low, below 2%.

In the three last cases, start-up costs have been removed from the objective function of the optimisation problem so as to simplify it. They are computed afterward in a sub-optimal manner. The dispatch found is therefore not the optimal one and the operational costs are higher than in the reference case. Differences brought by the modification of the model of thermal units are once again very low, below 2%.

Impact on unsupplied energy and LOLD

Unsupplied energy is slightly affected by the model of thermal units. When the model is simplified, load curtailments tend to be underestimated.

Neglecting the minimum up/down times constraints offers more flexibility to the power plants and therefore provides new solutions to balance the system. Some of them visibly permit to diminish the load curtailments. As a consequence, the unsupplied energy decreases when minimum up/down times are not taken into account. A similar reasoning can be made on the minimum stable power constraints.

Moreover, when start-up costs are not part of the objective function anymore, load curtailments slightly rarefy. In this configuration, solutions which propose to turn on new power plants to avoid load curtailments will indeed more likely minimise the problem.

In these test cases, the imprecision of the unsupplied energy brought by the simplification of the model is however low. Due to the high VOLL (10 000 €/MWh), solutions which minimise the operational cost are also inclined to minimise the unsupplied energy, even if it requires to delay the stops of some generators in order to respect the minimum up/down times constraints or to pay for the start-up of new power plants.

Impact on the energy in excess

The energy in excess is the indicator which is the most affected by the modelling of the thermal units.

Minimum up/down times constraints have a large influence on the energy in excess. In the intermediate scenario, almost all the energy in excess is cut when minimum up/down times constraints are removed from the model while it decreases by 36% in the scenario “high RES”. In this configuration, thermal units can indeed be switched off only for a few hours in order to compensate a valley in the load or a peak in RES generation. On the contrary, when minimum up/down times constraints are taken into account, thermal units will sometimes be forced to stay on, even if the system is facing a temporary high RES generation or low load.

In these test cases, energy in excess is not significantly impacted by the presence of the start-up costs in the objective function.

Impact on cross-border exchanges

The cross-border exchanges between France and Spain have been analysed.

It has been noticed that the modelling of thermal units does not significantly impact the distribution of the exchanges between the two countries of these test cases. Whatever the approach used, network needs will therefore probably be similar.

For instance, Figure 39 depicts the distribution of the cross-border exchanges of the scenario “high RES” for three cases: with the complete model (case 1), without the minimum up/down times constraints (case 2) and with the relaxed problem (case 5). The three distributions are very close.

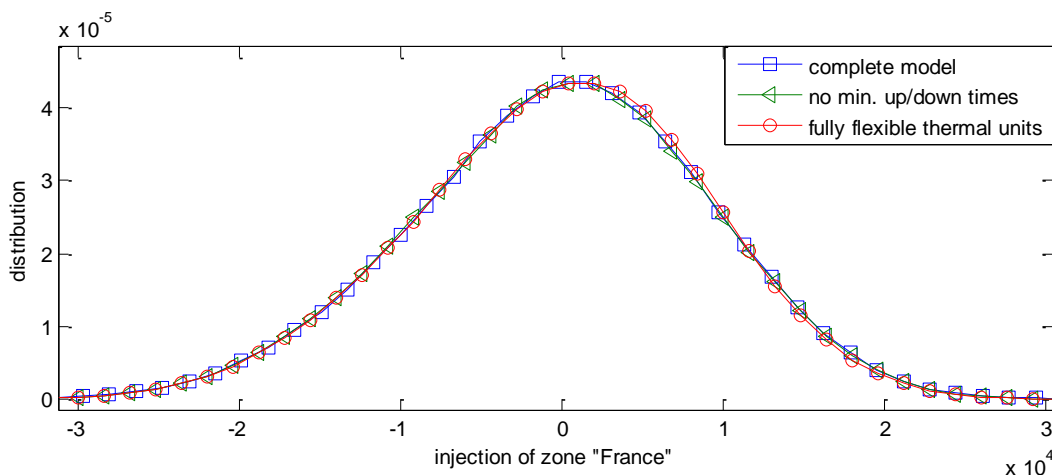


Figure 39. Distribution of the exchanges between France and Spain in the scenario “high RES” and for several thermal generators models

The time series of injection are used as a reference to calibrate the grid expansions in the following steps of the TEP methodology. Similar injection patterns will therefore probably lead to identical network expansion plans.

Impact on computational time

Computational time can be reduced by simplifying the model of the thermal generators.

Removing from the model only the minimum up/down times constraints or the start-up costs does not provide a significant reduction of the solving time. Those two elements are in a way redundant in the sense that they both encourage to limit the number of start-ups of the thermal power plants. Removing one of them without the other therefore does not permit interesting time savings.

However, removing both the minimum up/down times constraints and the start-up costs lead to a reduction of more than 65% of the computational time.

Finally, if the thermal units are made fully flexible so as to relax the integer variables of the optimisation problem, the solving time can be diminished by more than 75%. In this case, the resolution of the adequacy problem is very fast and most of the time is actually allocated to the reading and writing of data. For example, among the 3' 47" needed to solve the relaxed problem of the intermediate scenario, only 22" are used by the solver while 3' 25" are allocated by AMPL to load the data, build the model and write the outputs.

Week with the most unsupplied energy

Figure 40 depicts the week of scenario "High RES" with the highest amount of unsupplied energy. This week stretches from the 3rd of December to 9th. During the first three days of the week, demand in France and Spain is particularly high, with peaks of more than 130 GW, while wind power generation is low. It results in 46h of loss of load duration and a total of 352 GWh of unsupplied energy. As evidenced by the yearly averages of Table XII. Impact of the model of the thermal units on the results of adequacy simulations for the scenarios "low RES", "intermediate" and "high RES"

, this situation is exceptional.

In this test case, the thermal generation fleet has not been sized to supply the peaks of the residual load. Moreover, no backup solutions are proposed: the French/Spanish system is isolated (no exchanges with neighbouring countries are considered) and demand is strictly uncontrollable. During periods with an especially high consumption and a low RES generation, the system therefore lacks power and cannot supply all the demand.

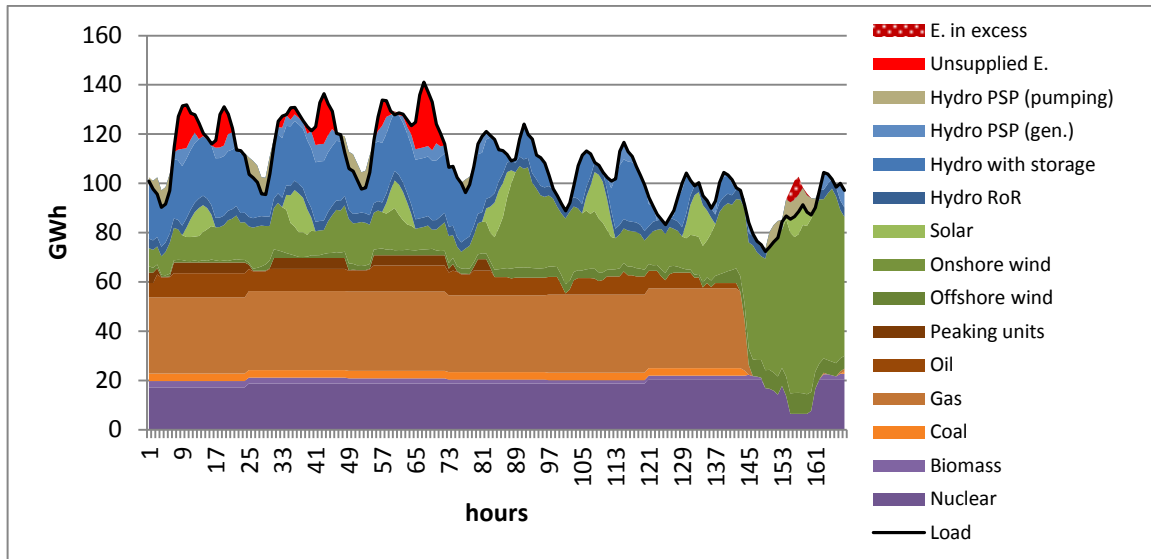


Figure 40. Generation schedule of the week with the most unsupplied energy of the scenario “High RES”, obtained with the complete model of thermal units

The generation schedule of Figure 40 also shows that hydroelectric energy brings lots of flexibility to the studied system. The test case includes more than 30 GW of hydro units with reservoir and PSPs. Hydropower absorbs one part of the intermittenancies of the residual load and loosens the requirement of flexibility of the thermal power plants.

In the first three days depicted in Figure 40, almost all the thermal units are always operated at their nominal capacity. Minimum up/down times and minimum stable power constraints are rarely activated. Load curtailments are here due to the lack of generating capacity and not to the limited flexibility of thermal thermal generators. Consequently, in this test case, unsupplied energy is not strongly sensitive to the thermal unit model (see Table XII. Impact of the model of the thermal units on the results of adequacy simulations for the scenarios “low RES”, “intermediate” and “high RES”

).

The next table focuses on hour 67 (Wednesday at 19h) which is the hour of the week with the highest amount of unsupplied energy – 24 GW of demand is curtailed during this hour. The table presents, for both countries, the generation during this critical hour and the available capacity of each type of energy. Note that the available capacities of thermal sources do not take into account units which are out-of-order or under maintenance.

Table XIII. Generation of France of Spain during hour 67 and available capacity of each source of energy

shows that the uncontrollable generation of both countries is especially low during hour 67. Solar generation is notably equal to zero as the sun is already down at 7 p.m. in December. On the contrary, all controllable generating units produce at their technical maximum. The system does not dispose of anymore lever to balance the consumption; all the available controllable generating units are already solicited.

		Spain		France	
		Generation (GWh/h)	Available capacity (GW)	Generation (GWh/h)	Available capacity (GW)
Controllable	Nuclear			18.7	18.7
	Biomass	0.8	0.8	1.3	1.3
	Coal			3.0	3.0
	Gas	22.5	22.5	9.7	9.7
	Oil	5.0	5.0	5.6	5.6
	Peaking thermal units	2.0	2.0	2.1	2.1
	Hydro with reservoir	15.1	15.1	9.1	9.1
	Pumped-storage hydro power plants (PSP)	2.7	2.7	4.3	4.3
Uncontrollable	Hydro run of the river (ROR)	0.4	2.0	3.4	11.7
	Offshore wind	2.2	4.0	0.1	8.0
	Onshore wind	7.4	39.8	1.7	79.6
	Solar	0	18.5	0	37.0

Table XIII. Generation of France of Spain during hour 67 and available capacity of each source of energy

Finally, Table XIV. Adequacy of both countries during hour 67

reports the generation and demand of each country during this critical hour. The imbalance is particularly problematic in France where the generation is very low compared to the load. On the contrary, Spain overproduces in order to compensate the lack of power of France.

	Spain	France
Generation (GWh/h)	58.1	58.9
Consumption (GWh/h)	38.6	102.5
Unsupplied energy (GWh/h)	24.1	

Table XIV. Adequacy of both countries during hour 67

These figures imply significant exchanges between the two countries: the 19.5 GW overproduced in Spain have to be transmitted to France. The copperplate approach retained in this Task allows unconstrained flows between the two countries. This result is however optimistic and may be revised in the following steps of the TEP, when the grid will be modelled.

6.3.3. Conclusions

The influence of the model of thermal units has been evaluated for different scenarios, integrating more or less uncontrollable renewable sources in their energy mixes.

For the studied scenarios, it has been shown that the energy in-excess can be significantly underestimated if the thermal generator model is simplified. On the other hand, the impact of the flexibility of thermal units on the unsupplied energy, operational cost and cross-border exchanges is low.

Furthermore, it has been noticed that consequent time savings (up to 75%) can be made by simplifying the modelling of the flexibility of the thermal units.

It has to be noted that the three studied test cases are fictional and have not been built on real data. The results obtained with them cannot be extrapolated to any power system. Moreover, assumptions made in this task (e.g. copperplate approach, reserves not modelled) may also conceal other concerns related to power system flexibility. For instance, the copperplate approach does not allow to rigorously assess the impact of the flexibility of thermal units on the location of the production.

6.4. The influence of demand response

The sensitivity of the results of the adequacy to the addition of Demand Response (DR) is finally analysed in this part.

6.4.1. Description of the test case

The studied test case is based on the French/Spanish system of the IT integration test of WP8. The scenario “High RES” presented for the previous example of Section 6.3.1 has been used. Its energy mix includes 65% of renewables, of which 55% are coming from uncontrollable sources (i.e. wind, solar or run of the river).

The proposed scenario has large shares of RES generation. The potentiality of demand response is indeed often associated to the requirement of flexibility of systems which possess a significant amount of non-controllable and intermittent renewable generation.

The model presented in Section 5.1.3 has been used to represent the controllable load.

Different levels of participation of DR have been tested, from 0 to 8% of the total consumption. The first case without DR programs is used as the reference case while the value of 8% corresponds to the order of magnitude of the potential of DR which is usually forecasted for direct load control programs [44]. Two intermediary rates, of 2% and 4%, are also considered so as to assess the sensitivity of the system to the participation rates of DR. In total, 4 cases are therefore considered with respectively 0, 2, 4 and 8% of the demand which is controllable.

In each of these cases, the load which participates in the DR programs is equally divided into:

- one third with a delay time of 4h,
- one third with a delay time of 8h, and
- one third with a delay time of 12h.

The demand controllable within short delay times usually refers to heating and cooling, the one with an intermediary delay time to the charging of electrical vehicles and the one with a longer delay time to the consumption of residential appliances.

All the types of demand response have the same cost. The cost has been chosen as in the second case presented in Section 5.1.3. In other words, DR is economically competitive in the electricity markets, it will favour re-dispatching toward less expensive generation units and will adapt to the intermittenencies of the RES. However, due to the small cost of DR, hydro pumping and storage is preferred to load shifting actions.

6.4.2. Results

100 Monte Carlo years have been simulated for the four cases, with respectively 0, 2, 4 and 8% of the consumption which can be shifted.

Adequacy between consumption and generation

For each Monte Carlo year, a few indicators have been retrieved: the total operational cost, the unsupplied energy, the loss of load duration (LOLD), the energy in excess (EIE), and the yearly generation of the peaking thermal power plants.

The total cost includes the value of ENS, considered equal to 10 000 €/MWh.

The expectation of the reliability indicators (i.e. their average on the 100 Monte Carlo years) is reported in Table XV. Impact of demand response on the results of adequacy simulations

	Total operational cost (G€/year)	Energy in excess (TWh)	Unsupplied energy (GWh)	LOLD (h)	Generation of peaking units (GWh)
Reference case (0% DR)	8.8	5.1	55	15	103
2% participation of DR	8.5	4.6	33	10	71
4% participation of DR	8.3	4.1	20	6	47
8% participation of DR	8.1	3.3	6	3	26

Table XV. Impact of demand response on the results of adequacy simulations

Note that the reference case contains more than 5 TWh of RES curtailments. This amount corresponds to 1.2 % of the uncontrollable RES generation and 0.7 % of the yearly consumption. The unsupplied energy is also significantly high, equal to 55 GWh. These figures evidence the frequent imbalances of the system which occur during periods with a high (or low) intermittent RES generation and low (or high) demand. They can mainly be explained by the highly intermittent energy mix.

The flexibility brought by demand response allows lessening the imbalance of the system. For instance, with the addition of DR, one part of the consumption can be decreased when the intermittent generation is low and shifted to periods when the intermittent generation is higher. This results in a reduction of the use of peaking power plants and load curtailments. In this test case, the addition of only 2 % of DR cuts 40 % of the unsupplied energy and reduces the generation of expensive peaking units by 31 %.

The ability of DR to reduce the imbalances of the system is illustrated in Figure 41. In the reference case (upper graph), a peak in the consumption of the first day accompanied by a low wind power generation forces the use of peaking power plants and load curtailments. In the case where 8% of the load is controllable (lower graph), one part of the morning peak is shifted to the previous night and drastically decreases the unsupplied energy.

Furthermore, by increasing the demand during the periods with a low load and a high RES generation, DR also allows reducing the amount of spilled energy. For instance, during the night between the 5th and 6th days of the week of Figure 41, the demand has been increased so as to absorb as much available RES as possible.

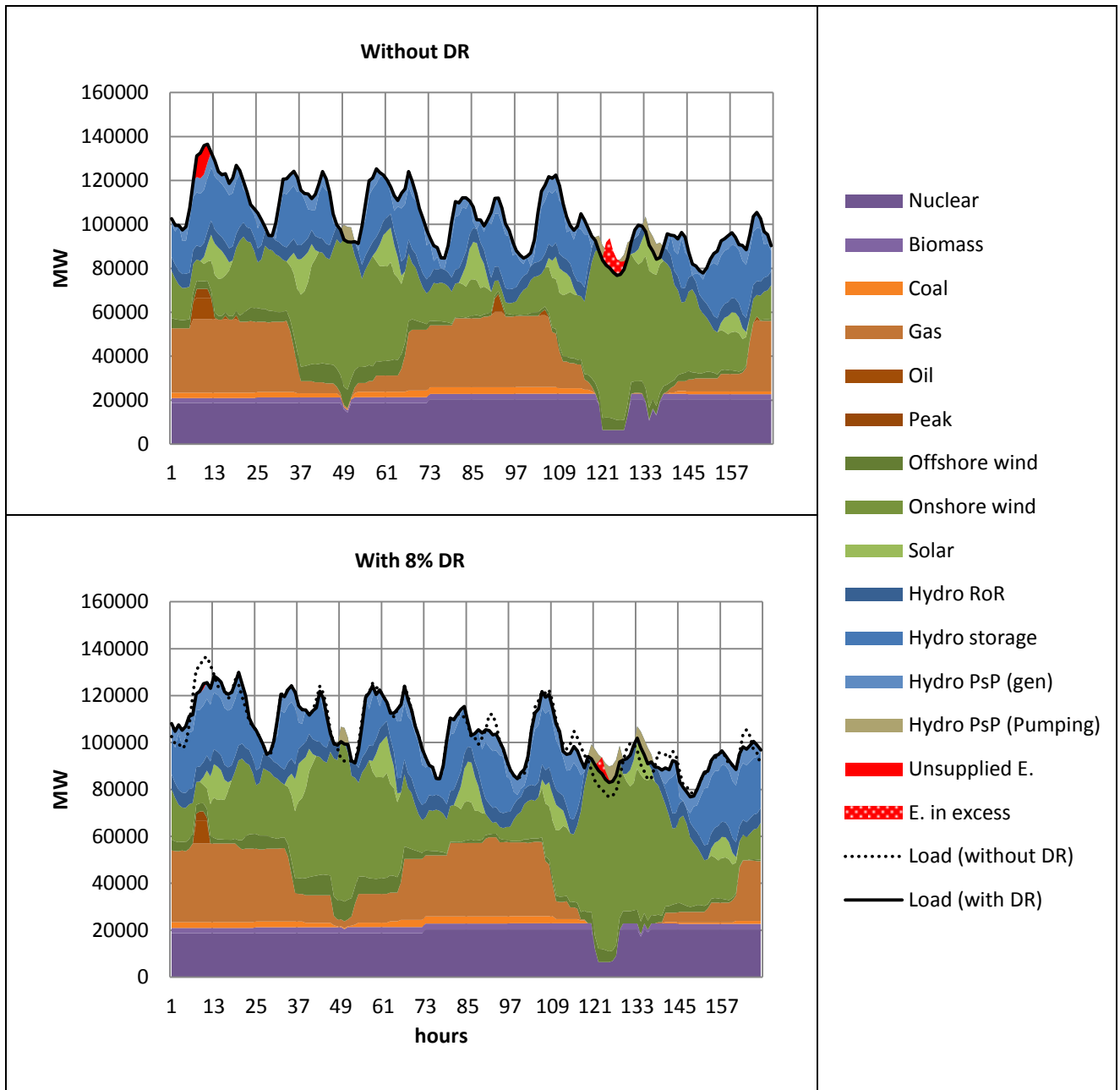


Figure 41. Generation schedule over one week of any MC year, with a fixed consumption (upper graph) and with 8% of the consumption which is controllable (lower graph).

In the studied test-case, a reduction of 1.8 TWh of spilled energy is made when 8% of the load is controlled via DR programs. A larger part of the available free renewable energy can be consumed and equivalently fewer fossil fuels are needed to balance the system. It indirectly results in the consequent saving of 1.8 TWh of thermal generation and the avoidance of their associated CO₂ emissions.

Finally, significant cost savings are made thanks to DR. The operational cost is cut by 3.2 % in the case with 2% of DR and by 7.8 % in the case with 8% of DR. Cost savings are due to:

- the reduction of load curtailments,

- the indirect reduction of thermal generation due to the decrease of the spilled renewable energy, and
- re-dispatching of thermal generators. For instance, the oil power plants which were initially switched on around hour 90 in Figure 41 can be switched off when DR is added to the system and replaced by less expensive thermal generation sources (e.g. biomass, nuclear).

The origin of the cost reduction for the different levels of participation of DR is depicted in Figure 42.

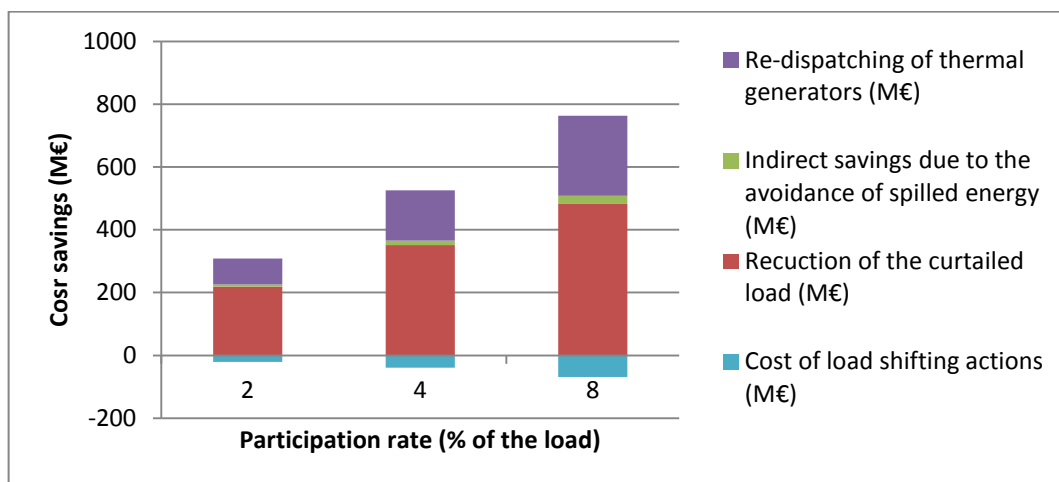


Figure 42. Cost savings associated to demand response (the indirect savings due to the reduction of the spilled energy is indexed on the cost of nuclear generation).

In this test case, the first advantage of demand response – in terms of costs – is its ability to reduce the unwanted load curtailments. DR is therefore particularly valuable in systems with imbalances issues¹¹. Typically in cases with lots of intermittent renewable energy, and so possible shortage of power, DR will have a substantial influence on the results of the adequacy simulations.

The re-dispatching of thermal generators is the second advantage brought by DR. It consists in shifting the load from periods when expensive units are on to periods when “base-load” units do not operate at their full capacity. In this test-case, it results in an increase of the energy produced with nuclear and biomass and a decrease of the energy produced by gas power plants and peaking units. For example, Figure 43 depicts the difference between the yearly thermal generation of the reference case and the one of the 4th case, with a participation rate of DR of 8%. The order of magnitude of the re-dispatching is of a few TWh/year for each type of energy.

¹¹ Note that similar simulations have been performed on cases with less intermittent generation or with an oversized thermal generation fleet. The role of DR in these cases has proved to be less pronounced.

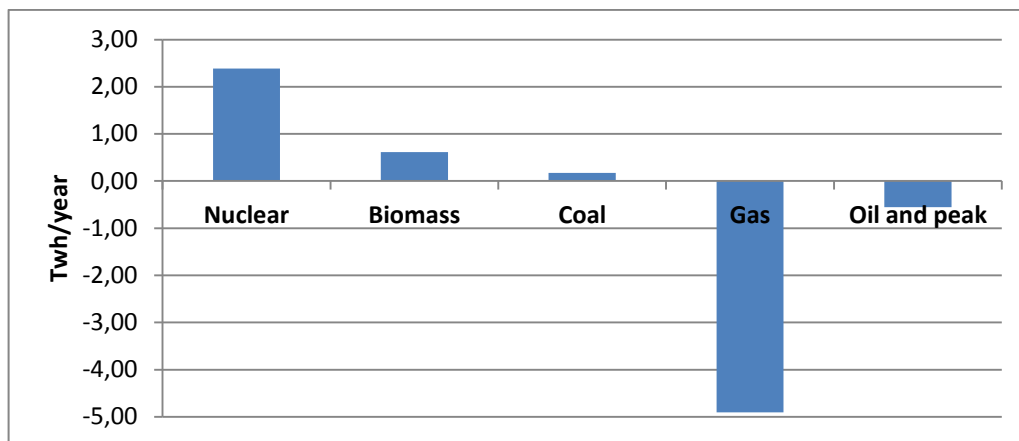


Figure 43. Re-dispatching of thermal generators when 8% of the load is controllable via DR.

In this test-case, the majority of the nuclear power is located in France while gas power plants are mainly deployed in Spain. The re-dispatching from one type of energy to the other therefore changes the average power flow between the two countries. More precisely, when 8% of the demand becomes controllable, the average flow from France to Spain increases by nearly 200 MW. Though the variability of the cross-border flow remains unchanged and its distribution is only slightly affected by the addition of DR.

Computational time

Table XVI. Impact of DR on the computational time

reports the average computational time over the 100 Monte Carlo simulations and for the four cases mentioned above.

	Total time (min)	Time in Ampl (min)	Time in solver (min)
Reference case (0% DR)	19' 21"	5' 18"	14' 03"
2% participation of DR	18' 19"	5' 13"	13' 05"
4% participation of DR	17' 32"	5' 06"	12' 26"
8% participation of DR	17' 22"	5' 12"	12' 10"

Table XVI. Impact of DR on the computational time

The “time in Ampl” refers to the time spent for loading the data in input, building the model and writing the results while the “time in solver” refers to the time actually spent to solve the adequacy’s MILP. The solver used is FicoXpress [62] with an optimality gap of 0.1%.

The time in Ampl is logically similar for all the simulations as the volume of data to read and write is identical in the four cases.

On the other hand, the time spent to solve the MILP is slightly affected by the modelling of DR. Time in solver is cut by 13% when 8% participation of DR is modelled.

In this test-case, when the participation rate of DR increases, the problem is quicker to solve. These results can seem counterintuitive as the addition of DR adds new constraints and variables in the optimization problem. However, for a fixed unit commitment, DR also offers a new flexible room for manoeuvre to approach the optimal solution. The branch-and-cut tree is therefore quicker to be processed when DR is added to the model.

6.4.3. Conclusions

One hundred Monte Carlo years have been simulated in this test case, with different participation rates of DR. It has been shown that DR can have a significant impact on the results of adequacy simulations, even if its participation rate is low. Reduction of curtailed load, re-dispatching of thermal generators and avoidance of spilled energy are the three main advantages of DR. However, these results should be put into perspective according to the scenario. We considered a “High RES” scenario, where the uncontrollability of RES generation is balanced with DR. In further studies, it would be interesting to investigate if it is more profitable to deploy DR or invest in new thermal units to bring flexibility to the system.

Moreover, DR does not increase the solving time of the adequacy simulator. On the contrary, it even slightly speeds the resolution of the MILP problem.

For these reasons, we advise to integrate the modelling of DR in the adequacy simulations, even if its deployment is at an early stage and its participation rate is low.

7. Conclusions

The prototype developed in task 8.2 converts the macro-assumptions of each scenario and time horizon into balanced time series of consumption and generation. A Monte Carlo method has been retained in order to tackle the stochasticity of the problem.

The proposed method contains 4 modules, namely:

- A maintenance scheduling heuristic, which plans the maintenance of the thermal power plants.
- A time series generator, which samples new possible behaviours of the uncertain phenomena which affect the power system (intermittent RES, demand, hydrological inflows and thermal plant outages).
- A routine which allocates the hydro resources among the 52 weeks so as to decompose the yearly problem.
- An hourly adequacy model with a complete description of the hydro and thermal power plants, extra-European exchanges and demand response programs which compute the hydro-thermal dispatch of the system.

Significant work has notably been done on the modelling of the dependencies between the uncertain phenomena of the system, both spatial and intermodal correlations, on the integration of an efficient unit commitment model, with consideration on the limited flexibility of thermal generators, and on the addition of demand response.

Recent literature has been reviewed on each of these points. A similar model is used in WP2 for adequacy simulations (see D2.1 “Data sets of scenarios for 2050”). However, some modelling aspects have been further studied in this deliverable in order to analyse the role they have in the adequacy simulator and the precision they bring to the results. The main results observed are:

- Spatial correlations can have a strong influence on the results of the adequacy simulator. It is recommended to take them into account in the Monte Carlo method. Neglecting them can notably lead to an over-optimistic assessment of the reliability of the system and a biased evaluation of the network needs.
- Although we could believe that wind generation, solar generation and load are not totally uncorrelated, the results of the study in which temperature is used as a common factor do not reflect this correlation. It would have been preferable if coherent time series of wind speed, solar irradiation and temperature were available.
- On the studied test cases, the modelling of the flexibility of thermal units has a strong influence on RES curtailments. Though its impact on unsupplied energy, operational cost and cross-border exchanges is low. Simplifying the model of thermal units can save up to 75% of the computational time.
- Demand response can have a substantial influence on the results of the adequacy simulations. The role of demand response is especially important in scenarios which include significant amount of uncontrollable generation. It is recommended to take it into account in the adequacy model, even if its deployment is at an early stage and its participation rate is low.

Further studies could be performed on the adequacy model, such as assessing the flexibility of RES generation in the system.

8. Annex A: Time series analyser

As described in Figure 6, the time series analyser is run *ex-ante* to extract, from a few historical data, the main characteristics of the studied phenomenon: its seasonality, stochastic characteristics and correlations. The historical trend of the process is also estimated in order to isolate the evolution of the time series due to external factors (e.g. increase of the installed capacity) from the intrinsic characteristics of the phenomenon.

The representation of univariate time series is presented in a first part. The estimation of the correlation between time series is then discussed in a second part.

8.1. Learning process of univariate time series

The TS analyser consists in studying historical data to learn the main characteristics of the studied phenomenon: its trend, seasonality and stochastic characteristics.

Trend

The trend is the multi-year evolution of the process. It describes the regular and diffuse changes in the power system. For example, the extension of the renewable generation park, or an overall growth of the consumption.

In most cases, a simple linear trend is enough to describe the behaviour of the historical data (9.1).

$$T_t = a_0 + a_1 t \quad (9.1)$$

Where T_t is the trend, t the time index, and a_i the regression parameters, further estimated.

Other sets of data however require a more complex model. In order to isolate properly the trend from the rest of the time series, it is indeed important to adapt its mathematical formulation to the specificities of the considered dataset. The general form of the trend is therefore:

$$T_t = \sum_i a_i h_i(t) \quad (9.2)$$

Where h_i are deterministic functions of the time and a_i the regression parameters.

Note that the trend estimated on the historical data is not the one used for the generation of the future realization of the time series. The future trend is an assumption which represents the forecasted restructuring of the power system. However, the interest of the calculation of the historical trend is twofold:

1. Remove the multi-year evolution from the historical data to isolate its intrinsic characteristics and strictly estimate its seasonality and stochastic properties.
2. Compute the future trend. For example, the future trend (e.g. in 2050) of intermittent RES generation will be equal to:

$$T_{2050} = T_{2013} \frac{capacity_{2050}}{capacity_{2013}} \quad (9.3)$$

Where the time index is given in years, and *capacity* is the installed capacity of the uncontrollable RES. If the scenario also contains information about the evolution of the average load factor of the RES which results from the integration of new generation technologies, it can also be multiplied to the capacity to refine the computation of the future trend.

Seasonality

The seasonality is the intra-year variation of the process. It represents the expected average behaviour of the studied phenomenon along the year and includes the periodic patterns observed in the historical data. Seasonality can mainly be explained by the yearly cycle of the climatic conditions, impacting the load (due to the presence of electrical heaters or air conditioners) as well as the intermittent renewable generation (due to changes in wind regimes, sunshine duration and irradiation angle).

As in [15], it has been decided to model the seasonality via Fourier series with a yearly periodicity (9.4).

$$\phi_0 + \sum_{i=1}^n [\phi_i \cos(2\pi i d_t) + \varphi_i \sin(2\pi i d_t)] \quad (9.4)$$

Where ϕ_i , φ_i are the regression parameters and d_t is the yearly ratio, equals to the number of days elapsed from the beginning of the year divided by 365. n is the Fourier order, usually small.

In practice, the seasonality also contains daily and weekly patterns. Daily frequency is for instance explained by the climatic diurnal cycle which affects the RES or by the differences in the consuming behaviour at different times of the day. Weekly periodicity affects the load and is mainly due to a specific consumption during weekends. Some irregularities can also appear in the seasonality, during certain type of days, as holidays, vacation or long week-ends.

These periodicities are also modelled in the seasonality by isolating the different hours and/or types of the day and by explaining each one of them by its own Fourier series. The generic formula of the seasonality is therefore:

$$S_t = \sum_{c \in \mathcal{C}} \mathbf{1}_c(t) \left\{ \phi_{0c} + \sum_{i=1}^n [\phi_{ic} \cos(2\pi i d_t) + \varphi_{ic} \sin(2\pi i d_t)] \right\} \quad (9.4)$$

Where S_t is the seasonality, \mathcal{C} is the set of time-categories and $\mathbf{1}_c$ is the indicator function of the time category c . For instance, if a distinction is made between the hours of the day, \mathcal{C} is defined as:

$$\begin{aligned} \mathcal{C} &= \{c_0, c_1, \dots, c_{23}\} \\ c_h &= \{t : \text{hour}(t) = h\}, \forall h \in \{0, 1, \dots, 23\} \end{aligned} \quad (9.5)$$

Where c_h is a time category associated to the hour h , and hour is a function which returns the hour, an integer from 0 to 23, from which the time index t comes from. In that case, the seasonality will therefore consists of 24 Fourier series, each one estimated on the data of only one specific hour.

The set of time categories depends on the studied phenomenon. For instance, 24 time categories, one for each hour of the day, are usually enough to describe the seasonality of the intermittent RES. On the other hand, the modelling of the load requires distinguishing the type of days as well as the hour. If we differentiate the weekdays (Monday to Friday), from the Saturday and the non-working days (Sundays, holidays and vacations), the model of the seasonality comprises 72 time categories and as much Fourier series. The model of the seasonality has to adapt to the specificities of the data: the load of the Mondays and Fridays should also better be represented by their own Fourier series in some countries.

Estimation of the trend and seasonality

The coefficients a_i , ϕ_{ic} and φ_{ic} of the trend, seasonality and thermo-sensibility are estimated via a regression of Y_t , the historical data, on $T_t S_t$

As trend and seasonality are multiplied, it results in a non-linear regression with multiplicative terms between the a_i and the ϕ_{ic} , φ_{ic} :

$$Y_t \approx \left(\sum_i a_i h_i(t) \right) \left(\sum_{c \in \mathcal{C}} \phi_{0c} \mathbf{1}_c(t) + \sum_{c \in \mathcal{C}} \sum_{i=1}^n \phi_{ic} \mathbf{1}_c(t) \cos(2\pi i d_t) + \sum_{c \in \mathcal{C}} \sum_{i=1}^n \varphi_{ic} \mathbf{1}_c(t) \sin(2\pi i d_t) \right) \quad (9.6)$$

The algorithm used to estimate the coefficients consists in computing successively linear regressions of Y_t/S_t on T_t , and of Y_t/T_t on S_t , fixing alternatively the seasonality and the trend until the convergence is reached. A similar approach has been used in [17].

Note on the stationarity of the stochastic component

Trend, seasonality and thermo-sensibility are deterministic patterns that would have been the same in all the range of the space of possibilities. On the contrary, the stochastic component includes all the random events which cannot be predicted with certainty. It represents the time-localized deviations from the trend and seasonality which do not repeat with a clear periodicity, such as the real-time speed of the wind, the nebulosity or unusual consuming behaviours.

The idea will be to generate, afterwards, a fully new stochastic component that represents one possible occurrence of future random events. It will be generated by a method which aims at replicating probabilistic properties of the past stochastic component: its probability density function (pdf), and autocorrelation function (acf). It is therefore assumed that the pdf and acf of the process are stationary, i.e. that they will remain unchanged in the future. One of the necessary prerequisites of this assumption is that the observed stochastic component is itself stationary on all the historical period.

Yet, some phenomena are not homoscedastic. In other words, the variance of their stochastic component is not constant over the year. This is notably the case of the thermo-sensitive consumptions (which have a higher variability in winter and/or summer) and the PV generation (which is more volatile in winter due to a more instable weather). For these time series, the remainder has been normalized by dividing them with their monthly standard deviation so as to obtain a stationary stochastic component. The monthly standard deviations are re-multiplied afterward, when new time series are synthesised.

Stochastic component

The stochastic component is characterized by its pdf and acf. Depending on their nature, one method or another will be more adapted to represent them. More precisely, two types of stochastic components will be distinguished:

- The ones with a Gaussian pdf, which are especially suited to an **ARMA-type** model.
- The other ones, whose acf will be supposed memoryless (exponential decaying function) and pdf will be approximated by a common marginal distribution (Gaussian, Weibull, Beta, Gamma, Uniform, etc.). Those stochastic components will be further re-generated with a **diffusion-type model**.

Both methods propose an iterative description of the stochastic component X_t , where X_t is calculated as a function of its past realizations, $(X_\tau)_{\tau < t}$, and an innovative Gaussian white noise, ε :

$$X_t = \hat{f}((X_\tau)_{\tau < t}, \varepsilon) \tag{9.7}$$

We refer the reader to the following papers for more information on the estimation of \hat{f} . The use of the Yule-Walker equations for the calibration of ARMA models is presented in reference [33] while the construction of diffusion-type models is addressed in [26].

Remark : On the tested datasets, the diffusion-type models are more appropriate to describe the inflows, photovoltaic and wind power generation while consumption time series are better represented by the ARMA-type models.

An adaptative learning process

The intrinsic characteristics of the time series are calibrated on a case-by-case basis. The above procedure is not fully automatic. The historical data have to be analysed to identify the models that could fit them. Several models are often tested, updated and improved, until one which properly fits the historical data is found.

8.2. Estimation of the correlations between the innovations

As explained in Section 3.2.3, spatial correlations are modelled between the innovations of the time series.

The challenge of this approach is the estimation of the correlation matrix R_ε .

Approaches adopted in the state-of-the-art

Reference [30] proposes to estimate R_ε based on the historical values of the innovation but this method gave bad results on the tested datasets. For example, the stochastic components of the load in two French zones – North and North-East – are highly correlated, with a correlation coefficient of more than 80 %. Both stochastic components are modelled with a seasonal ARMA of order $(1,0,0)_{24}(1,0,1)$ and historical values of the innovation are deduced from these models. The correlation of the two innovations is reported in the following table and seems surprisingly low (39%).

	Historical values	Generated sample
Correlation of the X	87 %	42 %
Correlation of the ε	39 %	39 %

Table XVII. Spatial Correlations of the stochastic components and innovations of historical and newly generated data

The generation of correlated stochastic components has been performed with this correlation of 39% between the innovations. The resulting correlation between stochastic components, after reconstruction with the ARMA model, is only of 42%. The method is therefore not able to catch the high correlations between the two time series.

Comparing the innovations at the same time is not sufficient to capture all the information on the spatial dependencies. Morales & al. [31] upgrade this approach by also modelling the lagged cross-correlations of the innovations, i.e. the correlations between $\varepsilon_{1,t}$ and $\varepsilon_{2,t-k}$ for different values of k . This improvement gives promising results.

However, the generation of correlated noises with lagged cross-correlation quickly becomes intractable for large problems. It has been used in [31] to generate time series of 24 time steps, but it can hardly be applied on numerous time series of 8760 time steps.

Another method has therefore been developed to estimate a coherent correlation matrix R_ε .

Method created for e-Highway2050's project

This method is an empirical research. It consists in updating iteratively the matrix R_ε and generating, for each iteration, long time series of new stochastic components X_{it} until they verify the correlations observed in the past.

The method is illustrated by Figure 44 for a pair of stochastic components with a correlation coefficient equal to r_X . The correlation coefficient r_X is the one calculated on the historical values of the stochastic components of the two time series.

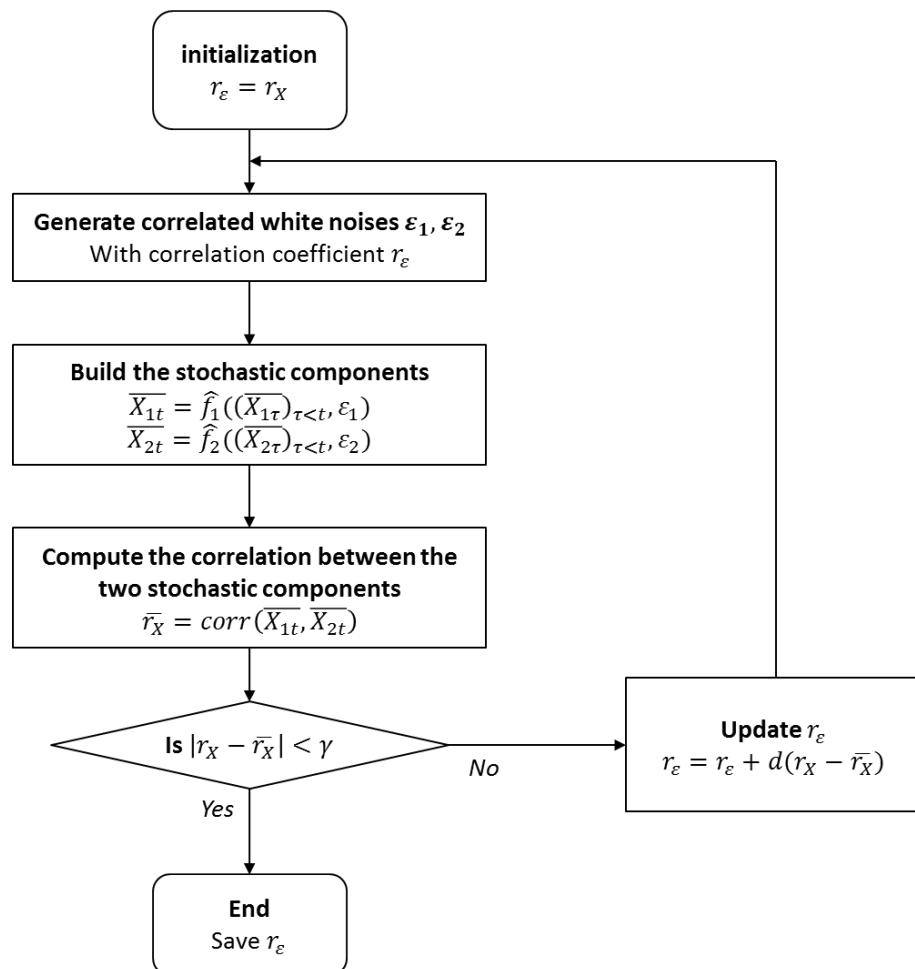


Figure 44. Empirical computation of the correlation coefficient r_ε

The correlation of the innovations is arbitrarily initialized to r_X .

Then, for each iteration:

1. Innovations are generated for a large amount of hours (typically, 100000 hours) with the correlation r_ε
2. Synthetic new stochastic components are built with these correlated innovations
3. The empirical correlation, \bar{r}_X , of the new stochastic components is calculated
4. If the empirical correlation is close enough to the historical correlation (typically, $|r_X - \bar{r}_X| < 0.01$), then r_ε is supposed to be the correlation of innovations which leads to the sought stochastic components. The algorithm stops and r_ε is saved.
5. Else, if the empirical correlation is not close enough to the historical correlation, then r_ε is updated and the algorithm returns to step 1. r_ε is updated by adding the weighed difference between the sought correlation r_X and the measured correlation \bar{r}_X . The difference is weighted by d , a positive coefficient which decreases at each iteration in order to refine the search after each step. A value of d equal to 0.95^{j-1} , where j is the index of the iteration, gave good results on the tested cases.

This algorithm gave good results on the tested time series. However, there is no mathematical proof that it should converge. The existence of a correlation coefficient r_ε which leads to the expected correlated stochastic components has not even been proven. Further work should be done in order to evaluate the consequences of this issue.

As presented in the next table, for two stochastic components which come from similar phenomena (i.e. stochastic models \hat{f}_1 and \hat{f}_2 are close), the correlation of the innovations is close to the correlation of the stochastic component and the algorithm converges after a few iterations.

	Time series 1	Load East of France	Load East of France	Onshore WPG Sicily	PV generation in south East of France
	Time series 2	Load North-East of France	Load West of France	Onshore WPG south of Italy	PV generation in North of Italy
Stochastic components	Model \hat{f}_1	S-ARMA (1,0,0) ₂₄ (1,0,1)	S-ARMA (1,0,0) ₂₄ (1,0,1)	Diffusion type with a beta distr.	Diffusion type with beta distr.
	Model \hat{f}_2	S-ARMA (1,0,0) ₂₄ (1,0,1)	S-ARMA (1,0,0) ₂₄ (1,0,1)	Diffusion type with beta distr.	Diffusion type with beta distr.
	Historical r_X	87%	54%	69%	48%
Results algorithm	Estimated r_ε	88 %	53%	72%	53%
	Number of iterations before convergence	3	6	5	4

Table XVIII. Estimated values of r_ε

This method is performed independently on each coefficient of the correlation matrix R_X .

Note that this algorithm is unusable for time series modelled by different methods (ARMA vs. diffusion-type). The relation which links the stochastic component, X_t , to the innovation, ε , differs for each type of model and the correlation of the stochastic part cannot be transposed to the innovations. More precisely,

the diffusion-type model requires an innovation with a subdivided hourly time step (typically, 60 values of ε per hour) while the innovation of an ARMA-model has an hourly time step. Thus, the comparison between innovations from the two different models is complex, if not impossible. However, this type of modelling is adapted to spatial correlations as time series models of a same phenomenon should be similar.

Given that the correlations r_ε are considered between each pair of innovations, the correlation matrix R_ε is built step by step without guaranteeing its mathematical consistency, i.e. its positive semi-definiteness. Yet, the Cholesky decomposition requires a positive semi-definite correlation matrix. If this property is not verified, the correlation matrix has to be adjusted. For instance, reference [34] proposes a method which aims at identifying the “closest” positive semi-definite matrix (according to the 2-norm).

9. Annex B: A few practical guidelines for the generation of time series

This section addresses some guidelines for the practical use of the TS generator, notably about some issues related to historical data. As explained in annex A, historical data are indeed required to estimate the intrinsic characteristics of the time series: seasonality, stochastic properties and correlations.

9.1. *Where to find historical data?*

This subsection directs towards websites hosting public data.

WPG, PV generation and load

Data of wind power generation, photovoltaic generation and consumption can usually be found at a country or regional scale on the websites of the European's TSOs.

Hourly load data for each European country are also available on the website of the European Network of Transmission System Operators for Electricity (ENTSO-E) [35].

Hydro inflows

Inflows data are the scarcest.

Remember that inflows can however be easily deduced from data of hydro generation and data of hydro reserve.

If such data cannot be found we advise to use instead data of run of the river generation, available at a monthly time step on the website of ENTSO-E [35] and to re-calibrate them respecting to the producible hydro energy. The power generation of run of the river units is influenced by the management of the hydro reservoir upstream, but it can give a first approximation of the inflows of the country.

9.2. *How to deal with the lack of historical data?*

In some cases, it is not possible to get historical data to calibrate the intrinsic characteristics of the models. For example:

- For “new zones”. Zones which do not have generation or consumption at this time. For example, potential offshore sites which are not yet exploited.
- For zones already exploited but without historical data (newly equipped zone, no metering system, no historical data published).
- To estimate the correlations: for time series possessing historical data, but on periods which do not overlap.

This subsection presents some guidelines to create the intrinsic characteristics of the time series in these cases.

Seasonality and stochastic properties

Seasonality and stochastic properties, i.e. (S_t) and \hat{f} , will be considered equal to the ones of a time series of a same type in a neighbouring zone.

Indeed, the seasonality and stochastic properties of a same phenomenon are usually similar in adjacent zones. For instance, Figure 45 and Figure 46 show the seasonality, pdf and acf of the stochastic component of the wind power generation in the west and east regions of France. The PDF are slightly different, but the seasonality and the ACF are following similar patterns.

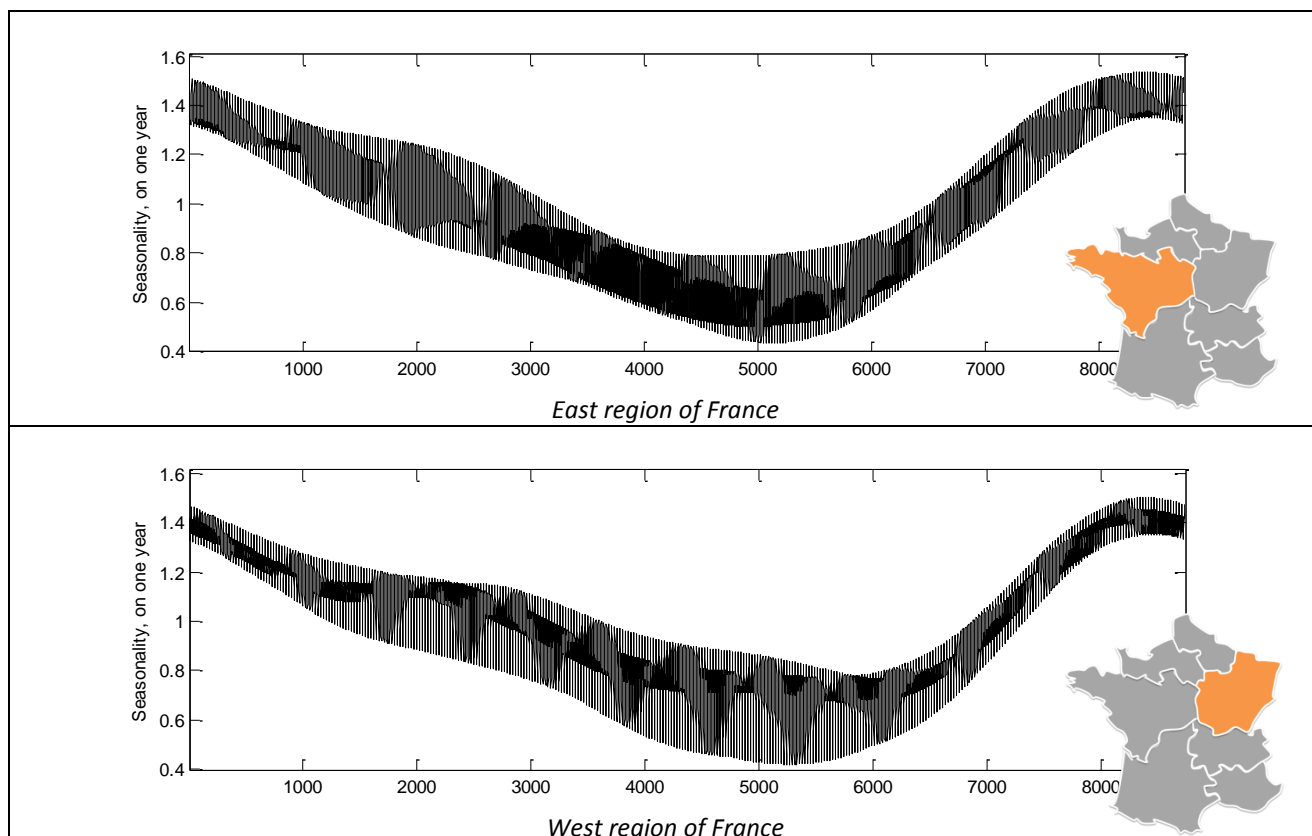


Figure 45. Seasonality of wind power generation in the east and west of France (dimensionless)

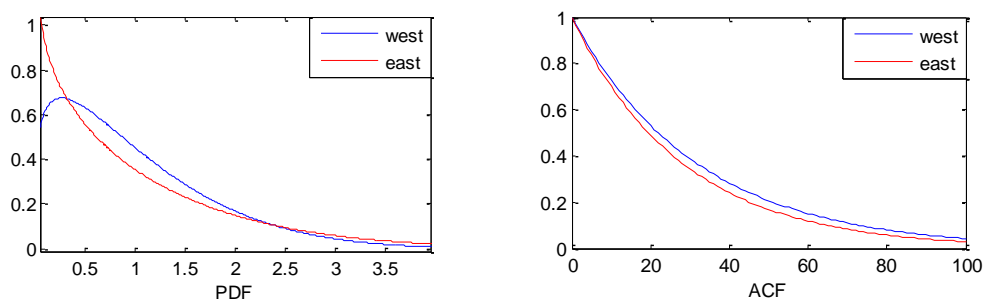


Figure 46. PDF and ACF of the stochastic component of the wind power generation in the east and west of France

Spatial correlations

A first estimate of the spatial correlations can be conjectured from a correlation vs. distance curve. Such curves can be found in the literature, as the one given in [14] for WPG and shown in Figure 47. They can also be deduced from the other correlations observed in the system.

The correlations can then be manually adjusted if needed, on a case-by-case basis according to the specificities of each area (e.g. winds from either side of a mountain range tend to be less correlated).

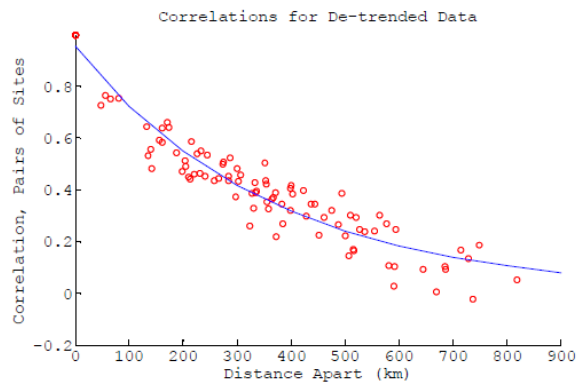


Figure 47. Correlation between two areas as a function of their distance apart [14]

The proposed methods are subjective and approximate but give the possibility to have a coherent estimation of the intrinsic characteristics of the time series when no historical data are available.

10. Annex C: Weekly allocation problem

This annex presents the mathematical formulation of the weekly allocation problem discussed in Section 5 and used to dispatch the hydro resources among the 52 weeks of the year.

Modelling choices are not explained here. They are presented in more details for the hourly adequacy model in Section 5.1.

The following notations are used:

Indexes:

- $t \in \mathcal{W} = \{w..104\}$, week index with w the considered iteration
- $c \in \mathcal{C}$, area index and set of areas
- $g \in \mathcal{G}$, thermal unit index and set of thermal units
- $e \in \mathcal{E}$, extra-European exchange and set of interconnection
- $h \in \mathcal{H}(c)$, aggregated controllable hydro unit index and set of aggregated controllable hydro units

Each country possesses at most two aggregated hydro units, one aggregated hydro unit with storage (reservoir) and one aggregated pumped-storage power plant.

Variables:

- $p_{g,t}^{th}$, power generated by the thermal unit g during the representative hour of the week t
- $p_{h,t}^{hy}$, power generated by the hydro unit h during the representative hour of the week t
- $q_{h,t}^{hy}$, power pumped by the hydro unit h during the representative hour of the week t
- $v_{h,t}$, volume in the reservoir h at the end of the week t
- $p_{e,t}^{ex}$, energy exchanged on interconnection e during the representation hour of week t
- p_t^{uns} , unsupplied energy during the representative hour of week t
- p_t^{exc} , energy in-excess during the representative hour of week t

The objective of the weekly allocation problem is to minimize total costs of the system.

$$\min \sum_{t \in \mathcal{W}} \left(\sum_{g \in \mathcal{G}} C_g^{lin} p_{g,t}^{th} + \sum_{e \in \mathcal{E}} C_e^{ex} p_{e,t}^{ex} + C^{uns} p_t^{uns} \right) \quad (11.1)$$

- Where C_g^{lin} is the generation cost of the plant g ,
- Where C_e^{ex} is the exchange cost on interconnection e ,
- C^{uns} is the value of loss load. The case when $p_t^{uns} > 0$ is particularly critical – it means that the security of supply cannot be insured in average conditions and may presage the worst in the peak hours of the week t .

The problem is subject to the following constraints:

Power Balance, $\forall t$: balances the generations (RES, Hydro and Thermal) with the load.

$$\sum_{g \in \mathcal{G}} p_{g,t}^{th} + \sum_{h \in \mathcal{H}} (p_{h,t}^{hy} - q_{h,t}^{hy}) + \sum_{g \in \mathcal{G}} p_{e,t}^{ex} + P_{c,t}^{RES} = L_{c,t}^0 - p_t^{uns} \quad (11.2)$$

- Where $P_{c,t}^{RES}$ is the averaged uncontrollable RES generation in country c during the week t (*real value* for $t = w$ and *expected seasonality* for $t > w$), sum of wind power generation (onshore and offshore), solar generation and RoR,
- $L_{c,t}^0$ is the averaged load of country c during the week t (*real value* for $t = w$ and *expected seasonality* for $t > w$).

Thermal limits, $\forall t, \forall g$: bound the power generated by a thermal unit by its nominal capacity.

$$0 \leq p_{g,t}^{th} \leq P_g^{max} (1 - M_{g,t}) \quad (11.3)$$

- Where P_g^{max} is the maximum output power of thermal unit g ,
- $M_{g,t}$ is the maintenance schedule, equal to 1 if unit g is in maintenance during week t , and 0 otherwise. It is obtained with the heuristic described in Section 2.

Exchange limits, $\forall t, \forall e$: bound the exchanges on the extra-European borders.

$$p_e^{min} \leq p_{e,t}^{ex} \leq P_e^{max} \quad (11.4)$$

- Where P_g^{min} and P_g^{max} are the minimal and maximal exchange capacities (P_g^{min} can be negative to model the exports of energy)

Hydro limits, $\forall t, \forall h$: bound the power generated and pumped by the aggregated hydro unit between a minimum power and a fraction of the capacity of the unit.

$$P_h^{min} \leq p_{h,t}^{hy} \leq \alpha_{hydro} \times P_h^{max} \quad (11.5)$$

$$0 \leq q_{h,w}^{hy} \leq \alpha_{hydro} \times Q_h^{max} \quad (11.6)$$

- Where P_h^{max} is the generation capacity of aggregated hydro unit h ,
- P_h^{min} : minimum stable power of aggregated hydro unit h ,
- Q_h^{max} : pumping capacity of aggregated hydro unit h ,
- α_{hydro} : real number between 0 and 1 added in order not to use the hydro unit at full capacity during all the hours of the week and to keep some room for manoeuvre (proposed value : $\alpha_{hydro} = 75\%$).

Volume limits $\forall t, \forall h$: the volume inside an hydro reservoir is bounded by the size of the reservoir.

$$0 \leq v_{h,t} \leq V_h^{max} \quad (11.7)$$

- Where V_h^{max} is the reservoirs limit of the aggregated hydro unit h .

Hydro balance $\forall t \geq w + 1, \forall h$: Balances the inflows with the evolution of the volume and the discharge in the hydro reservoirs

$$v_{h,t} = v_{h,t-1} + 168(I_{c,t}R_c^h + \lambda_h^{pump} q_{h,t}^{hy} - p_{h,t}^{hy}) \quad (11.8)$$

- Where $I_{c,t}$ is the averaged inflows of country c during the week t (*real value* for $t = w$ and *imperfect forecast* for $t > w$),
- R_c^h is the ratio of the inflows of country c which supply the aggregated unit h ,
- λ_h^{pump} is the pumping rate of the aggregated hydro unit h .

Hydro boundary conditions $\forall h$: Fix the initial volume of the reservoir and the final target

$$v_{h,1} = V_{h,w-1} + 168(I_{c,1}R_c^h + \lambda_h^{pump} q_{h,1}^{hy} - p_{h,1}^{hy}) \quad (11.9)$$

$$v_{h,104} = V_{h,0} \quad (11.10)$$

- Where $V_{h,w-1}$ is the volume of the reservoir at the end of the previous week (week $w-1$), computed in the previous iteration of the rolling planning,
- $V_{h,0}$ is the initial volume of the reservoir of aggregated unit h .

Post-processing

A post-processing optimisation is run in order to ensure that the hydro generation is logically divided among the hydro units.

The thermal generation, exchanges and unsupplied energy found in the weekly allocation problem are fixed. The hydro generation is balanced between all the units by minimising (11.11):

$$\min \sum_{t \in \mathcal{W}} \sum_{h \in \mathcal{H}} (p_{h,t}^{hy})^2 \quad (11.11)$$

Constraints (11.2) and (11.4-11.10) are reutilised to ensure the balance of the system and simulate the behaviour of the hydro units and reservoirs.

The post-processing is a convex non-linear program. It is however quickly solved as the number of variables is low (2 variables per country and per time step).

11. Annex D: State-of-the-art of demand response models

Demand Response (DR) refers to the changes in the electric usages of the consumers in response to signals transmitted by the System Operator (SO). Reference [55] identifies different actions by which a consumer response may be achieved. The most common one is the load-shifting, which consists in rescheduling – anticipating or postponing – one part of the demand. Some end-use consumptions of electricity are flexible and can therefore be rescheduled in exchange for a low loss of comfort. These end-use consumptions possess a good potential for DR, this is for instance the case of the charging of Electric Vehicles (EVs), heating and cooling, white goods (e.g.: washing machines, dryers, dishwashers) and some industrial processes.

DR offers a new flexibility to the load which can be used to balance the power system. The impacts of this new controllability of the load have been largely studied in the literature. DR has been proven efficient to reduce the operational cost of the system [44]-[45]-[47]-[48]-[50]-[51]-[52]-[53]-[54], to reduce the congestions in the network [44], to avoid the curtailment of intermittent Renewable Energy Sources (RES) [48]-[50]-[52]-[53], to decrease the emissions of CO₂ [48]-[50], to diminish the need of new peaking units [46], to strengthen the reserve [49] and to increase the reliability of the system [43]-[45]-[46]-[47]-[48]-[49].

Those benefits are substantial; for instance, Dupont & al. [48] evaluates the potential of DR in Belgium in the year 2025 when it is assumed that 45% of the demand is supplied by RES (wind, solar, biomass). The authors show that the participation of white goods (counting for 2% of the total demand) in DR leads to a reduction of the non-served energy of 1% and a reduction of the curtailed energy of 10% while the participation in DR of EVs (counting for 8% of the car park) reduces respectively the non-served and the curtailed energy of 7% and 40%. In this case, DR therefore also induces a slight reduction of the CO₂ emissions and operational costs of the system. Göransson & al. [46] studied the impact of DR on the congestion of the European transmission network for the horizon 2020. They show that DR is likely to reduce the congestions occurring during peak-load hours and that the penetration of 5 to 20% of controllable load can reduce the operational costs from 1.4 to 5.5%.

Furthermore, it can be expected that the presence of demand response programs in Europe will be assumed in most (or at least some) scenarios for 2050. One of the main purposes of DR is indeed to compensate the growing part of uncontrollable generation in the energy mixes; for this reason, future scenarios with a high penetration of intermittent RES will most likely go along with the instauration of demand response programs.

11.1. Different demand response mechanisms

The demand response programs – i.e. the mechanisms by which the elasticity of the load is operated – are classified into two major categories: price-based programs and incentive-based programs [49]-[55]-[56]. Price-based programs refer to programs in which electricity tariffs are not flat, but are fluctuating according to the real-time cost of electricity. In such programs, customers are faced to time-varying changes in the electricity prices and can reduce their electricity charges by decreasing their consumption at time of high prices, or shifting it to periods with lower electricity prices. In such programs, modifications in consumption are voluntary – they are incentivised by dynamic prices of electricity, but they are not fully predictable and controllable. Time Of Use (TOU) prices, Critical Peak Pricing (CPP), Extreme Day Pricing (EDP) are classical price-based programs with a few tariffs, typically two or three rates to distinguish off-peak from peak periods or normal days from days with a high expected demand. Real Time Pricing (RTP) is a more flexible

DR program in which the customers are charged hourly fluctuating prices reflecting the real cost of electricity in the market. Customers are informed about the prices one day in advance and can adapt their consumption accordingly. As it is more able to convey the power market needs, RTP is considered the most efficient price-based DR mechanism and the one on which future policy should preferentially focus [55]-[56].

Incentive-based programs are programs in which the customers receive incentives if they reduce their consumption at time required by the SO or the market – i.e. time of high electricity cost or when the system is in jeopardy. Typical incentive-based programs are Direct Load Control (DLC) mechanisms, Interruptible/Curtailable (I/C) Programs and Demand Bidding (DB). Within the framework of DLC and I/C programs, the SO has the ability to directly shut-down the demand of the consumers which participate in the DR program, via a direct control of some devices of these customers or the application of a pre-signed agreement. On the other hand, in Demand Bidding programs, the consumer has the possibility to directly intervene on the wholesale electricity markets by proposing load-clipping or load-shifting offers. Small consumers (residential) can participate with the intermediary of a third-party, an aggregator, which will gather the elasticity of the demand of a group of domestic customers to propose amounts of shiftable energy satisfying the minimum standard of the market. In such programs, demand can participate in the economic dispatch along with the generation and is an alternative to expensive generating units. Moreover, participation of DR in the intraday market offers a new flexibility to face unexpected events affecting the power system.

Demand can be controlled more precisely and in real-time via the incentive-based programs. The spatial resolution of the load controllability is more detailed, independent from the price zones, and can be used to solve diverse local problems (e.g.: congestions). On the contrary, the price-based programs only have one lever: a price profile which has to be fixed in advance and do not offer such controllability.

11.2. Demand response in adequacy models

Diverse modellings of DR have already been proposed and studied in the literature. Their affiliation to one type of DR mechanism or another (price-based and incentive-based) is however not always clearly identified.

11.2.1. Modification of the demand time series

A first modelling approach consists in modifying, *ex-ante*, the demand time series and to solve afterwards a classic adequacy problem with the modified time series as a fixed input. In [43], Zhou & al. propose a method in which the peak load is shaved and the corresponding curtailed energy is postponed in the off-peak hour. A similar approach is adopted in [45]. These two papers however consider fixed peak and off-peak periods, which are not so obvious in a system with a large penetration of RES. Reference [58] proposes a more complex method in which the variability of the residual demand time series (demand minus uncontrollable RES generation) is minimised. Rescheduling of three end-use consumptions – heating, EVs and appliances – are considered, in accordance with their maximum delay time and curtailable power.

With this first modelling approach, the time series of demand are modified with a logic which seems convenient with the expected effect of price-based DR. Demand is indeed reduced during peak hours, when the cost of electricity is supposed to be high, and rescheduled in off-peak hours, when the cost of electricity is supposed to be low. With such an approach DR cannot directly participate in the economic dispatch: the modified time series of demand are a fixed input of the adequacy problem. DR is thus motivated by a simple signal, but cannot respond to more complex balancing issues (e.g.: need of flexibility to compensate the inertia of thermal units).

11.2.2. Adjustment of the demand in the adequacy problem

A second approach consists in modelling the DR in the adequacy problem, i.e. in the optimisation program which aims at finding the optimal – less costly – dispatch of the generating units which balance the load. In that case, the load is not a fixed time series anymore; it is flexible and can directly participate in the economic dispatch. A set of new variables and constraints are therefore used to describe the possibilities offered by DR and to bound the modifications which can be made on the demand time series.

For instance, Göransson & al. [44] model the DR as a kind of storable load which can be consumed afterwards. The stored demand, dh_t , is the quantity of load which has been delayed until time t . It is linked to the positive and negative variations brought to the demand time series, d^+ and d^- , in accordance with constraint (12.1). The final demand, d , is equal to the initial time series of demand D_0 , adjusted by the variations due to DR (12.2).

$$dh_t = dh_{t-1} + d_t^- - d_t^+ \quad (12.1)$$

$$d_t = D_{0t} + d_t^+ - d_t^- \quad (12.2)$$

Note that capital letters are used to represent fixed parameters of the adequacy problem while lower cases are used for the variables of the problem.

The positive and negative variations of the demand curve are naturally bounded by the amount of available controllable demand (typically, a percentage of the total load). Furthermore, the load which is delayed has to be rescheduled before L hours, as imposed by constraints (12.3-12.4). Göransson & al. investigated different delay times, 6h and 24h.

$$dh_t \leq \sum_{l=1}^L d_{t+l}^- \quad (12.3)$$

$$dh_t \leq \sum_{l=1}^L d_{t+l}^+ \quad (12.4)$$

Dupont & al. [48] adopted a similar approach where the load modifications, d^+ and d^- , has to be balanced over one day. Constraints (12.3-12.4) are therefore replaced by constraint (5). It does not offer as much possibilities as the method of Göransson & al: it indeed implies a delay time of 24h and prevent from overlapping the load shifting on consecutive days. It however presents a simpler model, with less variables and constraints, which will probably be solved in a shorter time.

$$\sum_{t=1..24} d_t^+ = \sum_{t=1..24} d_t^- \quad (12.5)$$

Dietrich & al. [53] propose two types of load modifications: load shifting and load clipping. Load can be shifted in every hour of the same day and is modelled with constraints similar to (12.1-12.2) and (12.5). Moreover, a transaction cost, proportional to d^+ , is added in the objective function of the optimisation problem. The transaction cost is a compensation for the nuisance introduced by the load shifting (or in the case of DB, the price of the demand bid submitted in the electricity market). Load clipping allows net reductions of the demand time series, at a cost lower than the cost of the Energy Not Served (ENS) but higher than the cost of load shifting. Note that, in [48]-[53], the economic dispatch is solved over one day and constraint (12.5) can therefore be easily formulated.

In this approach, the adequacy problem is formulated as usual. The adjusted load d is balanced with the production. The operating costs of the system (including the costs associated with DR) are minimized.

The data on DR required by these methods are quite succinct, they are typically:

- The participation limit: the maximum amount of demand – or a percentage of the total demand – which can be reduced during one hour (the upper bound of d^-)
- the maximum amount of demand – or a percentage of the total demand – which can be recovered during an hour (the upper bound of d^+ , which is sometimes assumed equal to the participation limit)
- the delay time (L)
- the compensation cost

With this approach, different types of demand can be considered, with different parameters. A distinction by sectors [53] (e.g. residential, industrial and commercial), or by end-use consumptions [48] (e.g. heating/cooling, EVs, white goods) can be easily envisaged.

11.2.3. Maximisation of the social welfare

The previously mentioned papers aim at minimising the total costs of the system, equal to the cost of generation plus the cost of demand response plus the unreliability cost (cost of ENS). References [50]-[52]-[54] follow a different logic, they maximise the social welfare of the system, equal to the value that the consumers attach to energy minus the operating cost of the system.

As illustrated in Figure 48, one part of the demand is inelastic (price taking demand) as some consumers do not have the ability or the motivation to adjust their consumption to the price of electricity. The value attached to this demand is high; the price taking demand will therefore be supplied regardless of the price of electricity at this time. On the contrary, when DR is introduced, one part of the demand is price responsive. It will only be supplied if the price of electricity is lower than the marginal value attached to this demand. If the price of electricity is higher than its marginal value, consumers will prefer to reduce their consumption.

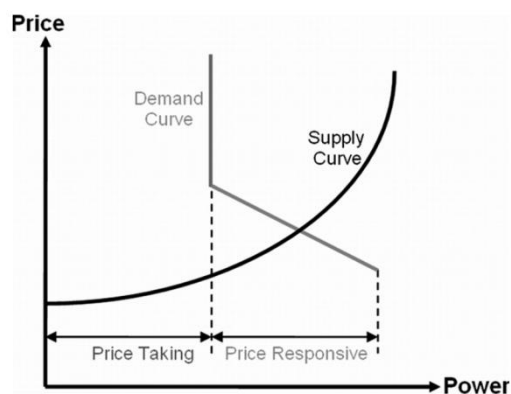


Figure 48. Price taking and price responsive demands. The amount of power which will be generated corresponds to the intersection between the demand curve and the supply curve. It covers the demand which has a marginal value higher than the marginal supply price [54]

In the model of Su & al. [54], the adequacy problem consists in maximizing the social welfare (12.6), which is the difference between the value of consumption, vc , and the operating cost oc .

$$\max \sum_t (vc_t - oc_t) \quad (12.6)$$

The demand curve is usually approximated by a step function and several segments of elastic demand are considered. The value of consumption is therefore linearized (12.7). d_{it}^R is the amount of price responsive demand of segment i which is accepted, and V_i the marginal value of demand for this segment. Moreover, the value of the price taking demand is constant and is therefore removed from vc .

$$vc_t = \sum_i d_{it}^R V_i \quad (12.7)$$

With this modelling of DR, the final demand, d , is equal to the price taking demand, D^{NR} , plus the accepted price responsive demand (12.8).

$$d_t = D_t^{NR} + \sum_i d_{it}^R \quad (12.8)$$

Finally, oc is the sum of the production cost and unreliability cost of the power system. The adjusted load d is balanced with the generation, as usual.

The difficulty of this approach is to build the demand curve, i.e. to ascertain the values of D_t^{NR} , V_i and the bounds of each d_{it}^R . Su & al. [54] modelled the different segments through an enumeration of bids submitted by the consumers on the electricity market. A set of constraints is added to describe the functioning of each bid. The bids can be quite flexible and overlap several hours. However, the construction of a set of bids requires detailed data on the implementation of DR in the considered scenario.

In the context of RTP programs, Sioshansi & al [52] use the own-price elasticity as an indicator to calibrate the slope of the demand curve. The own-price elasticity of the demand, ε_t , indicates the relative change in the demand in response to a change in the price of electricity (12.9), where P_{0t} and D_{0t} are respectively the initial price and demand, without DR. The price elasticity is an indicator which is usually used to characterize the impact of price-based demand response programs. Own-price elasticity observed in pilot projects are typically ranged between -0.01 to -0.4 [59]. It expresses how much percent of demand would change when an increase in price of 1% occurs.

$$\varepsilon_t = \frac{\partial d_t P_{0t}}{\partial p_t D_{0t}} \quad (12.9)$$

In order to build the demand curve for time step t , the initial pair (P_{0t}, D_{0t}) first has to be determined. D_{0t} is the time series of demand without DR. In order to estimate P_{0t} , the adequacy model is run a first time without DR. The hourly marginal cost (equal to the dual variable of the balance constraint when the unit commitment of the thermal units is fixed) is calculated and averaged in order to be representative of the assumed flat tariff that consumer face in the initial case. The price elasticity is then used as the slope of the demand curve. The demand curve is finally approximated by a step function in order to obtain a formulation similar as (12.7).

It should be noted that the method based on price elasticity [50] do not guarantee a strict conservation of the total consumption, moreover it does not consider the delay times: in most cases, demand will be reduced when the marginal cost is higher than P_{0t} and will be rescheduled when it is lower than P_{0t} , but no maximum delay is imposed between these two periods. The initial parameters, notably P_{0t} , should therefore be carefully assessed. This method is also quite time consuming as the adequacy model has to be run twice and the demand curve has to be built for each hourly time step.

In order to include the dynamic effects of DR that the own-price elasticity does not catch, De Jonghe & al. [50] complete this approach by also taking into account the cross-price elasticity, $\varepsilon_{t,t'}$, which indicates the change in consumption at time t in response to a change of price at time t' (12.10). It results in a more realistic modelling of DR, but also a more complex and non-linear formulation of the value of consumption vc .

$$\varepsilon_{t,t'} = \frac{\partial d_t}{\partial p_{t'}} \frac{P_{0t'}}{D_{0t}} \quad (12.10)$$

11.2.4. Other approaches

The previous paragraphs are not exhaustive. Other approaches have been reported in the literature which do not match the specific context of the WP8 of e-Highway2050 and will not be presented in details here. Among them, we can mention the non-sequential methods, such as the ones based on the load duration curve [47][47]. And the methods with a focus on the demand side, not adapted for a study at a large scale (Europe), including for example a modelling of the heating system of the consumers [57] or detailed considerations on the use of EVs [51].

12. References

On general issues of adequacy and market models

- [1] M. Ventosa, Á. Baíllo, A. Ramos, M. Rivier, “Electricity market modeling trends”, *Energy Policy*, vol. 33, no. 7, , pp. 897-913, May 2005.
- [2] P. Panciatici, M-S Debry, “High-level definition of a new methodology for long-term grid planning”, Deliverable D8.10 of the WP8 of e-highways 2050. Available at: <http://www.e-highway2050.eu/results/>.
- [3] W. Li. “System Analysis Techniques” in *Probabilistic Transmission System Planning*. Wiley-IEEE Press (Ed.), Ed. Hoboken, NJ: John Wiley & Sons, pp. 49-83, 2011.

On maintenance scheduling

- [4] L. M. V. G. Pinto, J. F. P. Filho, and M. V. F. Pereira, "A model for the maintenance schedule of an electrical generation/transmission system". *Proceedings of IEEE International Symposium on Circuits and Systems*, vol. 2, pp. 1216-1219, June 1991.
- [5] A. J. Conejo, R. García-Bertrand and M. Díaz-Salazar. "Generation Maintenance Scheduling in Restructured Power Systems". *IEEE Transactions on Power Systems*, vol. 20, no. 2, pp. 984-992, Aug 1999
- [6] J. Cao, K. R. W. Bell, I. Kockar, L. A. S. San Martin. “Generation Maintenance Scheduling in a Liberalised Electricity Market”. Presented in Universities Power Engineering Conference (UPEC), 31 Aug. - 3 Sept., Cardiff, Wales, 2010
- [7] E. Lobato, P. Sanchez-Martin, E. Saiz-Marin. "Long Term Maintenance Optimization of CCGT Plants". Presented in Power and Energy Engineering Conference (APPEEC), 27-29 March, Shanghai, China, 2012
- [8] L. Munoz Moro, A. Ramos. "Goal programming approach to maintenance scheduling of generating units in large scale power systems". *IEEE Transactions on Power Systems*, vol. 14, no. 3, pp. 1021-1028, Aug 1999

On the modelling of time series

- [9] I. J. Perez-Arriaga and C. Batlle, "Impacts of Intermittent Renewables on Electricity Generation System Operation", *Economics of Energy & Environmental Policy*, vol. 1, no. 2, 2012.
- [10] A. Zani and F.Lanati, "A scenario analysis of the impact of a large penetration of intermittent RES in the Italian power system," *10th Conference on the European Energy Market (EEM12)*, Florence, Italy, May 10-12, 2012
- [11] ENTSO-E’s “Summer Outlook Report 2012 and Winter Review 2011/ 2012”, 2012. Available: <https://www.entsoe.eu/publications/system-development-reports/outlook-reports/>
- [12] G. Papaefthymiou, P.H. Schavemaker, L. van der Sluis, W.L. Kling, D. Kurowicka, and R. M. Cooke, “Integration of stochastic generation in power systems”, *Elect. Power Energy System*, vol. 28, pp. 655-667, 2006.
- [13] G. Sinden, “Characteristics of the UK wind resource: Long-term patterns and relationship to electricity demand”, *Energy Policy*, vol. 35, pp. 112-127, 2007

- [14] D.C. Hill, D. McMillan, K.R.W. Bell and D. Infield, "Application of Auto-regressive Models to UK Wind Speed Data for Power System Impact Studies," *Sustainable Energy, IEEE Transactions on*, vol.3, no.1, pp.134,141, Jan. 2012.
- [15] A. Bruhns, G. Deurveilher and J.S. Roy, "A Non-Linear Regression Model For Mid-Term Load Forecasting and Improvements in Seasonality," 15th PSCC Conference, Liege, Belgium, Aug. 22-26, 2005.
- [16] M. Zugno, P. Pinson, H. Madsen, "Impact of Wind Power Generation on European Cross-Border Power Flows," *IEEE Transactions on Power Systems*, vol.28, no.4, pp. 3566-3575, Nov. 2013.
- [17] R. J. Hyndman and G. Athanasopoulos, *Forecasting: principles and practice*, OTexts, 2013.
- [18] E. H. Barakat, "Modeling of nonstationary time-series data. Part I. Data with regular periodic trends", *International Journal of Electrical Power & Energy Systems*, vol. 23, no. 1, pp. 57-62, 2001.
- [19] A. Papavasiliou and S. S. Oren, "Stochastic Modeling of Multi-area Wind Power Production ", in Proceedings of PMAPS 2012, Istanbul, Turkey, June 10-14, 2012.
- [20] A. Lojowska, D. Kurowicka, G. Papaefthymiou, L. van der Sluis, "Advantages of ARMA-GARCH wind speed time series modeling," *2010 IEEE 11th International Conference on Probabilistic Methods Applied to Power Systems (PMAPS)*, pp. 83-88, 14-17 June 2010.
- [21] N.S. Sisworahardjo, M.S. Alam, A.A. El-Keib, "An Improved Stochastic Load Model for Industrial Power Market," *Industry Applications Conference, 2006. 41st IAS Annual Meeting. Conference Record of the 2006 IEEE*, vol. 3, pp. 1352-1359, 8-12 Oct. 2006.
- [22] G. Papaefthymiou, B. Klockl, "MCMC for Wind Power Simulation," *IEEE Transactions on Energy Conversion*, vol. 23, no. 1, pp. 234-240, March 2008.
- [23] N. Barberis Negra, O. Holmstrøm, B. Bak-Jensen and P. Sørensen, "Model of a synthetic wind speed time series generator", *Wind Energy*, vol. 11, no. 2, pp. 193-209, 2008.
- [24] K. Brokish, J. Kirtley, "Pitfalls of modeling wind power using Markov chains," *Power Systems Conference and Exposition.PSCE '09.IEEE/PES*, March 15-18, 2009.
- [25] M. Doquet, "Use of a stochastic process to sample wind power curves in planning studies," *Power Tech, 2007 IEEE Lausanne*, pp.663,670, 1-5 July 2007.
- [26] B.M. Bibby, I.M. Skovgaard and M. Sorensen, "Diffusion-type Models with given Marginal Distribution and Autocorrelation Function," *Bernoulli Journal*, vol. 11, no. 2, 2005.
- [27] G. Papaefthymiou, D. Kurowicka, "Using Copulas for Modeling Stochastic Dependence in Power System Uncertainty Analysis," *IEEE Transactions on Power Systems*, vol. 24, no. 1, pp. 40-49, 2009.
- [28] H. Valizadeh Haghi, M. Tavakoli Bina, M.A. Golkar, S.M. Moghaddas-Tafreshi, "Using Copulas for analysis of large datasets in renewable distributed generation: PV and wind power integration in Iran", *Renewable Energy*, vol. 35, no. 9, pp. 1991-2000, 2010.
- [29] S. Westra, C. Brown, U. Lall, A. Sharma, "Modeling multivariable hydrological series: Principal component analysis or independent component analysis?", *Water Resources Research*, vol. 43, 2007.
- [30] J.R. MacCormack, D. Westwick, H. Zareipour, W.D. Rosehart, "Stochastic modeling of future wind generation scenarios," *Power Symposium, 2008. NAPS '08. 40th North American*, 28-30 Sept. 2008.
- [31] J.M. Morales, R. Mínguez, A.J. Conejo, "A methodology to generate statistically dependent wind speed scenarios," *Applied Energy*, vol. 87, no. 3, Pages 843-855, March 2010.

- [32] M. Doquet; C. Fourment; J. Roudergues, "Generation & transmission adequacy of large interconnected power systems: A contribution to the renewal of Monte-Carlo approaches," *PowerTech, 2011 IEEE Trondheim*, June 19-23, 2011
- [33] G. Box, G. Jenkins. *Time series analysis: Forecasting and control*, San Francisco: Holden-Day. 1970.
- [34] P. M. Lurie and M. S. Goldberg, "An Approximate Method for Sampling Correlated Random Variables from Partially-Specified Distributions", *Management Science*, Vol. 44, No. 2, pp. 203-218, Feb. 1998.
- [35] Data portal of ENTSO-E : <https://www.entsoe.eu/data/>

On the modelling of hydro units

- [36] M. Zambelli, I. Luna Huamani, S. Soares, M. Kadowaki and T. Ohishi. "Hydropower Scheduling in Large Scale Power Systems" in *Hydropower - Practice and Application*. Dr. Hossein Samadi-Boroujeni (Ed.), InTech, pp. 201-226, March 2012
- [37] M. Amelin and L. Soder. "On Monte Carlo simulation of electricity markets with uncertainties in precipitation and load forecasts". *Proc. 2001 Power Tech.*, pp.10-13, 2001
- [38] A. Helseth, G. Warland, and B. Mo. "A hydrothermal market model for simulation of area prices including detailed network analyses" in *International Transactions on Electrical Energy Systems*. Wiley online library, 2012
- [39] M. Zambelli, T.G. Siqueira, M. Cicogna, S. Soares. "Deterministic versus stochastic models for long term hydrothermal scheduling". *Proceedings of IEEE Power Engineering Society General Meeting*, 18-22 June, Montreal, Canada, 2006.
- [40] M. Pereira N. Campodónico R. Kelman. "Long-term Hydro Scheduling base on Stochastic Models". Presented at EPSOM'98, Zurich, Switzerland, September 23-25, 1998.
- [41] B. Tong, X. Guan, Q. Zhai and F. Gao. "Long-term Scheduling of Cascaded Hydro Energy System with Distributed Water Usage Allocation Constraints". Presented in IEEE Power and Energy Society General Meeting, 24-29 July, San Diego, CA, 2011

On the modelling of thermal units

- [42] G. Morales-España, J.M. Latorre, and A. Ramos, "Tight and Compact MILP Formulation of Start-Up and Shut-Down Ramping in Unit Commitment", *IEEE Transactions on Power Systems*, Vol. 28, no. 2, pp. 1288-1296, May 2013

On Demand response

- [43] Ming Zhou, Gengyin Li and Peng Zhang, "Impact of Demand Side Management on Composite Generation and Transmission System Reliability," *Power Systems Conference and Exposition*, pp.819-824, Oct 2006.
- [44] L. Göransson, J. Goop, T. Unger, M. Odenberger and F. Johnsson, "Linkages between demand-side management and congestion in the European electricity transmission system," *Energy*, vol. 69, pp. 860-872, May 2014.
- [45] D. Huang, R. Billinton, W. Wangdee, "Effects of demand side management on bulk system adequacy evaluation," *Probabilistic Methods Applied to Power Systems (PMAPS)*, pp. 593-598, June 2010.

- [46] A. Keane, A. Tuohy, P. Meibom, E. Denny, D. Flynn, A. Mullane, M. O'Malley, "Demand side resource operation on the Irish power system with high wind power penetration," *Energy Policy*, vol. 39, no. 5, pp. 2925-2934, May 2011.
- [47] K.S. Malik, "Simulation of DSM resources as generating units in probabilistic production costing framework," *IEEE Transactions on Power Systems*, vol. 13, no. 4, pp. 1528-1533, Nov 1998.
- [48] B. Dupont, K. Dietrich, C. De Jonghe, A. Ramos, R. Belmans, "Impact of residential demand response on power system operation: A Belgian case study," *Applied Energy*, vol. 122, pp. 1-10, June 2014.
- [49] M. Parvania, M. Fotuhi-Firuzabad, "Demand Response Scheduling by Stochastic SCUC," *IEEE Transactions on Smart Grid*, vol. 1, no. 1, pp. 89,98, June 2010.
- [50] C. De Jonghe, B.F. Hobbs, R. Belmans, "Value of Price Responsive Load for Wind Integration in Unit Commitment," *IEEE Transactions on Power Systems*, vol. 29, no. 2, pp. 675-685, March 2014.
- [51] J. Wang, C. Liu, D. Ton, Y. Zhou, J. Kim, A. Vyas, "Impact of plug-in hybrid electric vehicles on power systems with demand response and wind power," *Energy Policy*, vol. 39, no. 7, pp. 4016-4021, July 2011.
- [52] R. Sioshansi, W. Short, "Evaluating the Impacts of Real-Time Pricing on the Usage of Wind Generation," *IEEE Transactions on Power Systems*, vol. 24, no. 2, pp. 516-524, May 2009.
- [53] K. Dietrich, J.M. Latorre, L. Olmos, A. Ramos, "Demand Response in an Isolated System With High Wind Integration," *IEEE Transactions on Power Systems*, vol. 27, no. 1, pp. 20-29, Feb 2012.
- [54] C. Su, D. Kirschen, "Quantifying the Effect of Demand Response on Electricity Markets," *IEEE Transactions on Power Systems*, vol. 24, no.3, pp. 1199-1207, Aug. 2009.
- [55] M.H. Albadi, E.F. El-Saadany, "Demand Response in Electricity Markets: An Overview," *Power Engineering Society General Meeting*, June 2007.
- [56] Q. Zhang, J. Li, "Demand response in electricity markets: A review," *9th International Conference on the European Energy Market (EEM)*, May 2012.
- [57] K. Bruninx, D. Patteeuw, E. Delarue, L. Helsen, W. D'haeseleer, "Short-term demand response of flexible electric heating systems: The need for integrated simulations," *10th International Conference on the European Energy Market (EEM)*, May 2013.
- [58] Deliverable of the WP2 of e-highway 2050, annex on Demand Side Management.
- [59] A. Faruqui and S. Sergici, "Household Response to Dynamic Pricing of Electricity – a Survey of the Experimental Evidence", 2009.
- [60] Capgemini Consulting, "2020/2025 Demand Response Study", 2012.

Others

- [61] AMPL Optimization, <http://ampl.com>.
- [62] FICO Xpress Optimization Suite, FICO, <http://www.fico.com/en/products/fico-xpress-optimization-suite/>.
- [63] RTE, *Generation Adequacy Report 2012*.
- [64] National Climatic Data Center database : <http://cdo.ncdc.noaa.gov/>